University of Stavanger

Faculty of Science and Technology

MASTER'S THESIS

Study program/ Specialization: Msc. Petroleum Technology	Spring semester, 2011.. Open / Restricted access
Writer: Nina Iren Kåsa	………………………………………… (Writer's signature)
Faculty supervisor: Aly Anis Hamouda External supervisor(s): Øyvind Midttveit Anastasios Siamos	
Titel of thesis: Production Performance Analysis of Well With Different Inflow Technologies	
Credits (ECTS): 30	
Key words: Petroleum Technology Production Optimization Well Performance Inflow Control Technology Near Wellbore Simulation NETool	Pages: ………77………… + enclosure: ……10…… Stavanger, …15.06.2011…………….. Date/year

Preface

This thesis is completed during the spring of 2011 on behalf of the Troll Petroleum Technology Group within Statoil ASA. It is the last part of a five year long study in Petroleum Technology at the University of Stavanger (UiS).

It has been a challenging process since there is not much material available on this subject, and the external advisors and experts on this area have been located in Bergen whereas the thesis has been completed in Stavanger. The faculty supervisor Aly Anis Hamouda from UiS has been a great resource and was always available for discussions if needed.

A special thank you is given to the external advisor Anastasios Siamos at Statoil ASA for good guidance and counselling during this whole process. He would contribute with relevant insights and comments whenever requested. Another great thank you is handed to the other external advisor Øyvind Midttveit and the contact person for the Troll Petroleum Technology group Martin Halvorsen. Both have together with Anastasios Siamos been involved in routine updates via video conferences, and have suggested ideas and shared information. Svend Magnus Pettersen, Gunn Helen Tonning and Erlend Gudding have all been helpful in the process of learning and understanding the simulation software used called NETool. All involved people are hereby thanked.

A big thank you is also sent out to the members of the Production Support Centre at Statoil ASA in Stavanger. They gladly lent me an office and were always there with a joke or a cup of coffee to lighten up even my darkest day.

Nina I. Kåsa

Abstract

Due to the limited gas handling capacity at the Troll Oil platforms the objective is to produce at the lowest possible gas-oil ratio (GOR). This can be achieved by installing inflow control equipment, preferably with the ability to restrict the flow of gas more than it does the oil.

The well considered in this thesis is a new multi lateral sub-sea well completed with different inflow control valves. The ICD technology implemented in branch BY1H shows the ability of attaining a higher volumetric flow rate of the oil in long horizontal sections. This is achieved by balancing the inflow better over the whole production section. The RCP valve found in the other branch called BY2H restricts the gas flow and presumably the water too better than other conventional inflow control devices. It has also an ability to give a more uniform inflow.

The expected theoretical performance of these two inflow control technologies are described and summarized through estimated pressure drop curves developed with the respective characteristics given for the tools. The different advantages of the technologies stated above are confirmed theoretically.

To investigate the real performance of the two valves, a simulation model is built in NETool on the basis of results from three of the 15 available production well tests. Many assumptions are required, but the intention is to make it as realistic as possible and then investigate what these conditions imply. A control of the model is performed by comparison of other test not used for matching. Simulation results indicate a more uniform inflow profile of oil for the RCP valves.

Also, a theoretical evaluation of the productivity index (PI) in the two branches is performed. The pressure drops across sandface and completion is evaluated based on these findings and available production well tests. It is found that both branches have high PI values; 8700 Sm3/d/bar in BY1H with ICD valves and 13700 Sm3/d/bar in BY2H with RCP completions. These findings imply that the majority of the drawdown seen in the well is due to the pressure drop across the completion, not the formation, and that the production is highly dependent on how these valves are operated.

Contents

Acronyms

AICD	autonomous inflow control device
BHP	bottom hole pressure
DCP	downstream choke pressure
DCT	downstream choke temperature
DHP	downhole pressure
DHSV	downhole safety valve
DL	dog leg
FCV	flow control valve
GBT	gas break through
GKGL	gasskappe gassløft
GOC	gas-oil contact
GOR	gas-oil ratio
HC	hydrocarbons
HSV	havbunn sikkerhetsventil
ICD	inflow control device
ICV	interval control valve
IPR	inflow performance relationship
LGR	liquid-gas ratio
MD	measured depth
NPD	Norwegian petroleum directorate
NPV	net present value
OWC	oil-water contact
PLT	production logging tool/production testing
PSS	pseudo-steady state
PSV	platform sikkerhetsventil
RCP	rate controlled production
RGL	riser gassløft
RKB	rotary kelly bushing
S-FCV	shrouded flow control valve
sg	specific gravity
SIP	shut in pressure
SMG	side mounted gun
SS	steady state
ST	standard
TD	true depth
TOGI	Troll Oseberg gas injection
TVD	true/total vertical depth
TWT	two-way time (seismic)

UCP	upstream choke pressure
VLP	vertical lift performance
WH	wellhead

Nomenclature

a	a user-input 'strength' parameter
A	area [m^2]
B	formation volume factor [Rm^3/Sm^3]
C	compressibility [bar^{-1}]
f	friction factor
f(ρ,μ)	analytic function of the mixture density and viscosity
h	formation thickness [m]
ID	inner diameter [m, in]
L	length [m]
OD	outer diameter [m, in]
P	pressure [bar]
PI	productivity index [Sm^3/d/bar]
Q	flow rate [Sm^3/d]
r	radius [m]
s	skin
T	transmissibility
V	volume [m^3, l]
x	length in x direction [m]
y	length in y direction [m]
z,Z	vertical distance [m]
α	volume fraction
θ	well deviation from vertical [deg]
κ	permeability [mD]
κ'	effective permeability perpendicular to the well axis
λ	mobility
μ	viscosity [cP]
ρ	density [kg/m^3, sg.]

Subscripts

AICD	characteristic marker for AICD valve
av	average
b	bubble point
c	completion
cal	calibration
d	damage
DR	downstream restriction
DSC	downstream surface choke
DSV	downstream safety valve
e	equivalent rectangle
F	friction
fm	formation
g	gas
H	horizontal
m	Moody
o	oil
p	perforated
PE	potential energy
phase	relevant phase; oil, water or gas
R	reservior
r, phase	relative value of phase
sep	separator
USV	upstream safety valve
V	vertical
w	wellbore, well, water
wf	flowing bottom hole
wfs	flowing sandface
WH	wellhead

Figures

Tables

1. Introduction

1.1. Objective

One goal in this thesis is to perform well inflow control evaluations of two different completion device technologies. They have been installed in a new dual lateral sub-sea well located in the Troll field. This is achieved by the use of available reservoir and well test data.

To investigate if the equipment is functioning in accordance with the given performance specifications, an estimation of the pressure drops across sandface and the inflow control technologies is performed based on production well test results. In addition to this, a near wellbore simulation model is prepared to aid in the investigation. The production performance from the well tests is compared with the a-priori available reservoir simulation results. A discussion and comparison of results is carried out with emphasis on production optimization.

The process of completing this thesis can be characterized by the learning-by-doing principle. This is especially valid for the creation of the simulator. Often a mistake was made in order to eliminate a theory rather than programming the correct assumptions from the beginning and then just improving it further. It was also experienced that there are many uncertainties to be considered, so many that a whole chapter is dedicated to this discussion.

The well is new and still developing with respect to production conditions, which at the moment are not optimal for the purpose of this thesis. The same investigation could be continued with the results obtained here functioning as the basis for future evaluations.

1.2. Background

The Troll field is characterized by a large gas cap and a relatively thin oil column representing a huge challenge considering both drilling and completion operations. Through time the implementations of multilateral well technology, longer horizontal sections and new sand screen technologies have made the Troll oil subsea development one of the largest oil producing fields on the Norwegian continental shelf today [1].

Regarding production optimization, the aim is to maximize the oil production within the gas handling capacity available. This means producing at the lowest possible gas-oil ratio (GOR) [2]. This is done by having inflow control devices in the production zones of the wells with the ability to choke the reservoir fluids, preferably with more restriction of the gas than the oil/liquid. The particular well considered in this thesis is a bi-lateral well with horizontal branches completed with different inflow control devices having unequal characteristics. Since the branches have comparable lengths and are drilled in similar sands, the conditions allow for a comparison of the two technologies [3]. 15 well tests have been performed in this well, and are used as a basis to perform near wellbore simulations and to estimate the pressure drops across sandface and inflow control completion.

1.3. Outlay

The Troll field and the particular well called Well X BY1H/BY2H in this thesis are presented in Chapter 2 and 3 respectively as an introduction. The information given is also relevant for understanding the reasons behind the choice of completion and how this well is producing. In Chapter 4 the two particular inflow control technologies placed in each branch are described and compared theoretically with regards to expected performance. Also a method of analyzing the number of valves filled with from the well tests is suggested. Other relevant equipment in addition to the valves is presented last in this chapter. Following this is a chapter (Chapter 5) on well testing; why they are performed and the procedures followed at Troll Well X BY1H/BY2H. A technique for performing pressure drop evaluations from these well test results is provided in Chapter 6. Several considerations must be made in order to obtain the correct values, and all of these are mentioned here. Given in Chapter 7 is an outlay on how the near wellbore models are developed and what assumptions they are based on. Then in Chapter 8 the specific results obtained from the simulation runs are presented together with a comparison between these and the production performance obtained through well tests. Following this are the results of the pressure drop analysis given in Chapter 9. Chapter 10 is used for the discussion and evaluation of the performance of the inflow control technologies before Chapter 11 debates uncertainties. Last, a conclusion is formed in Chapter 12.

2 The Troll Field

2.1. General

Approximately 300 meters below sea level, a bigger than 750 km^2 sized oil and gas field was discovered in 1979 by Norske Shell, and it was declared viable in 1983. This is now known as the Troll field, and it is located in the four blocks 31/2, 31/3, 31/5 and 31/6 in the northern part of the North Sea, about 65 kilometres west of Kollsnes in Hordaland. This position is shown in Figure 1 below. Almost 1/3 of the reserves are situated in block 31/2 originally belonging to Norske Shell, while Statoil, Norsk Hydro and Saga Petroleum were awarded the three other blocks initially. In 1985 the licenses were arranged so that Troll could be developed as one single unit. Hydro commenced the production of Troll Oil in September 1995, while Statoil took over as operator in the production of Troll Gas in June 1996. At this moment, Statoil is accountable for the operations and the lines leading onshore while Gassco on behalf of Gassled is the operator of the gas processing facility at Kollsnes [5], [6].

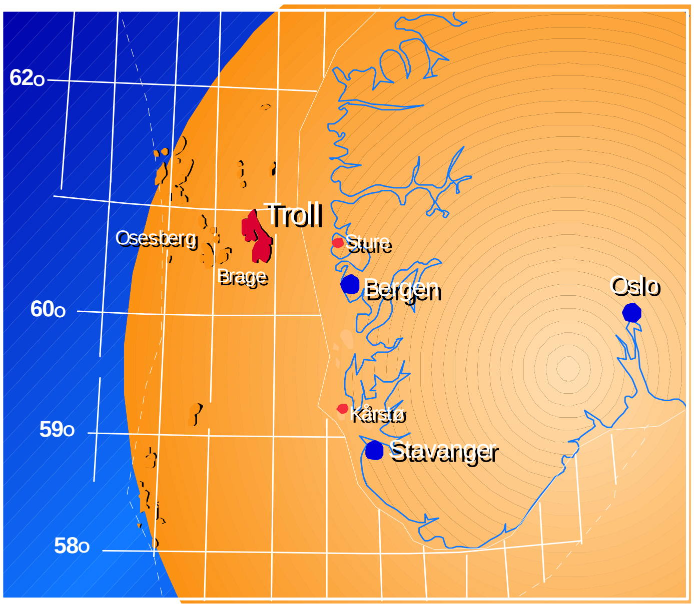

Figure 1: Location Troll field [3].

Two main structures called Troll East and Troll West divides the field. It is estimated that about two thirds of the gas reserves are situated in Troll East, and even though there is a thin oil layer below this huge gas cap reaching throughout the entire field, it is in Troll West that it was thick enough (ranging between 8-26 m) to be produced for profit initially. Troll West is also divided in two provinces based on what type of reservoir fluid it contains, the Gas Province and the Oil Province. The division of the field is shown in Figure 2. It should also be mentioned that oil production from the northern part of Troll East was initiated in November 2008 [4], [5], [6].

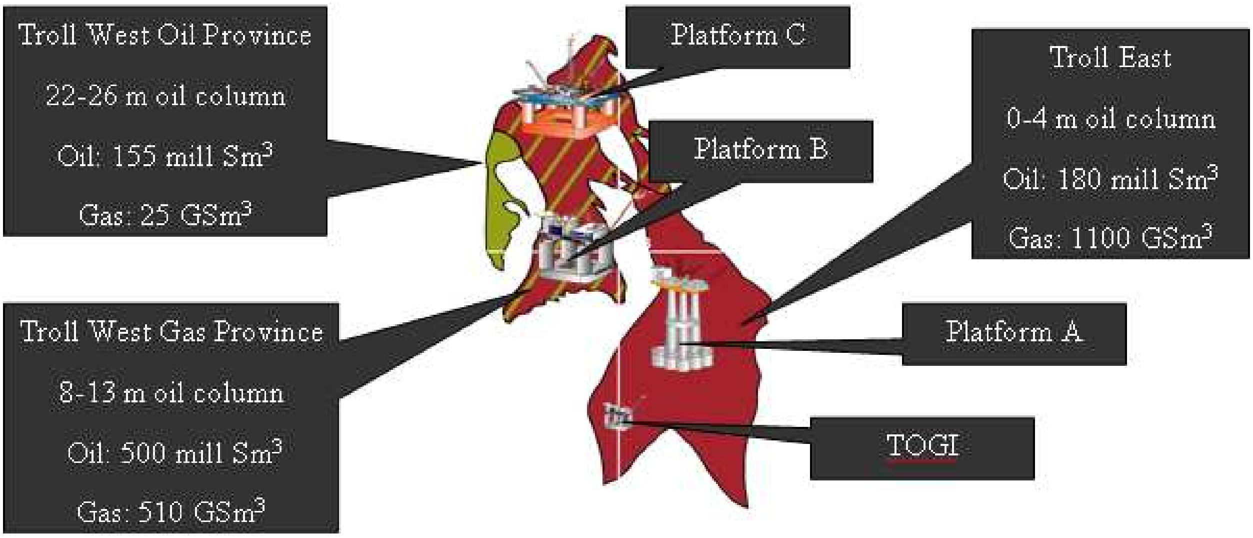

Figure 2: Division of Troll East and West with platforms [4].

The field has been developed in several phases. Phase 1 involves the gas reserves in Troll East with the production platform A. The Troll Oseberg Gas Injection (TOGI) is also found south of Troll A in the eastern part of the field. Phase 2 involves the oil reserves in Troll West, and it is platform B and C that are responsible for this [3], [7].

2.2. Ownership [5]

Petoro 56 %
Statoil 30,58 %
Norske Shell 8,10 %
Total E&P Norge 3,69 %
ConocoPhillips Skandinavia 1,62 %

The Troll findings led to the biggest investment project in Norwegian history, requiring 130 billion NOK to develop processing facilities on shore, offshore platforms and other infrastructure nationally and internationally [6].

2.3. Reservoir Information

The oil and gas found in the Troll field are situated mainly in shallow marine sandstones from the Sognefjorden Formation of late Jurassic age. There are also reserves in Fensfjord Formation (middle Jurassic), deposited prior to Sognefjorden Formation. Three rotated fault blocks, which are relatively big, define the Troll field. To the east the reservoir is located at approx. 1330 m., with a proven oil column of 6-9 m. in Fensfjord Formation the northernmost part of Troll East. In Troll West oil province, the oil column is found to be 22-26 m. thick situated at 1360 meters deep below a small gas cap. When it comes to Troll West gas province, the oil column is smaller and varying between 12-14 m., and a gas column reaching as far as 200 m. immediately below the oil column in Troll West, considerable amounts of residual oil have been found. Below the main reservoir, in the Brent Group (middle Jurassic) a smaller oil reservoir has been discovered as well. A pressure communication between Troll East and Troll West has been established [7].

2.4. Reserve Estimates as of 31.12.2010[1, 2]

The recoverable and the estimated remaining reserves given for the field as of 31.12.2010 are given in Table 1:

Recoverable reserves				**Remaining reserves**			
Oil	Gas	NGL	Condensate	Oil	Gas	NGL	Condensate
[10^6 Sm^3]	[10^9 Sm^3]	[10^6 tonn]	[$10^6 Sm^3$]	[10^6 Sm^3]	[10^9 Sm^3]	[10^6 tonn]	[10^6 Sm^3]
250	1330,7	25,7	1,6	36,6	942	20,8	-2,7

Table 1: NPD reserves [7].

2.5. Troll Gas

Troll is said to be the very cornerstone of Norwegian gas production, responsible for almost 40 per cent of the total gas reserves on the Norwegian Continental Shelf [5]. It is found to be the 16th largest gas field in the world [6]. Troll Gas consist of the platform Troll A, the pipes linking the platform to the main land and the facility for gas processing at Kollsnes.

Two compressors powered by electricity from onshore were installed on Troll A in 2005 to provide pressure support and ensure maintained production as the gas is transported onshore. This solution ensures no emission of CO_2 and NO_x from either the platform or the processing plant onshore [7].

2.5.1. Transportation

The gas from both Troll East and West is transported through multiphase pipes to the gas handling system found at Kollsnes. Here the condensate is separated from the gas, and transported further on, partly to Stureterminalen and partly to Mongstad. The dry gas goes through Zeepipe II A and II B [5]. Some of the produced gas is being used in Norway, but most of it is exported to countries such as Germany, France, Belgium and Spain to mention some. This is made possible by five different pipe systems throughout Europe [6].

---

1 NGL = butane + ethane + isobutane + propane + LPG + gasoline + NGL mix.

2 Negative figures for remaining reserves are due to mismatch between the approximate recoverable reserves and actual production numbers.

2.6. Troll Oil

Today Troll is among the fields with the highest oil production on the Norwegian continental shelf, but it was initially recognized as unprofitable. Some reasons for this are [9]:

- The oil columns are thin, ranging from 4 to 26 m. in thickness.
- The oil columns, as well as the field itself, reach out over a great area, over 750 m^2.
- The reservoir quality varies between the different sand layers that are present.
- Experience showed movement in the res. fluids when producing the oil, making the planning for new wells more difficult.
- The oil being produced will gradually contain more and more gas and water.

The solutions to these problems were many, including the following:

- Drilling horizontal wells over great distances with accurate precision.
- Developing the field with multiple installations on the sea floor and fewer floaters.
- Multiphase transportation.

As of 31.01.2011, there are a total of 110 production wells being planned, all of them horizontal with some of them reaching as far as 3200 meters along the oil zone. 28 of them will be multi laterals, meaning that there exist two or more branches connecting back to the same bore hole [10].

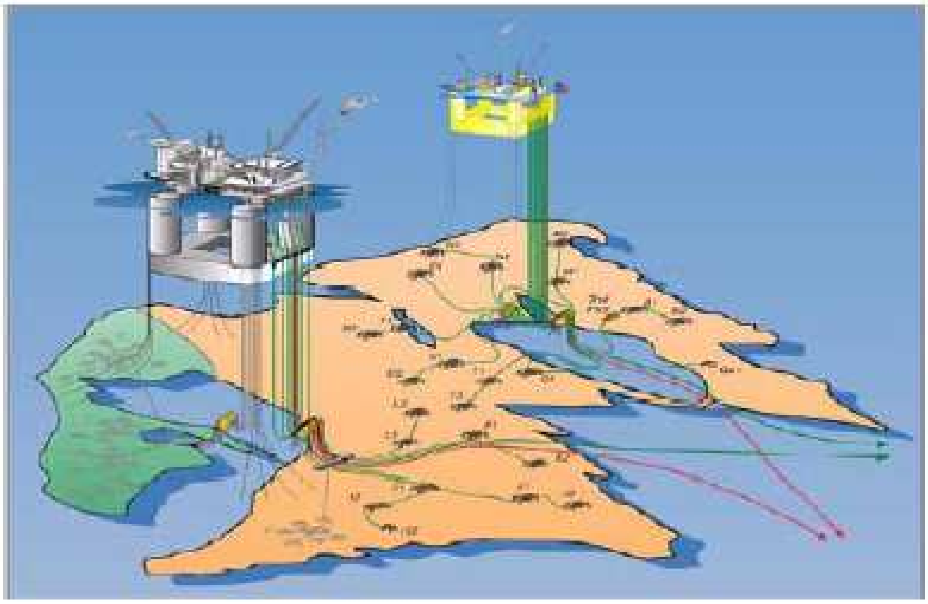

Figure 3: Field map Troll Oil with B and C[1].

There are two platforms responsible for production of Troll Oil, namely Troll B and C shown in Figure 3 above. Platform B is a concrete floater whereas Plaatform C is a steel unit semi-floater. Both platforms are equipped with living quarters and production facilities [10].

2.6.1. Transportation

The oil from platforms B and C are transported to the oil terminal at Mongstad through Troll Oljerør I and II [7].

3. Well X BY1H/BY2H

The relevant well for this assignment is a multilateral well with two completed horizontal branches named BY1H and BY2H. The completion diagram with relevant equipment is found in Figure 9 on page 12. It is situated in the Troll West Oil Province in block 31/2-1, a well known area. In July 2010 Songa Trym performed the drilling operation, while West Venture was responsible for the completion job. On the 1st of October 2010 the production of oil was initiated [3]. The black square in Figure 4 show where the well is situated in the Troll field. The different colors characterize different sand types.

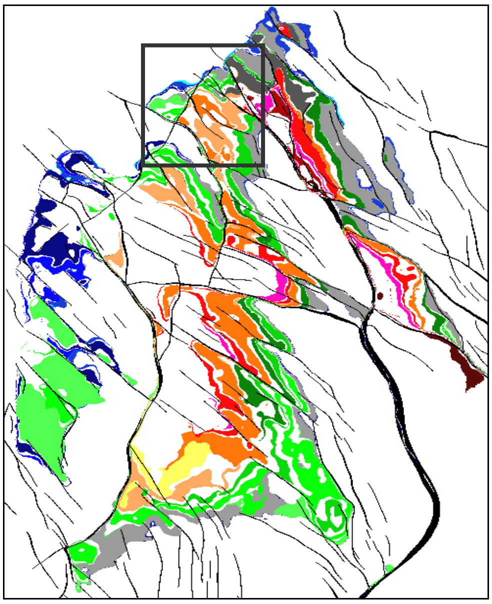

Figure 4: Placement of well within square [3].

3.1. Target Placement

The lowermost arrow in Figure 5 shows the main target sand 3Dc which is an elongated sand package striking NW-SE thinning distally to the NW. The sand quality is also improving in this direction. It is found to be up to 40 m. thick. The bottom section of both branches was planned in the 4series. 4Bc and 4Cc were observed as northwards dipping sand packages, with a thickness of approximately 5-8 m. This is represented by the uppermost arrow in Figure 5. Figure 6 simulate the location of the well through these sands. The branches are placed approximately 0,5 m. above the OWC [3].

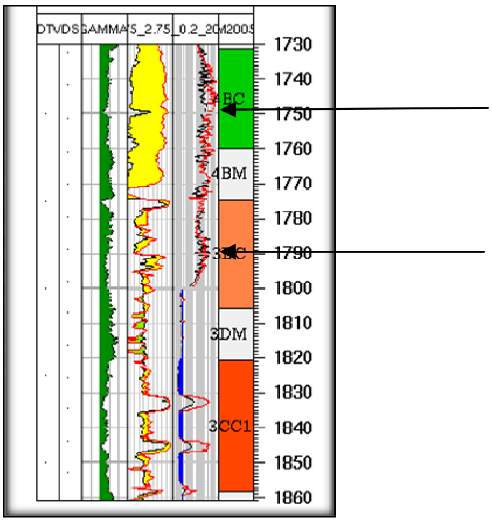

Figure 5: Log for Well X. [3].

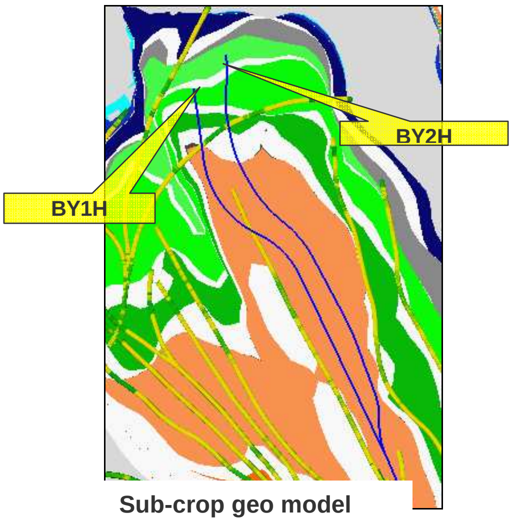

Figure 6: Well X in different sands [3].

In Figure 7 and Figure 8 below are the cross sections of the model in Figure 6 shown for BY1H and BY2H respectively. Following the blue line one can trace the placement of the branch through the different sands. Initial oil-gas-contact (GOC) and oil-water-contact (OWC) are also marked with red and green lines in both figures.

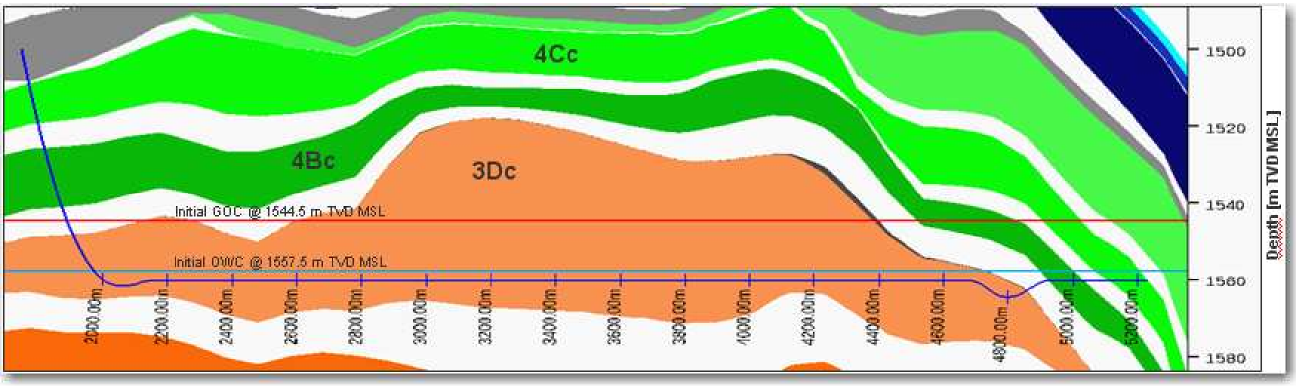

Figure 7: Well path of BY1H [3].

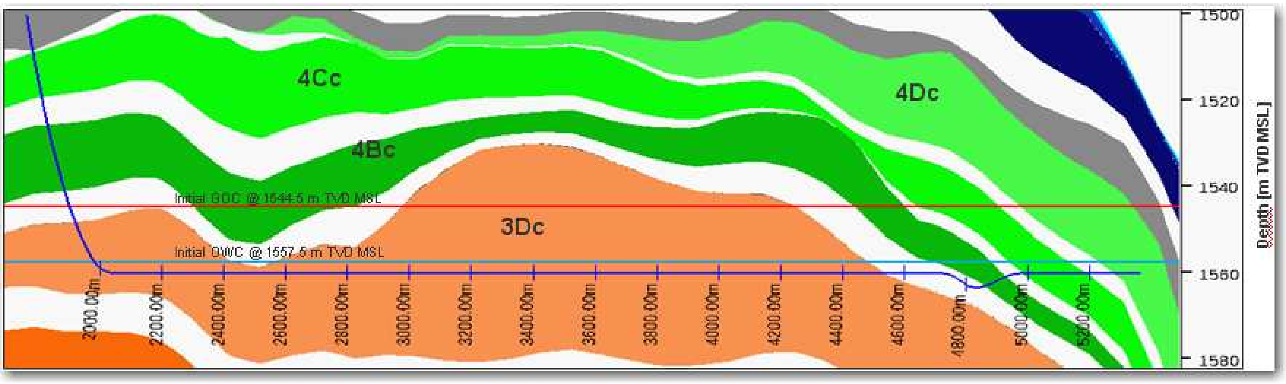

Figure 8: Well path of BY2H [3].

3.2. Layout and Completion

The well starts out from a vertical position on the sea floor and gradually builds up a DL so that the two branches become horizontal [11].

3.2.1. Deviation Data for BY1H

Max deviation [deg]	93,1 (at 4075,30 m)
Av. angle through pay zone [deg]	90
TD MD [m]	5240

Table 2: Deviation data BY1H [12].

3.2.2. Deviation Data for BY2H

Max deviation [deg]	91,5 (at 4339,90 m)
Max DL [deg]	9,3 (at 2009,70 m)
Av. angle through pay zone [deg]	90
TD MD [m]	5343,5

Table 3: Completion data for BY2H [12].

3.2.3. Relevant Lengths

To get a feeling on the size and range of this well, relevant parameters are listed in Table 4.

Total well length from sea floor [m]	8560
Approx. cumulative length from start sand screen in both branches [m]	6456
Horizontal length BY1H [m]	3170
Horizontal length BY2H [m]	3370
Producing interval BY1H [m]	2333
Producing interval BY2H [m]	2809,5
Total producing interval [m]	5142,5

Table 4: General well data [3], [11].

3.2.4. Casing programme

In Table 5 the casing programme for the well is given. The relevant parameter for this thesis is ID in column 4.

Size	MD Top	MD Bottom	Nom. Weight	ID	Matl.	
[inch]	[m]	[m]	[kg/m]	[inch]	Specifications	Threads
30	371,1	435,7	460,88		X-52	Quick Stab
18,625	370,1	861	130,21		X-56	Multi
13,375	370,5	1588	107,15	12,35	P-110	Vam Top
10,75	1528,5	1997,6		9,66	13 Cr-80	Vam Top
10,75	370,9	1534,5	90,33	9,66	13 Cr-80	Vam Top
9,625	1997,6	2102	79,62	8,54	P-110	Vam Top

Table 5: Casing programme [12].

3.2.5. Placement of Important Equipment

The placement of important equipment is given in Table 6:

Completion	**Placement in well [m MD RKB]**
WH datum	370,12
7" DHSV	439
Production packer	1699
GLV	1736
Perforated interval (from – to)	1765 – 1795
5 ½" Single DHG	1944
3 ½" Dual DHG	1978
FCV (BY2H)	1968,5
S-FCV (BY1H)	1980
Junction	2220

Table 6: Placement of important equipment [11].

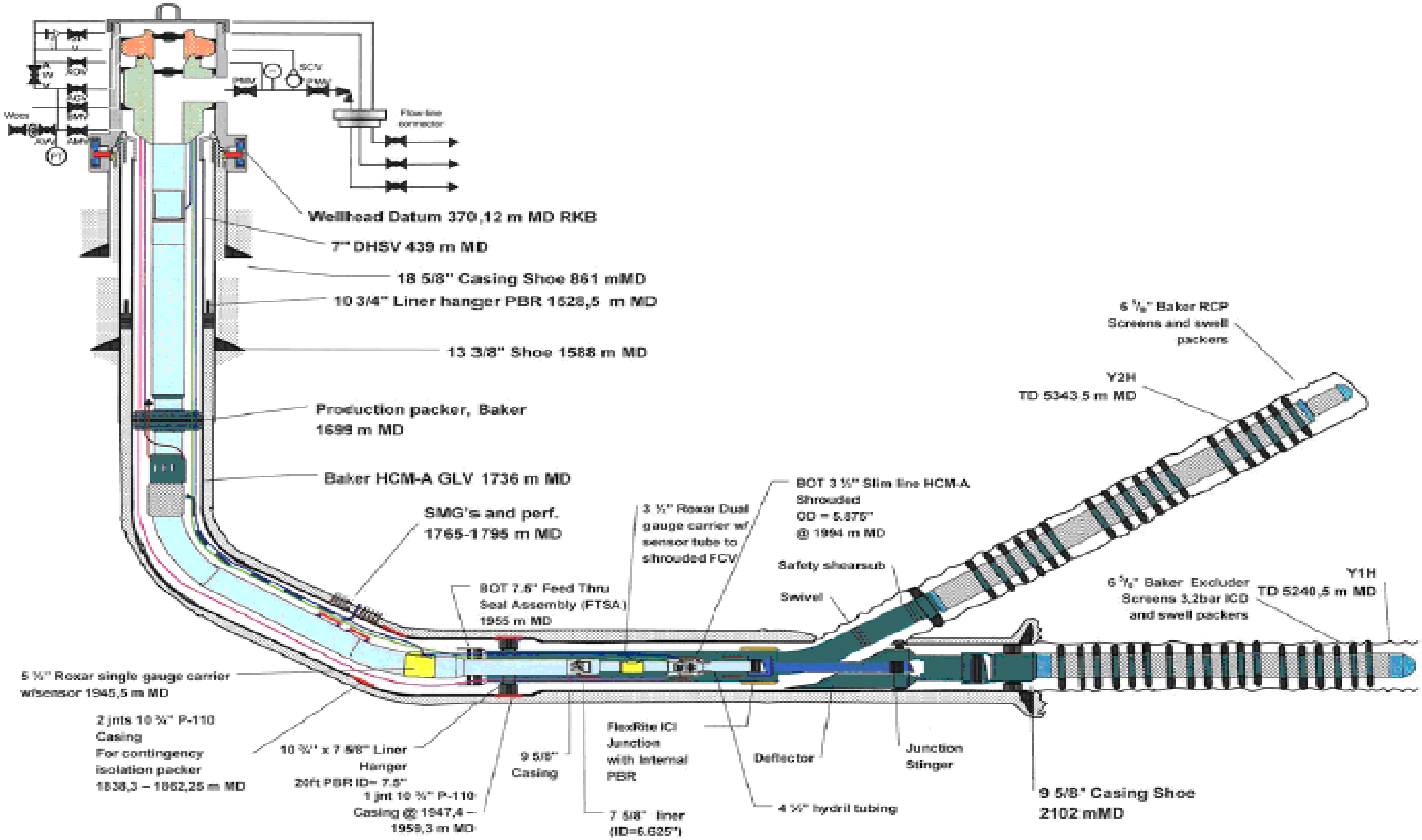

Figure 9: Completion diagram Well X BY1H/BY2H [11].

4. Relevant Equipment

4.1. Background for Selection of Tools

This well is producing from a loose sand reservoir [9] so the relevant sections are completed with sand screens in order to hold back the formation. A sand screen is defined by ExproBase [13] as *"A special tubular section assembled as part of the completion string with the filter component build up around a base pipe with holes"*. There are inflow control devices mounted at the end of the joints. This is to avoid possible coning effects or too early gas break-through (GBT) due to uneven flow distribution in the horizontal branches. Installing these devices give the possibility of controlling the inflow, creating a more evenly distributed flow and mitigating or reducing the possible problems [9], [13]. Integrating the device into a screen base without holes ensures that all the fluid passes through the filter along the OD of the pipe. This way it is forced to move through the manually regulated valve before entering the tubing.

The ability to manage gas at Troll C is limited, so to optimize the production of oil one has to take into account the gas handling capacity. It is therefore beneficial to implement a device that will restrict or choke the inflow of gas without limiting the flow of oil. The two branches of Well X are completed with different inflow control technologies; BY1H is equipped with 200 3,2 bar ICD valves, while 216 RCP valves are found in BY2H [14], [15].

4.2. Inflow Control Device (ICD)[1]

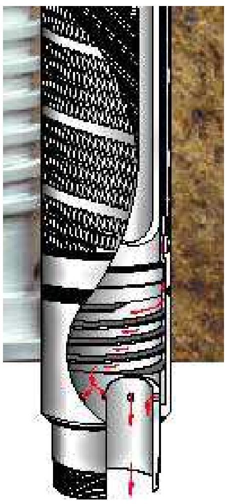

In branch BY1H, a Baker developed spiral type ICD valve called the "Equilizer" is used. Compared to conventional sand control completions it has been proven to yield a higher volumetric recovery of oil in wells with long horizontal sections. This is because it balances the inflow better. The principle of the valve with flowing direction is shown in Figure 10 to the left.

Figure 10: Equalizer ICD screen [1].

It has been observed that the longer the section of the well completed with ICD is, the smoother the well can be operated with respect to GOR control. Another experience is that the wells with short intervals with ICD valves are very sensitive to changes in choke position. This may give instabilities in the production network, making the wells are more demanding to operate. It is also verified through radioactive tracer technology that the ICDs have a positive effect in the clean up phase. Due to the functionality of the ICD, the flow in the lowermost section of the well (also called the toe) is assisted.

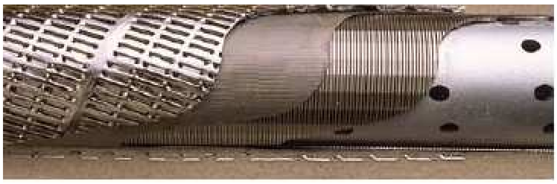

Figure 11: Premium screen used in the Troll field [1].

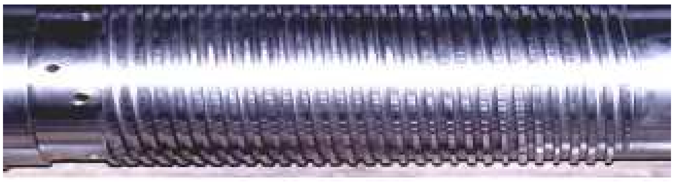

Figure 12: Helical flow channel inflow control device [1].

Baker has developed a general equation for calculating the “Equilizer” ICD performance for various designs, according to the following equation:

$$\Delta P = a \cdot \left[\frac{\mu}{\mu_w}\right]^w \cdot \left[\frac{\rho}{\rho_w}\right]^w \cdot Q + b \cdot \left[\frac{\mu}{\mu_w}\right]^y \cdot \left[\frac{\rho}{\rho_w}\right]^z \cdot [[Q]]^2 \quad \text{...(1)}$$

This was developed from the general equation (x)

$$\Delta P = \tilde{a} \cdot Q + \tilde{b} \cdot [Q]^2 \quad \text{...(2)}$$

The subscript w refers to the properties of water at standard conditions. Q must also be given at standard (ST) conditions. This equation is continuous in the mathematical sense and is suitable Table 7:

ICD Design	a	b	w	x	y	z
0.2	0,001454	0,0000728	0,843	-1,372	0,336	-3,45
0.4	0,002902	0,0001309	0,843	-1,372	0,336	-3,45
0.8	0,003454	0,0003621	0,843	-1,372	0,336	-3,45
1.6	0,006903	0,0006775	0,843	-1,372	0,336	-3,45
3.2	0,011023	0,0014561	0,843	-1,372	0,336	-3,45

Table 7: Coefficients and exponents Baker.

Baker states that it is important to note that the ICD design nomenclature (i.e. 0,2) refers to the pressure drop [bar] of the valves at the original design flow rate with the original design fluid properties. For other applications, the name is just an indication of flow resistance. For example, a 3,2 ICD design has approximately twice the flow resistance of a 1,6.

Statoil ASA have based on the theoretical performance for the "Equilizer" developed an equation for various designs with the input parameters given at actual downhole conditions. This is the equation that will be used in this thesis:

$$\Delta P = \left(\frac{\rho_{cal}}{\rho_{mix}} \cdot \frac{\mu_{mix}}{\mu_{cal}}\right)^{1/4} \cdot \frac{\rho_{mix}}{\rho_{cal}} \cdot a_{ICD} \cdot Q^2 \quad \text{...(3)}$$

The relevant parameters for the 3,2 ICD at downhole conditions on Troll are listed in Table 8:

Variable	**Value**
a_{ICD} [bar/(Rm³/d)²]	$3,46 \cdot 10^{-3}$
ρ_{cal} [kg/m³]	1000,3
μ_{cal} [cP]	1,45

Table 8: User defined variables for ICD.

4.3. Rate Controlled Production (RCP)

The RCP valve is an autonomous inflow control device (AICD) that Statoil ASA has developed. It ensures a more uniform inflow along a wellbore in addition to choke the gas and presumably the water more compared to oil compared to conventional inflow control devices [14]. The principal of the RCP is shown in Figure 13.

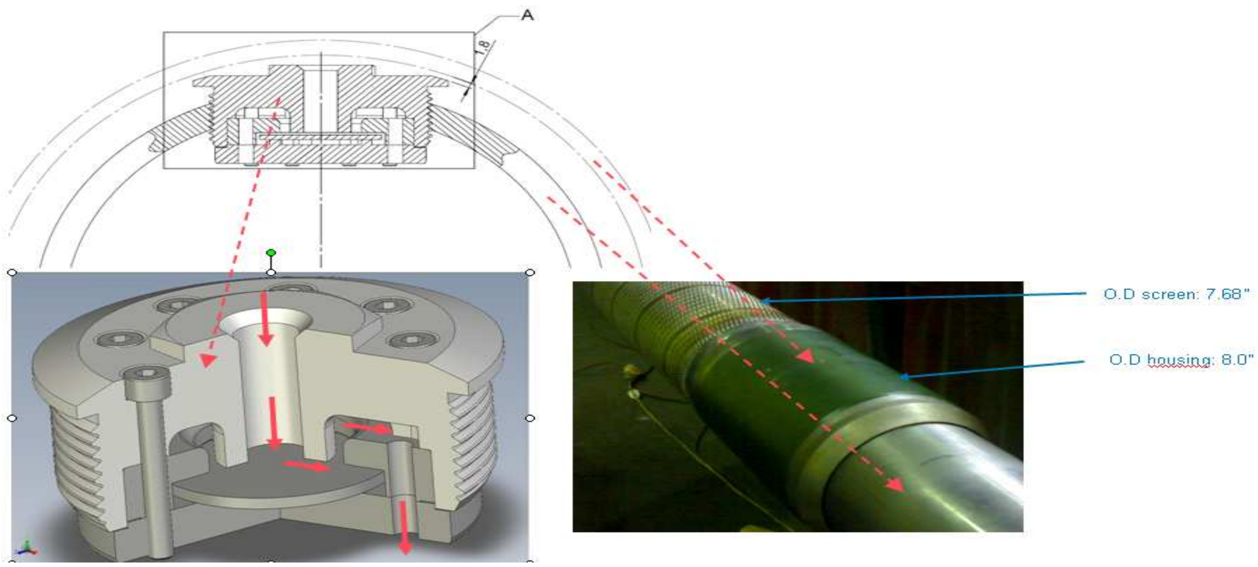

Figure 13: The principle of RCP [2].

The reservoir fluids will go through a screen to a housing where the RCP valve is located, via an annulus and an end-ring. The screen is shown to the right in Figure 13. The valve is integrated in such a way that the fluid must pass through it before entering the tubing [2], shown to the left in Figure 13.

Since oil and gas have different viscosities the flow velocities through the valve will be different and so will the stagnation pressures be. This becomes apparent in the Bernoulli equation for fluid flow along a streamline presented with respect to the stagnation point (the point at which the fluid is at rest, hence the velocity is zero):

$$P_0 = P_1 + \frac{1}{2} \cdot \rho \cdot u^2 \quad \text{...} (4)$$

This states that the stagnation pressure (P_0) is the sum of the static pressure and the dynamic pressure at a point further upstream. [17]. Since the gas has a lower viscosity the stagnation pressure will be lower and less gas is let through the valve [2]. This principle is shown in Figure 14.

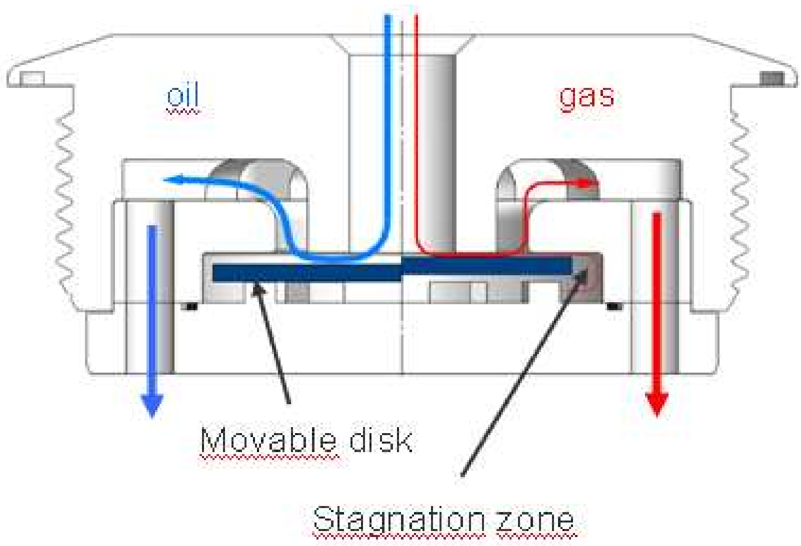

Figure 14: Integration of the RCP valve into the Baker screen [2].

A model for the differential pressure across the valve was developed from experiments performed in 2006-2008, and suggests that it is a function of fluid mixture parameters and volume flow as shown in equation (5).

$$\Delta P = f(\rho, \mu) \cdot a_{AICD} \cdot Q_{AICD}^{x} \quad \text{...} (5)$$

The x represents a user-input constant exponent found in Table 9.

The following function is proposed when it comes to the analytic function of the mixture density and viscosity;

$$f(\rho, \mu) = \left(\frac{\rho_{mix}^2}{\rho_{cal}}\right) \cdot \left(\frac{\mu_{cal}}{\mu_{mix}}\right)^y \quad \text{(6)}$$

The y represents a user input constant found in Table 9.

The mixture density and viscosity are defined as the sum of the local values of the phases obtained from the PVT data in Appendix B

$$\rho_{mix} = \alpha_{oil} \cdot \rho_{oil} + \alpha_{water} \cdot \rho_{water} + \alpha_{gas} \cdot \rho_{gas} \quad \text{(7)}$$

$$\mu_{mix} = \alpha_{oil} \cdot \mu_{oil} + \alpha_{water} \cdot \mu_{water} + \alpha_{gas} \cdot \mu_{gas} \quad \text{(8)}$$

The relevant values are found in Table 9 below:

Variable	**Value**
a_{AICD}	$1{,}0 \cdot 10^{-6}$
x	4,0
ρ_{cal} [kg/m^3]	890
μ_{cal} [cP]	1,75
y	0,2

Table 9: Troll RCP characteristics [14].

RCPs with different designs will have different functions.

Plotting the pressure drop curves with the specified user variables representative for Troll together with experimental data one can see the quality of the formulas in use. In Figure 15 it appears that the equation (x) underestimates the actual water production rate for pressure drops below 6 bars. Otherwise the experimental data fit well with the functions developed for each of the three phases.

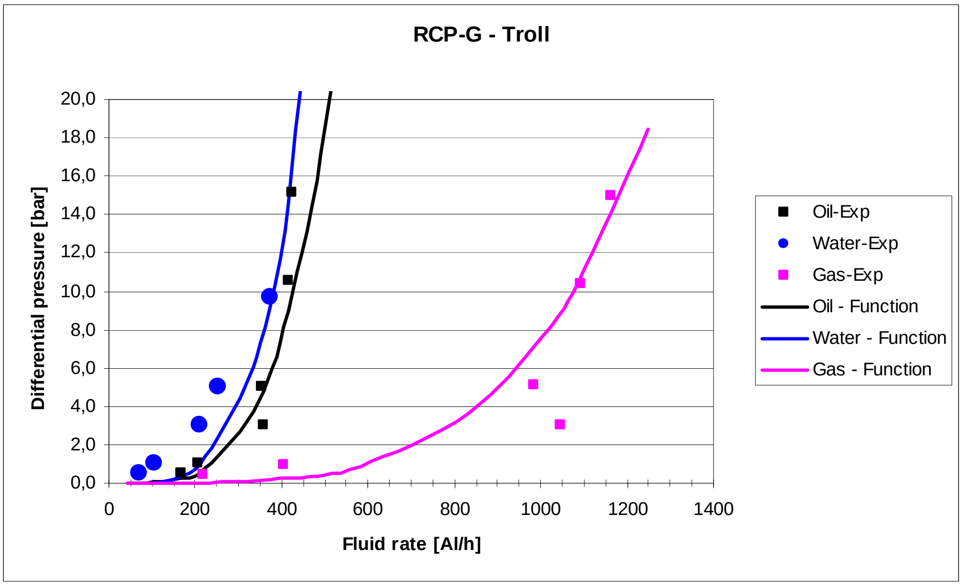

Figure 15: Functions for the different fluids through a RCP valve [2].

Well tests performed in another well completed with RCP valves, located in the same area as Well X, *indicate* that the valves operate within the given specifications. Still, an early GBT and high rates made it difficult to conclude on the effect of the valves in that particular well.

4.4. RCP vs. ICD

To be able to compare the performance of RCP and ICD, it is favourable that [3]:

- The branches have comparable lengths
- The branches are drilled in similar sands

Table 10 below gives the relevant parameters showing that Well X is a qualified candidate for testing the RCP vs. the ICD.

Branch	Horizontal length [m]	Target sand
BY1H	3170	C-sand
BY2H	3370	C-sand

Table 10: Ssimilarity between the two branches [11].

Earlier simulations imply an increase in reserves with RCP valves instead of ICD valves in branch BY2H. This is illustrated in Figure 16 where the red line represent production with RCP inflow technology and the black line represent production with ICD.

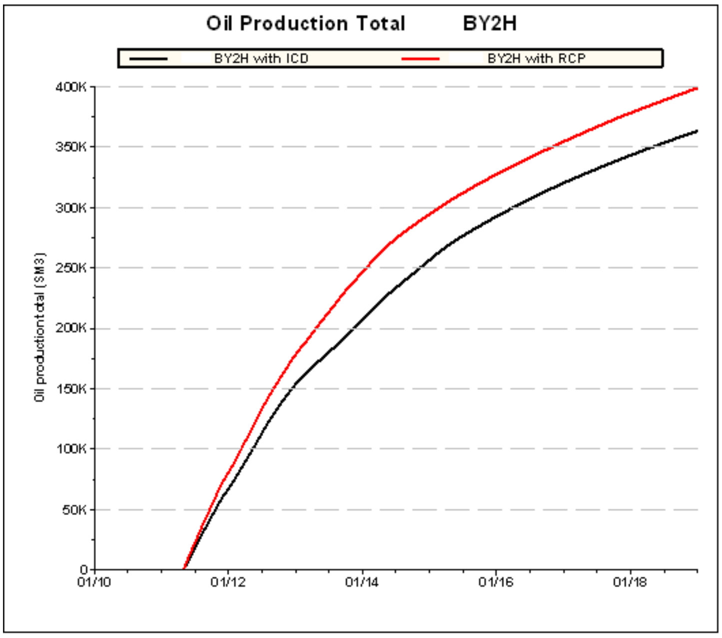

Figure 16: RCP vs. ICD valve [3].

Pressure drop curves for the two valve technologies may be developed from the relevant PVT data given in Appendix B and the equations for the respective valve presented earlier in this chapter. These are seen in Figure 17:

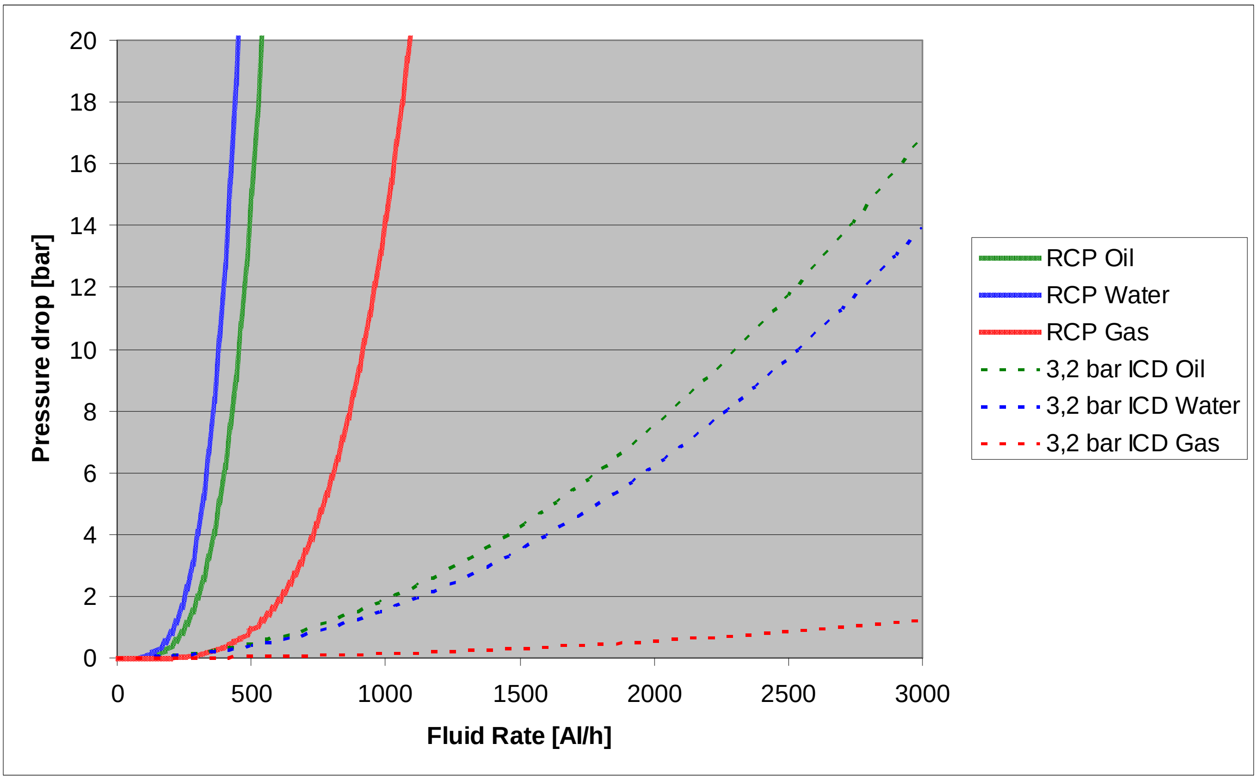

Figure 17: Pressure drop curves at 139 bar and 68 °C ICD and RCP.

Figure 17 shows that for all given pressure drops the actual downhole liquid rates are higher when making use of an ICD valve compared to a RCP valve. Unfortunately for the purpose of this well, we see that the ICD valve also will produce large amounts of gas for small pressure drops.

There are no production logging tools (PLT) available on either of the two branches considered in this thesis, but it has been run on ICD wells on Grane. The calculation method of pressure drop through the valve and the inflow profile modelling implemented was then verified [1].

4.5. Calculation of Number of Valves Filled With Fluid

For the performance of the valves to be in accordance with the theoretical characteristics the minimum gas and liquid filled valves should be less than total number of valves installed. This can be investigated by rearranging Equation (3) for ICD and Equation (5) for RCP to be solved with respect to Q, and solving it with the respective ÄP calculated for each test. Number of valves filled with gas and liquid are found by dividing flow rate from test by obtained flow rate for valves. The gas rate must also be corrected for downhole conditions.

$$\textbf{No of valves with gas} = \frac{Q_{gas,test}}{\left(\frac{Q_{gas,valve}}{B_g}\right)} \quad \ldots\ldots\ldots\ldots\ldots\ldots\ldots\ldots\ldots\ldots\ldots \textbf{(9)}$$

$$\textbf{No of valves with liquid} = \frac{Q_{liquid,test}}{Q_{liquid,test}} \quad \ldots\ldots\ldots\ldots\ldots\ldots\ldots\ldots\ldots\ldots\ldots \textbf{(10)}$$

The outcome of this analysis is given in Chapter 10.

4.6. Other Relevant Equipment [11]

4.6.1. Flow Control Valves

The well is also equipped with one shrouded flow control valve (S-FCV) in BY1H and one FCV in BY2H. They are operated in accordance with applied pressure control signals, typically 30-330 bars measured at wellhead (WH), and they only move when pressure is applied. Since they are run on dual lines (separate), one must be ventilated if the other one is pressurized. There exist 14 steps/positions for both of the valves, referring to 5 unique opening areas including closed and fully open. The opening areas in percent refer to the smallest area of the FCV, with a diameter of 2.75 in.

Position	**Opening area [%]**	**Flow area [m^2]**
1	Closed	0,0000
2	100	0,0038
3	2	0,0001
4	100	0,0038
5	5	0,0002
6	100	0,0038
7	Closed	0,0000
8	100	0,0038
9	27,1	0,0010
10	100	0,0038
11	27,1	0,0010
12	100	0,0038
13	27,1	0,0010
14	100	0,0038

Table 11: Opening area [%] for the S-FCV BY1H.

Position	**Opening area [%]**	**Flow area [m^2]**
1	Closed	0,0000
2	100	0,0038
3	27	0,0010
4	100	0,0038
5	27	0,0010
6	100	0,0038
7	27	0,0010
8	100	0,0038
9	2	0,0001
10	100	0,0038
11	5	0,0002
12	100	0,0038
13	Closed	0,0000
14	100	0,0038

Table 12: Opening area [%] for the FCV BY2H.

5. Production Well Testing

5.1. What Why, and How

OilGasGlossary.com defines a production test as a test of the well's producing potential, which is the maximum volume of HC that can be extracted at a given pressure [18].

The reasons for performing a well test is that we are looking for some information about the oil, gas and water flow that can aid in making decisions regarding the surveillance of the well. Information that may be obtained in relation to these tests is [19]:

- Productivity or injectivity
- Permeability and potential well damage
- Composition and features of the reservoir fluid by taking samples

Periodical testing provides allocated rates of the reservoir fluids. It can also contribute in the update of reservoir simulations. Different types of tests are performed in different types of wells at various frequencies. What is common for them all is that the results can play a role in ensuring optimal well productivity and integrity [20].

5.1.1. Test Separators

In a test the produced fluid is sent to a pressure container at surface that is called the test separator. It is defined by the Schlumberger Oilfield Glossary [21] as: *"a vessel used to separate and meter relatively small quantities of oil and gas. Test separators can be two-phase or three-phase, or horizontal, vertical or spherical. They can also be permanent or portable."* The liquid phases are measured by turbines whereas the gas phase is measured by an orifice meter. As the three phases are recombined, the fluid can be further analyzed [23].

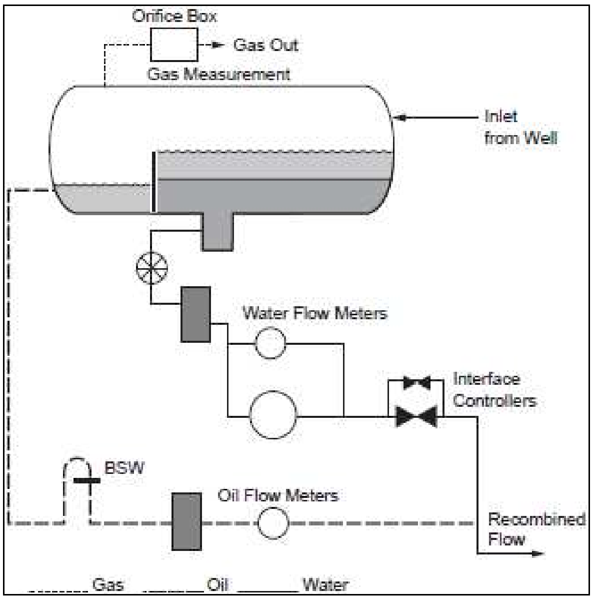

Figure 18: A typical test separator [22].

If there are any problems with e.g. sand or slugging, this may also be detected in a well test procedure. When the main process is not running, the equipment may be used to produce fuel gas for power generation [23].

5.2. Well Testing Program for Troll Well X BY1H/BY2H[11], [26]

There are two types of tests being executed in Well X:

1. **Well test:** The well that shall be tested is routed in on the test separator. The well pressure (well condition) is maintained as equal as possible as the well is producing to 1. step separator. This is in order to have the well production representative to the real production conditions.
2. **Deduction test**: The difference between two test lines are the basis for this test, valid for a well or branch that is closed in the time period between the two tests. In Well X a pressure is measured in BY2H when both branches are open. Then BY1H is closed, and the well is choked to obtain a pressure in BY2H equal to when both lines were producing. It is now assumed that BY2H is producing at same conditions as in the first test. Then the result for BY1H will be the total result for both lines subtracted the result for BY2H.

When performing a test the water cut is measured by the 6 in. water rate meter and the fluid rate is fixed to 3000 Sm^3/d. The rest results are gathered as the well produce at a steady state for 12 hours. If for some reason (e.g. maintenance) the 6 in. is unavailable, the 2 in. meter must be used. This requires a fluid flow rate below 70 Sm^3/t. When this is obtained and the WC is known, a single test of BY1H is performed in accordance with the test program given in Table 13 below:

Position number of S-FCV in BY1H	**Position number of FCV in BY2H**	**Branches open**	**Max. fluid rate [Sm^3/t]**	**Time (steady state production) [h]**
2	14	BY1H+BY2H	3000	12
2 [3]	1	BY1H	N/A	12
2	2	BY1H+BY2H	N/A [4]	12

Table 13: Well production test program.

When the well tests are performed the FCVs are fully open and the measured pressure does not have to be corrected. See Chapter 4.6 for explanation of FCV positions.

[3] DHP BY1H must equal previous test in order to obtain a deduction test of BY2H.
[4] Rate is determined after test is completed.

From the beginning of production on the 1st of October 2010 until the 15th of June 2011 there have been performed 15 tests. Three of these tests are deduction tests of BY1H. One of the tests with commingled production does not have a measured water flow rate, and is discarded in the NETool analysis performed later in this thesis. The other values obtained from this particular test, such as GOR, are still considered representative in order to investigate the trend of the well.

	Commingled production	**Single BY1H**	**Single BY2H**
Tests performed	8	4	4
Model match	1	1	1
Model control	6	3 [5]	3

Table 14: Number of different tests performed and used for NETool model matching and control.

[5] These tests are deduction tests.

6. Pressure Drop Evaluations

6.1. Introduction

During the production process, the pressure of the HC is reduced in several steps from initial reservoir pressure to atmospheric pressure.

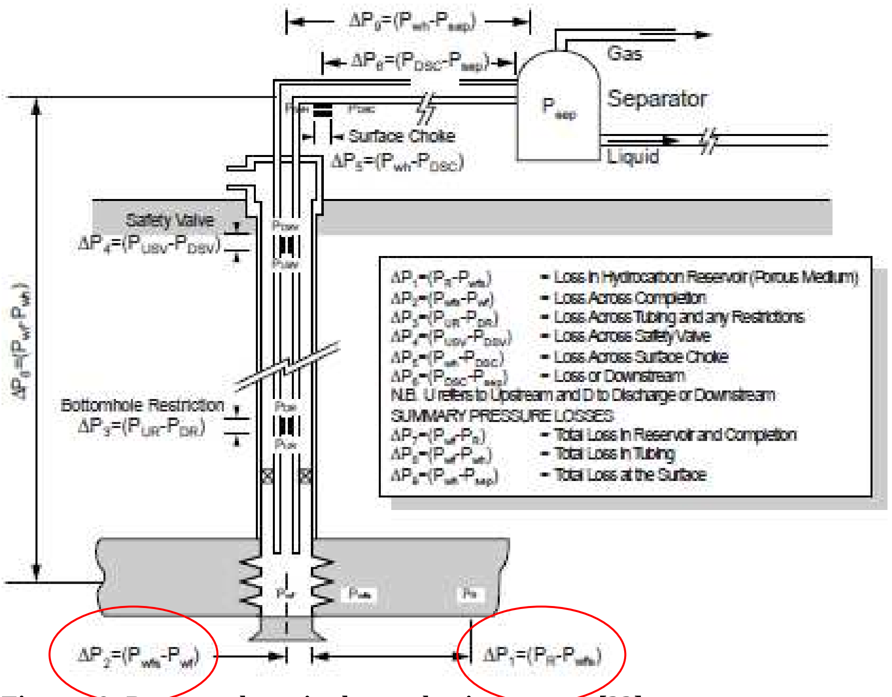

Figure 19: Pressure drops in the production process [22].

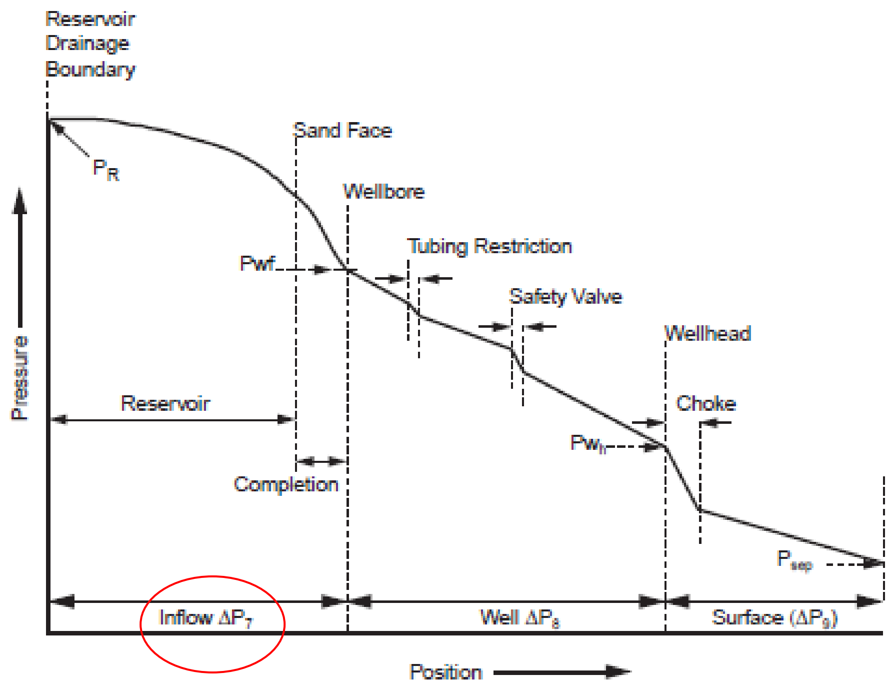

Figure 20: Pressure drops in the production process [22].

In this thesis the relevant parts of the production process are when the HC enters the wellbore through the reservoir and as it goes through the inflow control devices located in each branch, marked in red in Figure 19 and Figure 20 above. Since the gauges are not positioned at the top of the first screen in each well, there is a pressure drop due to friction over the length of the pipe in addition to a pressure drop due to height difference. This is the total pressure measured in a well test, and the factors will be evaluated one by one.

The pressure at top of the first screen [bar] is then given as:

$$P_{top\ screen} = P_{test} + \Delta P_F + \Delta P_{PE} \quad \text{..........}(11)$$

Then for each branch we have:

$$\text{Drawdown} = \Delta P = (SIP - P_{top\ screen}) = SIP - \Delta P_{fm} - \Delta P_c = \frac{Q_{liquid}}{PI} - P_c \quad \text{.....}(12)$$

As for the pressure on top of the first screen, the SIP must also be adjusted for the vertical distance from the gauge. Since there is no flow when the branch is shut in, the frictional pressure drop is not considered.

6.2. Frictional Pressure Drop ΔP_F [22]

Since the top of the first screen in both branches and the gauges are not at the same location of the well, there is a frictional pressure drop present over this distance that must be considered. The Fanning equation (13) is utilized:

$$\Delta P_F = \frac{f_m \cdot \rho_{mix} \cdot u^2 \cdot L}{2D} \quad \text{..........}(13)$$

The Moody friction factor, f_m, depends on the flow regime which is determined by calculating the Reynolds number (Re).

$$Re = \frac{\rho \cdot u \cdot D}{\mu} \quad \text{..........}(14)$$

Re < 2000 → laminar flow, indicating that the frictional pressure drop is proportional to the fluid velocity and inversely proportional to Re but independent of pipe roughness:

$$f_m = \frac{64}{Re} \qquad \text{……(15)}$$

Re > 2000 → turbulent flow, the frictional pressure drop is very sensitive to both the Reynolds number and the exact condition of the inner pipe wall. It has been shown that the important parameter is the relative roughness ε/D of the pipe. The Chen equation (Chen, “An explicit equation for friction factors in pipes”, Ind. Eng. Chem. Fund., 18, p296, 1979) is one alternative for the determination of the friction factor in this flow regime.

$$\frac{1}{\sqrt{f_m}} = -4 \cdot \log\left[\frac{\varepsilon}{3},71065 - 5,\frac{0452}{Re} \cdot \log\left(\varepsilon^1,\frac{098}{2},8257 + \left\{7,\frac{149}{Re}\right\}^0,8981\right)\right] \qquad \text{.(16)}$$

Assuming a three phase flow (oil, water and gas), the velocity, the density and the viscosity must be calculated in accordance with mixing rules. ρ_{mix} and μ_{mix} are calculated from Equations (7) and (8). u_{mix} is given as below:

$$u_{mix} = \frac{Q_o}{A} + \frac{Q_w}{A} + \frac{Q_g}{A} \qquad \text{……(17)}$$

Where

$$A = \frac{\pi \cdot ID^2}{4} \qquad \text{……(18)}$$

The roughness of the pipe is set according to the value presented in [22], given in Table 15 below:

Material	**Roughness**
Plastic pipe or coating	0,0
New tubing	0,00005
Dirty well tubing	0,00075

Table 15: Typical pipe roughness values.

6.3. Pressure Drop Due To Change in Potential Energy (ΔP_{PE})

$$\Delta P_{PE} = \rho \cdot g \cdot \Delta Z \qquad \text{……(19)}$$

Branch	Top first screen TVD [m]	ΔZ single gauge [m]	ΔZ dual gauge [m]
BY1H	1584	Not relevant	26,5
BY2H	1585	31	27,5

Table 16: Height difference between top screen and gauge.

Distance to top first screen is calculated in Completion String Design using the TVD calculator.

To estimate the pressure drop across sandface, the productivity index (PI) must be determined and used together with corrected well test pressures as discussed in the previous sections. Subtracting the sandface results from the total drawdown gives the pressure drop across the valves in accordance with Equation (12).

6.4. PI Calculations

In a naturally producing well it is the differential pressure between the reservoir and the wellbore that drives the fluids into the well, often referred to as the drawdown. It is often controlled by chokes, and it delimits the production rates [27]. The RCPs in BY2H and the ICDs in BY1H have thin function in Well X.

Schlumberger's Oilfield Glossary [28] defines the PI as *"a mathematical means of expressing the ability of a reservoir to deliver fluids to the wellbore. The PI is usually stated as the volume delivered pr. psi of drawdown at the sandface (bbl/d/psi)"*. The general steady state (SS) and pseudo-steady state (PSS) formulas for PI are given as Equation (20).

$$PI = \frac{\dot{Q}}{P_R - P_{wf}} = \frac{\kappa h}{B\mu\left(\ln\left[\frac{r_e}{r_w} + S\right]\right)} \qquad (20)$$

In this thesis the productivity computations called Cases 1-4, developed by Leif Larsen and modified by Faram Ahmadhadi for Statoil ASA [23], are developed from the Goode and Kuchuk [23] formulas for inflow performance evaluation.

The main result is a PSS PI based on a set of well parameters that are included in the following formula:

$$PI = \frac{\dot{Q}}{(P_{av} - P_{wf})} = \frac{\kappa \cdot h}{18.66 \cdot B \cdot \mu \cdot PIDrec} \qquad (21)$$

Here P_{av} represents the average pressure within rectangle and PIDrec is the symbol for a modified version of the earlier mentioned Goode and Kuchuk's dimensionless drawdown function for horizontal wells [23]. These calculations assume production with pressure depletion at stable conditions which is proven valid for this well in Chapter 9.

The relevant input parameters for both branches are given in Table 17:

Input variable	**BY1H**	**BY2H**
h [m]	100	100
r_w [m]	0,10795	0,10795
L_p [m]	2809,5	2333
0/1	0	0
θ [deg]	90	90
z_w [m]	50	50
s_d	1	1
x_e [m]	5600	5600
y_e [m]	2000	2000
x_w [m]	2809,5	2333
y_w [m]	1000	1000
κ_H [mD]	5915	5232
κ_V/κ_H ratio	0,60	0,60
B [Rm^3/Sm^3]	1,14	1,14
μ [cP]	2,07	2,07

Table 17: Input parameters in PI calculations.

Figures 21 and 22 show how some of the variables concerning the geometry of the well are defined:

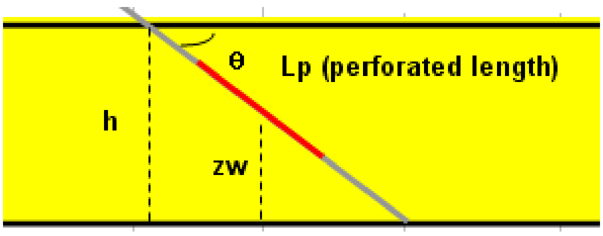

Figure 21: Well schematic.

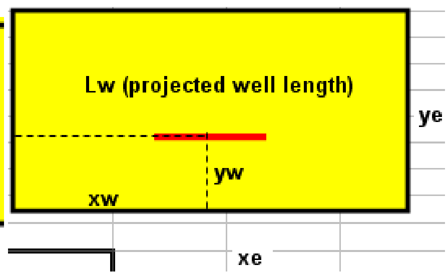

Figure 22: Reservoir schematic.

0/1 denominates a flag used to turn off/on a direct shape factor (Dietz) based on an algorithm for short wells. It is needed for (effectively) extremely short wells, and triggered automatically in the calculation spread sheet for wells with effectively small deviations.

If desired, skin can be estimated from Hawkins' formula (22):

$$s_d = \left(\frac{k'}{k_d} - 1\right) \cdot \ln\left(\frac{r_d}{r_w}\right) \quad \text{......}(22)$$

6.5. Pressure Drop Across Sandface and Inflow Control Completion (ΔP_{fm} and ΔP_c)

When determining the pressure drop across sandface by using flow rates from well tests, the reference level must be the same for all pressures. Table 16 is referred to for the corrections of ΔZ between top screen and the gauges. The SIP must also be corrected with respect to this, but the depletion of the reservoir must also be considered for this parameter. The pressure drops can now be evaluated for Equation 12.

7. NETool Simulations

7.1. Building the Model

The model is based on the first three well tests ever performed; one well test and two single tests, one of each branch. They are found in Table 18. The emphasis is placed on matching the liquid flow rates for the purpose of this thesis. There are many different assumptions to be made on the various parameters in the program, but only the best fit will be accentuated here. If relevant, the others will also be presented together with the reason why it was not successfully implemented.

7.1.1. Test Values Simulated

The following table shows the tests that are attempted to be matched in the simulator. All relevant pressures are exported from a tag on the well in question in Aspen Process Explorer.

Parameter	**Test 1**	**Test 2**	**Test 3**
Start [dd.mm.yy]	02.10.10	03.10.10	04.10.10
Stop [dd.mm.yy]	03.10.10	03.10.10	04.10.10
Q_{oil}[Sm^3/d]	1603,1	852,1	1253,6
Q_{water}[Sm^3/d]	1670,2	1325,0	714,9
Q_{gas}[Sm^3/d]	174696	48840	70164
Q_{liquid} [Sm^3/d]	3273,3	2177,0	1968,5
GOR	109	57,3	56
Water cut [%]	51	60,9	36,3
Valve opening (open = 100 %)	Y1 open Y2 open	Y1 open Y2 closed	Y1 closed Y2 open
DHG (Y1 + Y2) [bar]	131,244	132,611	127,511
DHG Y1 [bar]	134,959	131,791	135,083
DHG Y2 [bar]	133,613	135,558	129,172

Table 18: Relevant parameters from well tests chosen for making of a NETool model.

7.1.2. The Reservoir Model

The Eclipse res. model used as basis was updated early 2011, and the restart file is simulating 7578 days after 01.01.1990 – that is 01.10.2010 which is at production start up.

There is an interval between approximately 3900 and 4100 m MD that lacks information. It is assumed to be a fault here.

7.1.3. Specifications and Assumptions in the Program

- The well is a producer
- All three phases are present; oil, gas and water
- Hydrostatic pressure
- Homogeneous pressure drop in tubing and annulus
- PI calculations based on a semi-steady state model (Appendix C).
- The relevant variables related to this are set in accordance with the theoretical PI calculations performed in Chapter 6.4:
  - *Horizontal PI*
    Res. thickness: 100 m
    Res. width: 2000 m
    Res length: 5600 m
    Depth position of well: 50 m
    Width position of well: 1000 m
    Length position of well: 2600 m
- Precision of calculations: 0,001
- Stability: 1,0
- The flow may change direction in:
  - Tubing
  - Annulus
  - Annulus-tubing
  - Reservoir-tubing
- Well pressure limits: 100-160 bar
- Improved momentum balance
- Max Mach number: 0,9
- Bernoulli for diameter variations is almost precise
- Multilateral junction type is tubing → tubing
- Transition flow regime at Reynolds number lower than 2000
- Boundary condition
  - Bottom hole pressure (BHP) = given bottom hole pressure at top node
  - Total liquid rate

The last parameter above is very important because it sets the premises for the results of the simulations. Originally the BHP was used. Knowing that the top node in the simulator is set at the position of the dual gauge, the combined pressure denoted as

DHG (Y1 + Y2) was used. The simulations were also performed with the total liquid rate obtained in the tests as the boundary condition. The results are presented in the following chapter and further discussed in Chapter 10.

7.1.4. Segment Setting/Completion

The trajectory of the well is set to be divided into 12 meter long segments. One node is assigned to each segment in order to simulate one joint pr. segment. By default, the first segment is set to be a cemented blank pipe. Following, the rest of the well is completed with the relevant type of valves, packers and blank pipes with corresponding dimensions in accordance with the tally [14], [15]. See Appendices E and F for segment divisions implemented in simulator.

In Figure 23 and Figure 24 below the packers are coloured red, grey indicates blank pipes and blue indicates the ICD and RCP valves in BY1H and BY2H respectively.

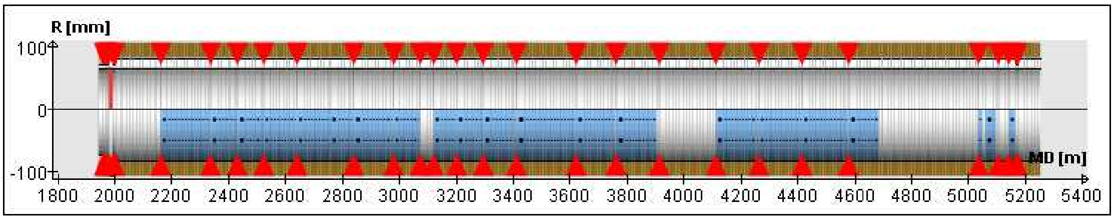

Figure 23: Completion in BY1H.

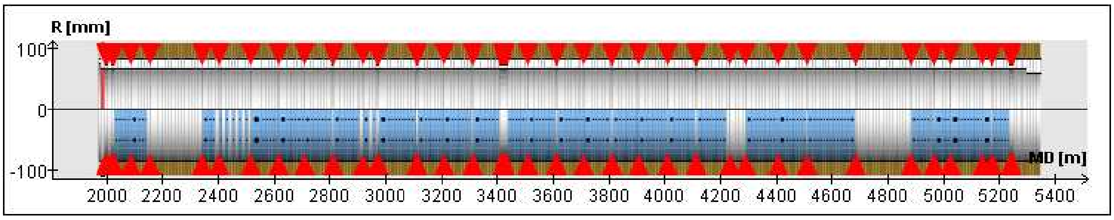

Figure 24: Completion in BY2H.

The mainbore (BY1H) is set to start at 1550 m TVD MSL since the single gauge is set at approximately 1554 m TVD MSL. The beginning of the well, also called the heel, is set to simulate the dual gauge. The positioning of the lateral (BY2H) is in accordance with this. It should be mentioned that in order to perform the simulations the two branches are not allowed to have the same starting point, explaining why BY2H is set to start at the next measured trajectory point after 1550 m TVD MSL in Appendix F.

We know that the well is located approximately 0,5 meters above the OWC (see Figure 29 and Figure 30 in the following pages), and this is not obtained in the NETool simulator when using the values presented above. Since the grid in the reservoir model has a vertical distance of 2 meters, the trajectory for both branches are moved the same distance (2 m.) in order to have a better placement of the well. The distance to the OWC is reduced but still larger than 0,5 m as seen in Figure 25 and Figure 26 below. The part of the model without information as mentioned in paragraph 7.1.2. is visible in the first of these Figures.

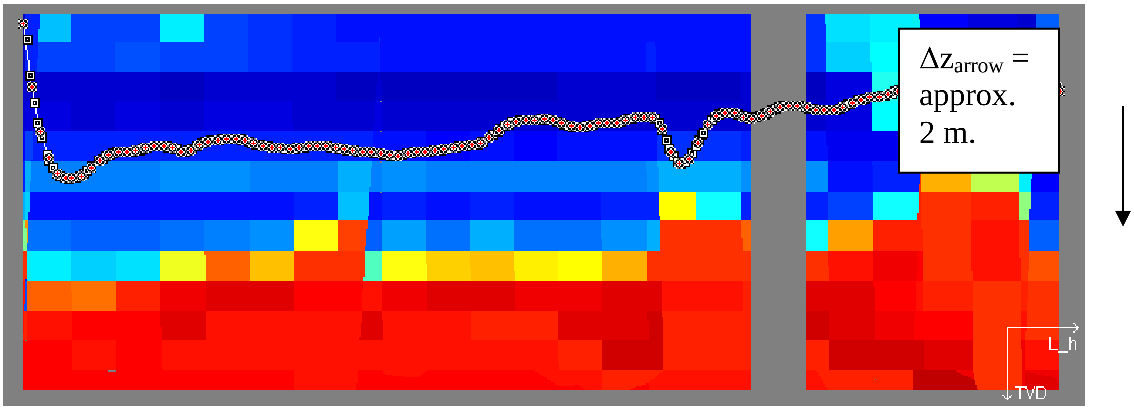

Figure 25: The positioning of BY1H in relation to the water saturation. More red represents higher water saturation.

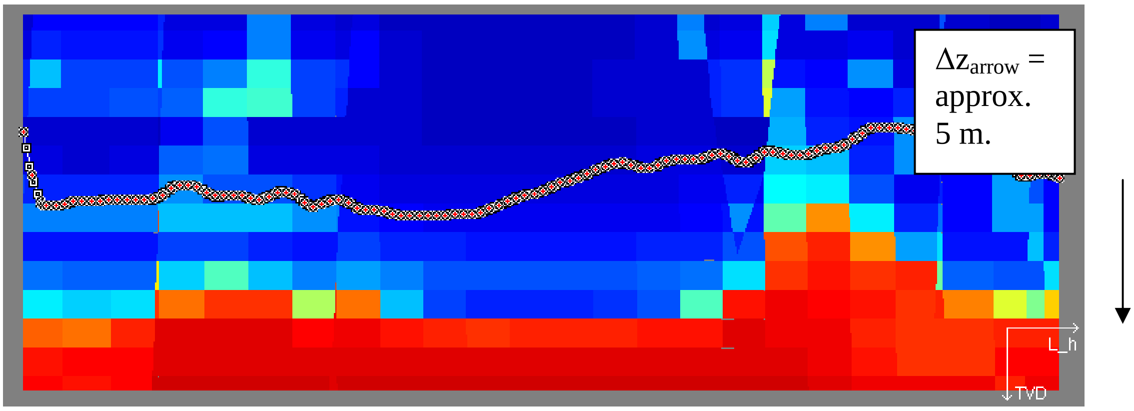

Figure 26: The positioning of BY2H in relation to the water saturation. More red represents higher water saturation.

In NETool the first possible position where the two branches may combine is at 1971 m MD MSL (1553,1 m TVD MSL). Assuming the given value in [14] to be correct (2013 m MD RKB and 1585 m TVD MSL), this is accepted.

For simulations of single tests, a tubing plug/choke is set at the same position in both branches. It is placed close to where the two branches combine, at 1980 m MD MSL (1556 m TVD MSL). It is set to have an annulus, since the experience within the Troll production technology suggests at least some flow present here. If the valves are 100 % open in both branches the well is producing fully from both of them. Closing it in BY1H simulates a single test performed in BY2H and vice versa.

7.1.5. Reservoir Parameters

Transmissibility

The best fit found in this thesis is a transmissibility obtained from the PI model, with a transmissibility multiplier of factor 0,1. This corresponds to a sensitivity of 10 mD and implies that the PI model overestimates the values obtained in the tests. More on the meaning of this parameter is found in Appendix D.

Permeability

The horizontal permeability values are imported from open hole logs, and the values implemented in NETool are found in Appendix G and H. Segments with undesirable or incorrect figures were either removed completely or entered manually as the average between the segment directly before and after. The comparison between model and log is shown below for both branches. Having a closer look in these charts it is seen that the blue values obtained in the simulations are hidden behind the log values, making the two sets look different when in reality they fit well.

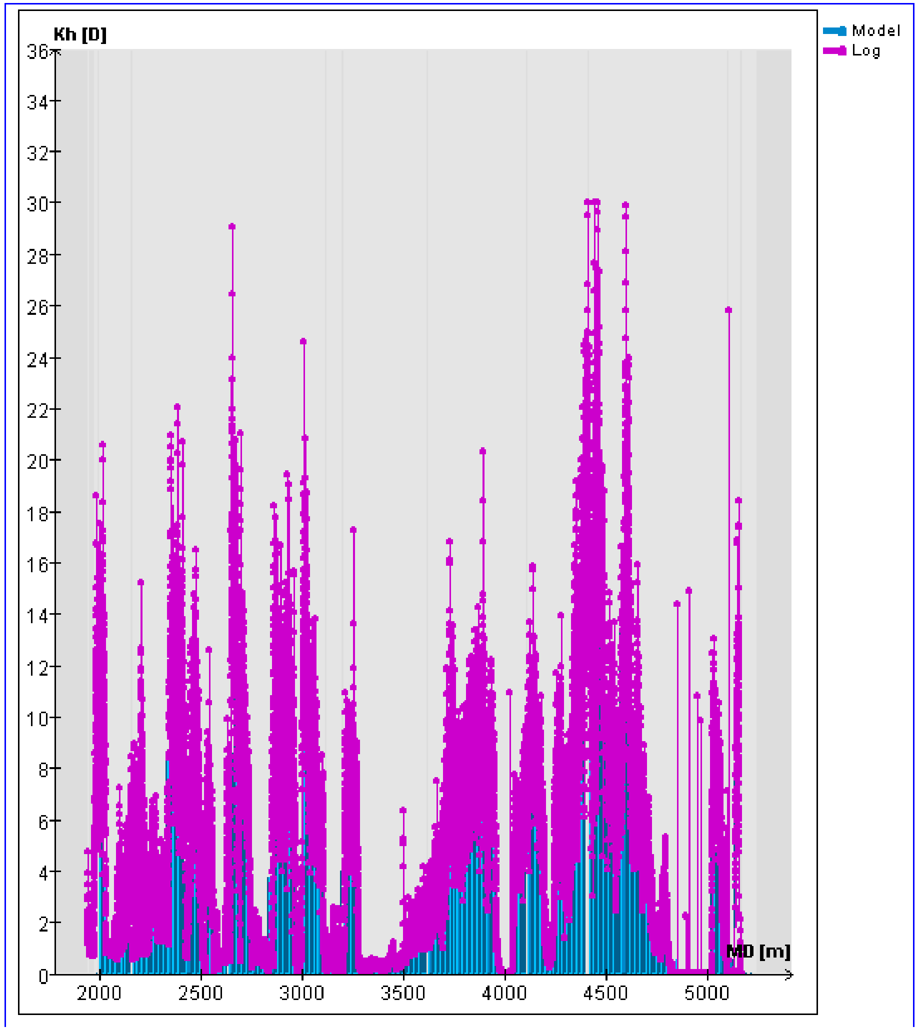

Figure 27: Comparison permeability data from log and model BY1H.

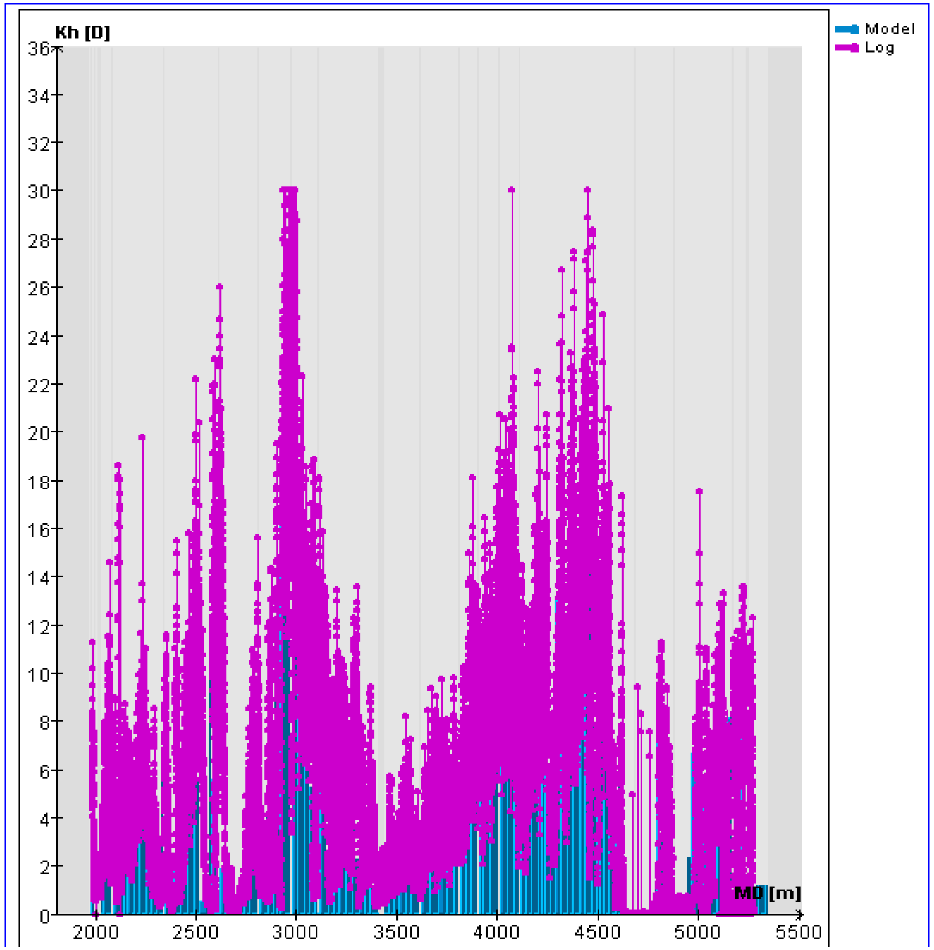

Figure 28: Comparison permeability data from log and model BY2H.

The ratio between horizontal and vertical permeability is assumed to be 0,6 based on experience within the Statoil ASA Troll production technology group.

Mobility

Since we for this well have logs for the water saturation (S_w), the flowing fraction definition is chosen and the relevant values are imported from Appendices I and J. Segments without values are set manually when considering Figure 29 for BY1H and Figure 30 for BY2H. The green line represents the well path while the blue, dotted line represents the OWC. The completion is also shown at the bottom of these Figures.

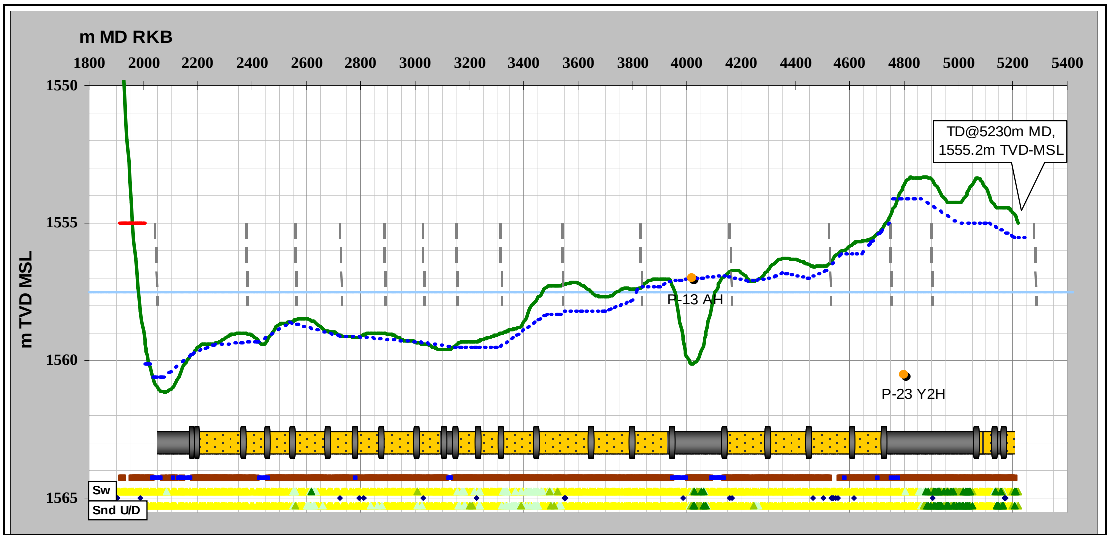

Figure 29: Basis for interpretation of water saturation in area without log for BY1H [30].

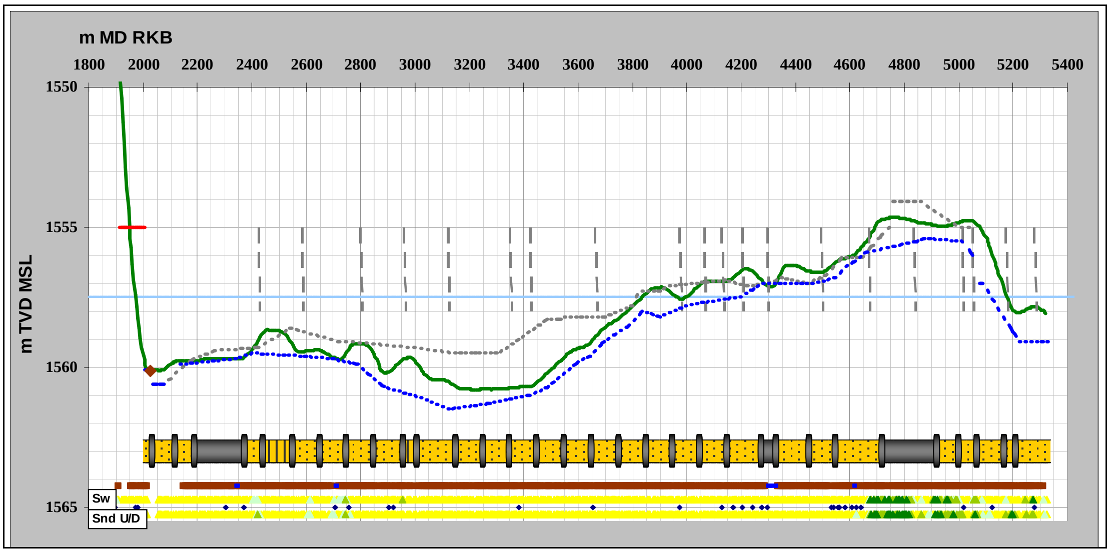

Figure 30: Basis for interpretation of water saturation in area without log for BY2H [31].

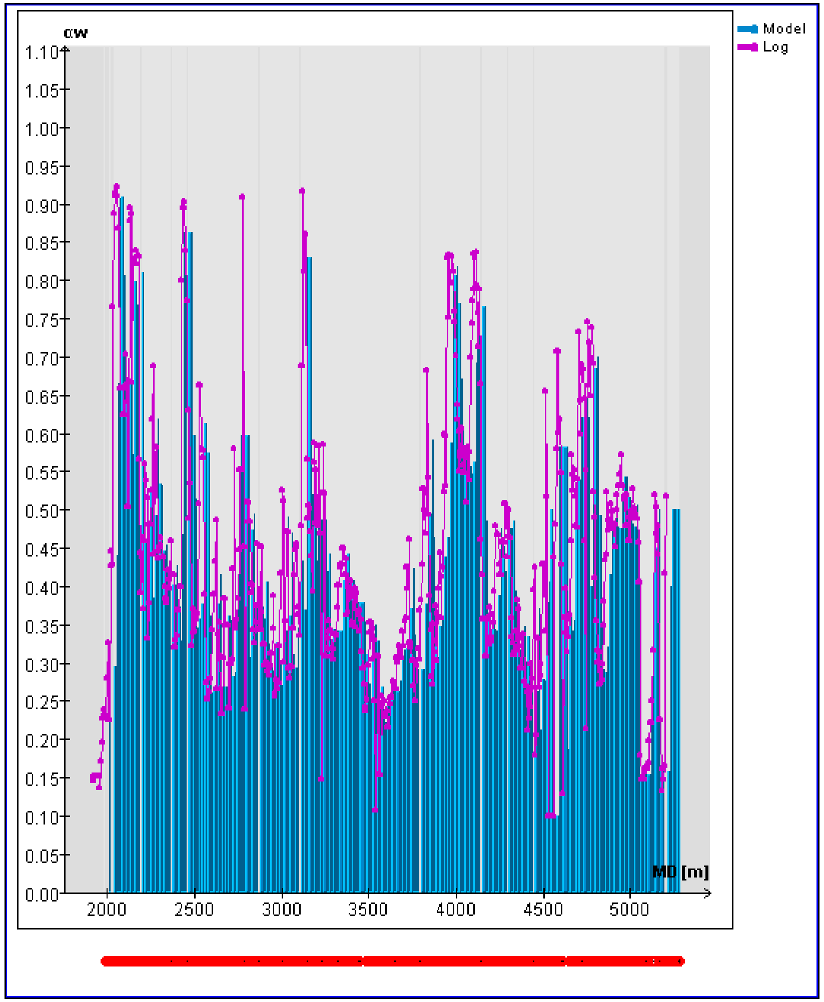

Figure 31: Comparison water saturation between model and log BY1H

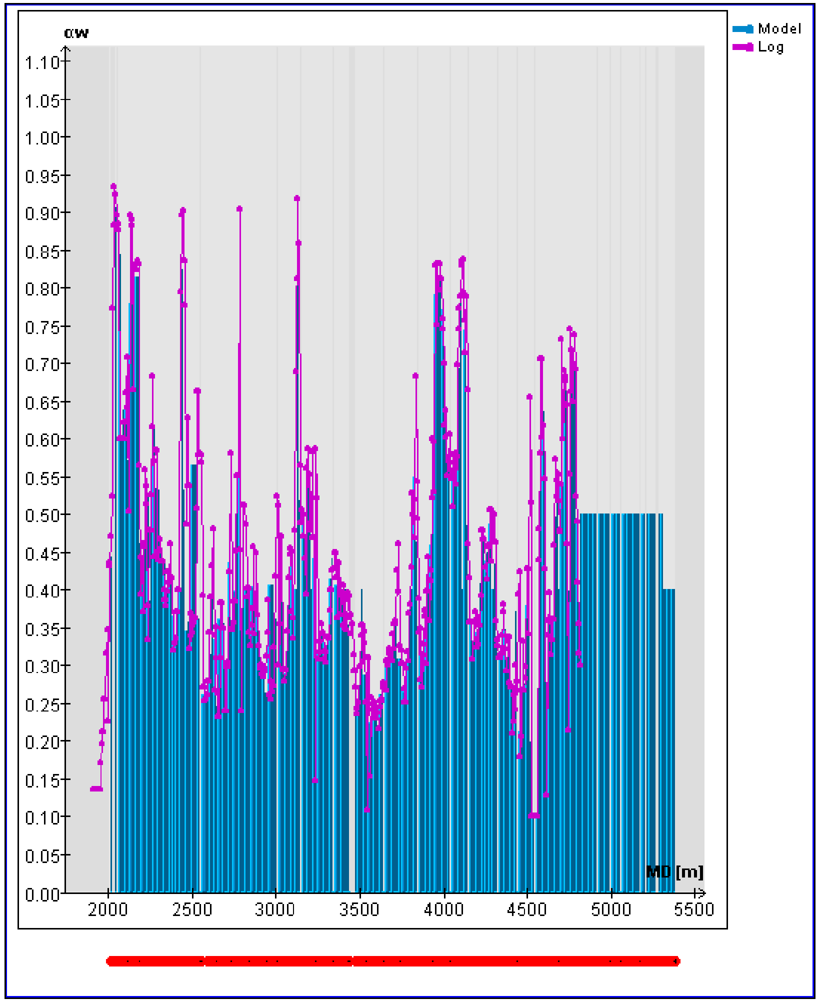

Figure 32: Comparison water saturation between model and log BY2H

We see from the PVT data in Appendix B that the solution GOR at assumed Troll conditions 68° C and 139 bar is 48 Sm^3/Sm^3. This could indicate that there in the first test may be some free gas in the well and that the gas fraction (S_g) should be considered, see Table 18. When considering the development in GOR of the commingled tests, it appears that the value obtained from the first test is not representative, and should instead be assumed to be somewhere close to 50 Sm^3/Sm^3. This conclusion sets the premises for the oil saturations (S_o), which are given as:

$$S_o = 1 - S_w - S_g = 1 - S_w \quad \textbf{(23)}$$

Advanced Settings

For both BY1H and BY2H the inner tubing roughness is set to 0,015 mm and the annular space roughness is set to 0, 15 mm by default.

8. NETool Model Analysis and Results

8.1. Quality of Model; How Accurate Is It?

There is some uncertainty linked to most of the considered variables in the model, so it is of interest to investigate how comparable the results are with test values.

8.1.1. Boundary condition: BHP

The simulation model found to best fit the data Table 18 giving the BHP as the boundary condition gives the following results:

Parameter	Simulation 1	Simulation 2	Simulation 3
BHP [bar]	131,244	132,611	127,511
Q_{liquid} [Sm^3/d]	3868,3	2228,1	1589,7
Q_{oil} [Sm^3/d]	2107,2	1213,9	871,5
Q_{water} [Sm^3/d]	1761,1	1014,2	718,2
WC [%]	45,5	45,5	45,2
Q_{gas}[Sm^3/d]	101135	58492,7	41475,2
GOR [Sm^3/Sm^3]	48	48,2	47,6

Table 19: NETool simulation results with boundary condition BHP.

In Table 19, Simulation 1 represents Test 1 in Table 18. Simulation 2 is the equivalent of Test 2, and Simulation 3 is based on test 3. Below are the deviations in Q_{liquid} for all three simulation runs compared to the test values:

Q_{liquid} production test [Sm^3/d]	Q_{liquid} simulation modell [Sm^3/d]	Deviation [%]
3273,3	3868,3	18,2
2177	2228,1	2,3
1968,5	1589,7	-19,2

Table 20: Difference in values of Q_{liquid} when using BHP as the boundary condition.

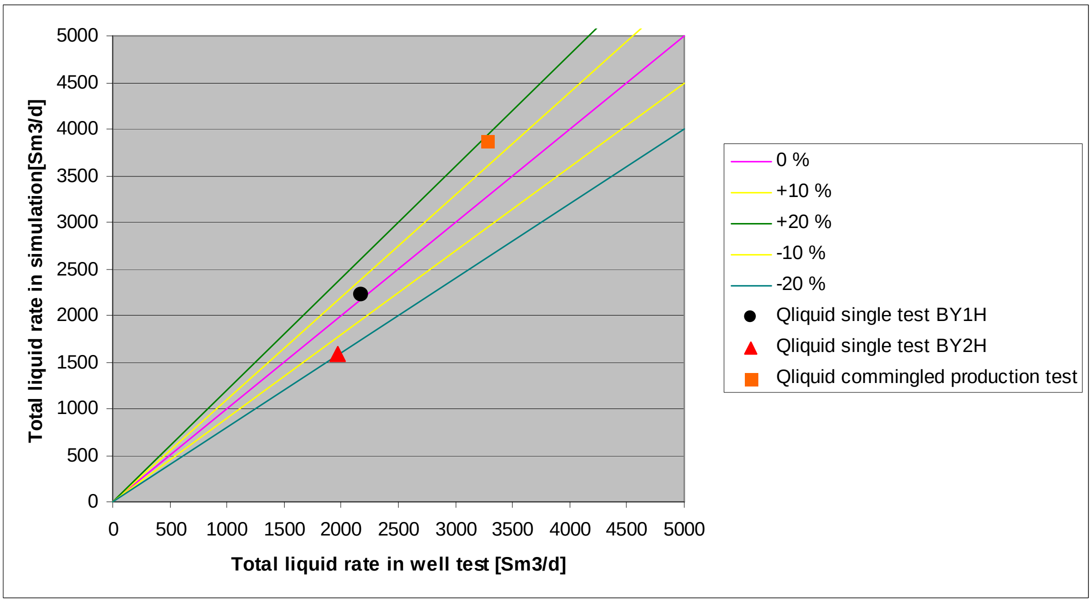

Figure 33: Discrepancy in simulated values compared to values from tests, BHP.

It is seen in Figure 33 that the developed model has a good fit when it comes to the simulation of the single test in BY1H, and for the other two tests the offset is approximately 20 %. Note that the commingled test has an overestimated total liquid rate while the single test of BY2H has a comparable underestimate of Q_{liquid}.

Pressure Sensitivity

It is of interest to investigate how sensitive the rates are to a change in BHP. Table 21 summarizes the new estimates of the relevant variables when lowering BHP by 1 bar:

Parameter	Simulation 1	Simulation 2	Simulation 3
Q_{liquid} [Sm^3/d]	4279,2	2539,8	1657,2
Q_{oil} [Sm^3/d]	2331,1	1368,6	908,8
Q_{water} [Sm^3/d]	1948,1	1171,2	748,4
Q_{gas}[Sm^3/d]	111888,6	67392,5	43248,6

Table 21: Discrepancies between NETool simulations and well test data for the relevant tests used in matching, BHP lowered 1 bar.

Table 22 shows the relative increase in flow rate when BHP is lowered 1 bar:

Parameter	Simulation 1	Simulation 2	Simulation 3
Increase Q_{liquid} [%]	10,6	14,0	4,2
Increase Q_{gas} [%]	10,6	15,2	4,3

Table 22: Percentage change in production rates when lowering BHP by 1 bar.

The results show that changing the pressures will give the largest percentage increase in production in the ICD branch, indicating that it has a larger PI than BY2H.

8.1.2. Boundary condition: Q_{liquid}

In Table 23 and 24 below are the outcomes of the simulations locked on Q_{liquid} and the discrepancies in BHP compared to the ones obtained in tests:

Parameter	**Simulation 1**	**Simulation 2**	**Simulation 3**
BHP [bar]	132,49	132,8	120,3
Q_{liquid} [Sm^3/d]	3273,37	2177	1968,64
Q_{oil} [Sm^3/d]	1780,9	1186,19	1081,68
Q_{water} [Sm^3/d]	1492,47	990,81	886,96
WC [%]	45,6	45,5	45,05
Q_{gas}[Sm^3/d]	85473,1	57158,9	51386,8
GOR [Sm^3/Sm^3]	48	48,2	47,5

Table 23: NETool simulation results with boundary condition Qliquid.

The difference between the measured pressure and that obtained from simulations with the total liquid rate as the boundary condition was also investigated:

BHP production test [bar]	**BHP simulation model [bar]**	**Deviation [%]**
131,244	132,49	0,9
132,611	132,8	0,1
127,511	120,3	-5,7

Table 24: Difference in values of BHP when using Qliquid as the boundary condition.

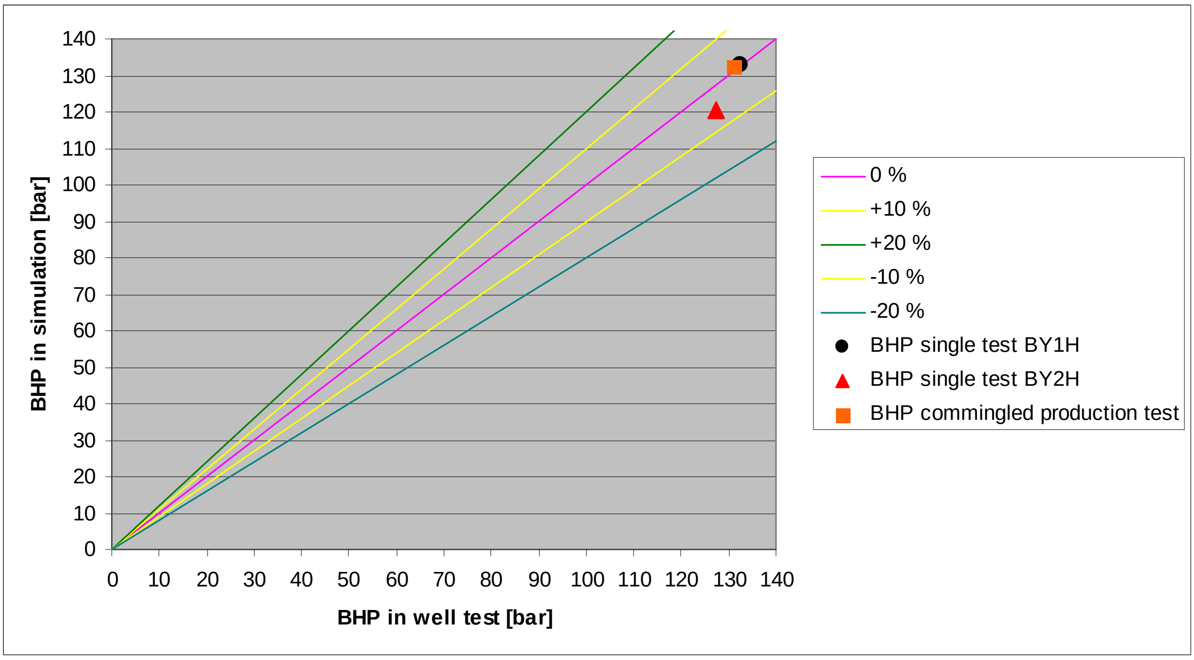

Figure 34: Discrepancy in simulated values compared to values from tests when using total liquid flow rate as the boundary condition.

For the commingled test and the single test of BY1H the deviation is less than 1 %, for the single test in BY2H the simulation underestimates the BHP with 5,7 %. This is seen in Figure 34.

It was not expected that the simulations performed with the two different boundary conditions would give unequal deviations. The discrepancies between model and test data are further considered in Chapter 10 and 11.

8.2. Commingled Production Results

A lot of information can be obtained from the simulations, but regarding the performance of the valves in each branch the relevant parameters to investigate are:

- Pressures and pressure differences
- Flow rates and influx
- WC

Factors like completion, permeability and saturation could have impact on these results, so having the Figures 23 and 24, 27 and 28 and 31 and 32 available was found to be beneficial for the interpretation.

8.2.1. Pressures in BY1H

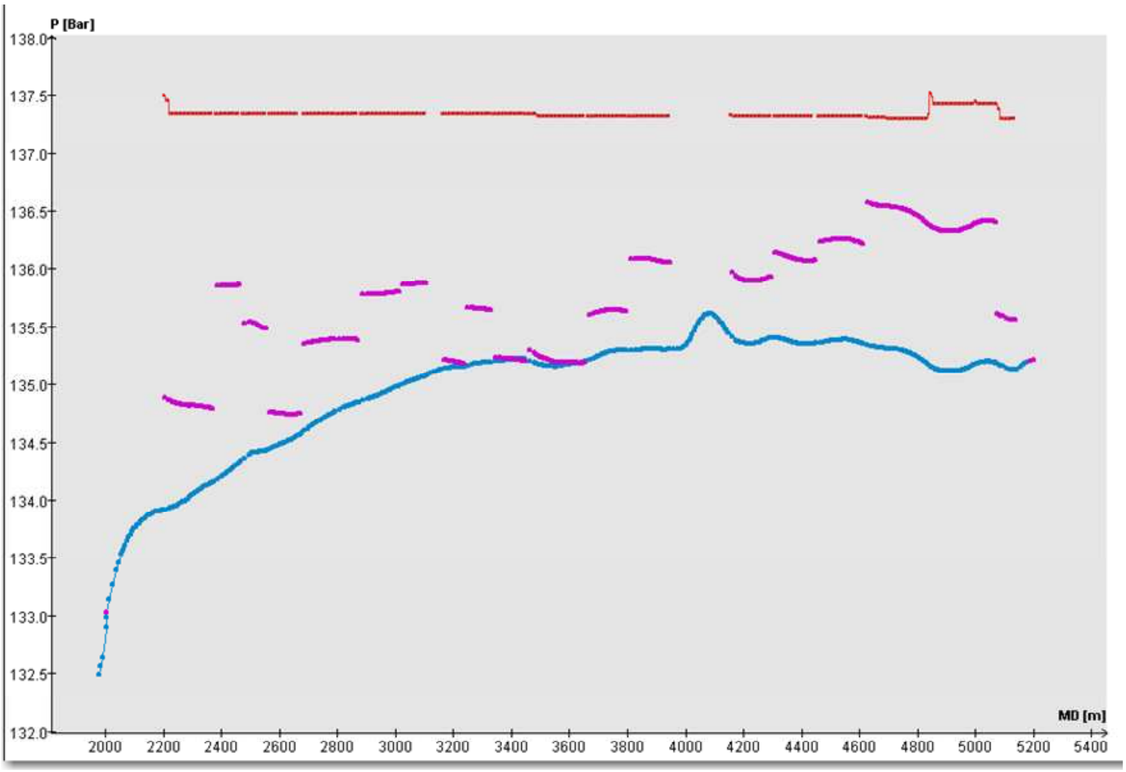

Figure 35: Different pressures in BY1H.

The red values represent the reservoir pressure, the pink are the annulus pressure and the blue give the tubing pressure. It is seen that the reservoir pressure stays fairly stable; the tubing pressure gradually decreases whereas the pressure in annulus varies a lot in comparison. The difference between the reservoir pressure and the tubing pressure is called the drawdown as discussed earlier. This is given in Figure 35 below:

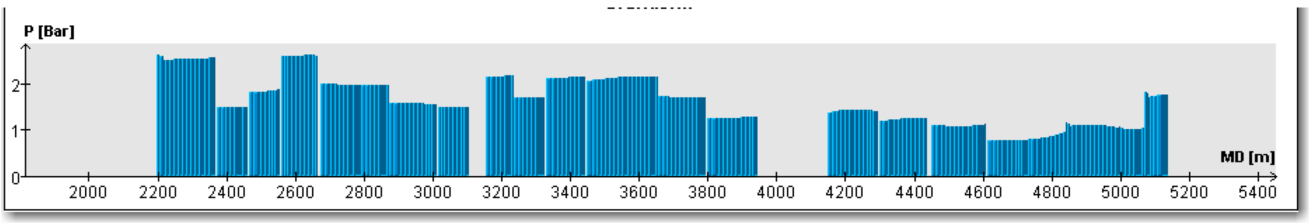

Figure 36: Drawdown in BY1H.

The drawdown in the well (Figure 36) is gradually higher towards the heel of the branch and it is also increased at the very tip of the toe. The latter is explained by a higher reservoir pressure in that area. This is a value imported from the Eclipse model. The intervals with no pressure difference are completed with blanks. Over the total length of the branch the drawdown appears to vary between 1 and 2,5 bar.

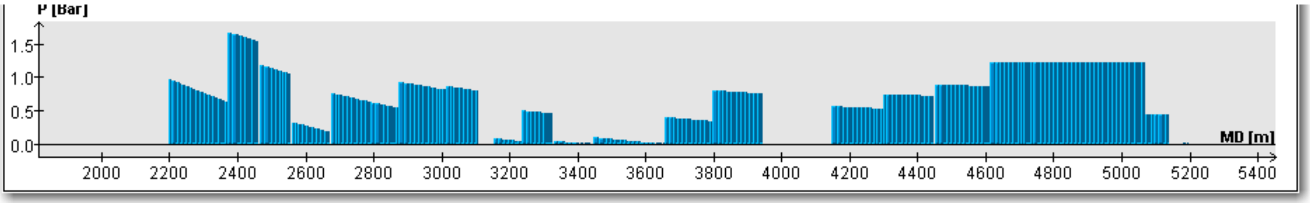

Figure 37: Pressure drop across completion in BY1H.

The pressure drop across the completion is very stable near the toe, before it varies in the mid section of the well until it is higher again near the heel. This is also where the highest values are seen. As in the previous discussion, the parts of the well completed with blank pipes will naturally not see any pressure drop across the completion. But this does not explain the low drawdown in the midsection of the well. Seen in Figure 28 the horizontal permeability is low here, giving results as expected with a low pressure drop across the completion compared to that across sandface.

8.2.2. Flow Rates in BY1H

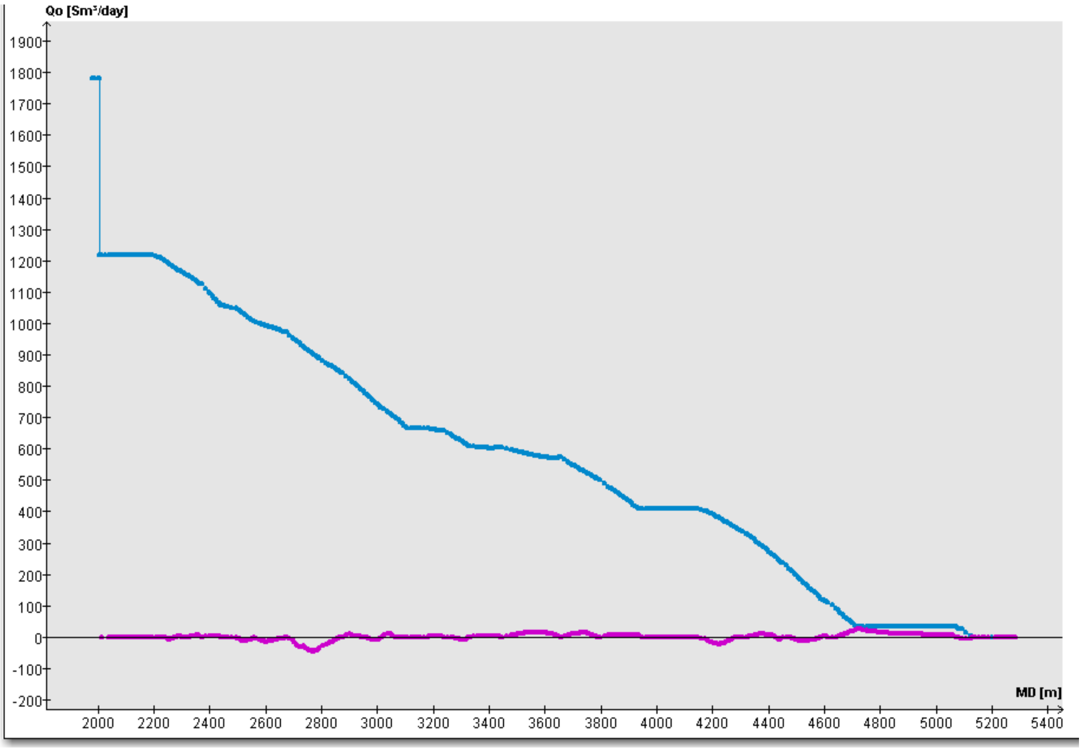

Figure 38: Cumulative oil flow rate in BY1H.

In Figure 38 there is hardly any production seen from the toe of the branch and approximately 400 meters towards the heel because this is a part completed with blank pipes. This is also valid for the interval between 2000 and 2200 m MD. The horizontal section between 3900 and 4100 m MD is explained by the incomplete res. model because of the fault. The sudden leap in flow rate at around 2000 m MD is caused by the contribution from BY2H as the production becomes commingled. The inflow of oil is lowest in the interval between 3000 and

3600 m MD which is a part of the producing length of the branch where the permeability is low.

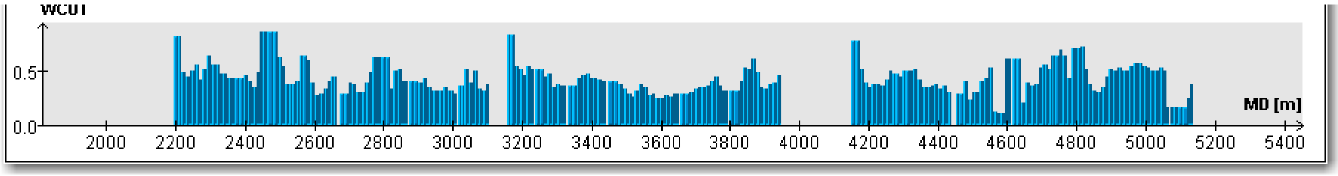

Figure 39: WC in BY1H.

Since the WC is seen to vary along the well from Figure 39 above, it is of interest to consider not only the oil but the total liquid (water and oil) flux from the reservoir.

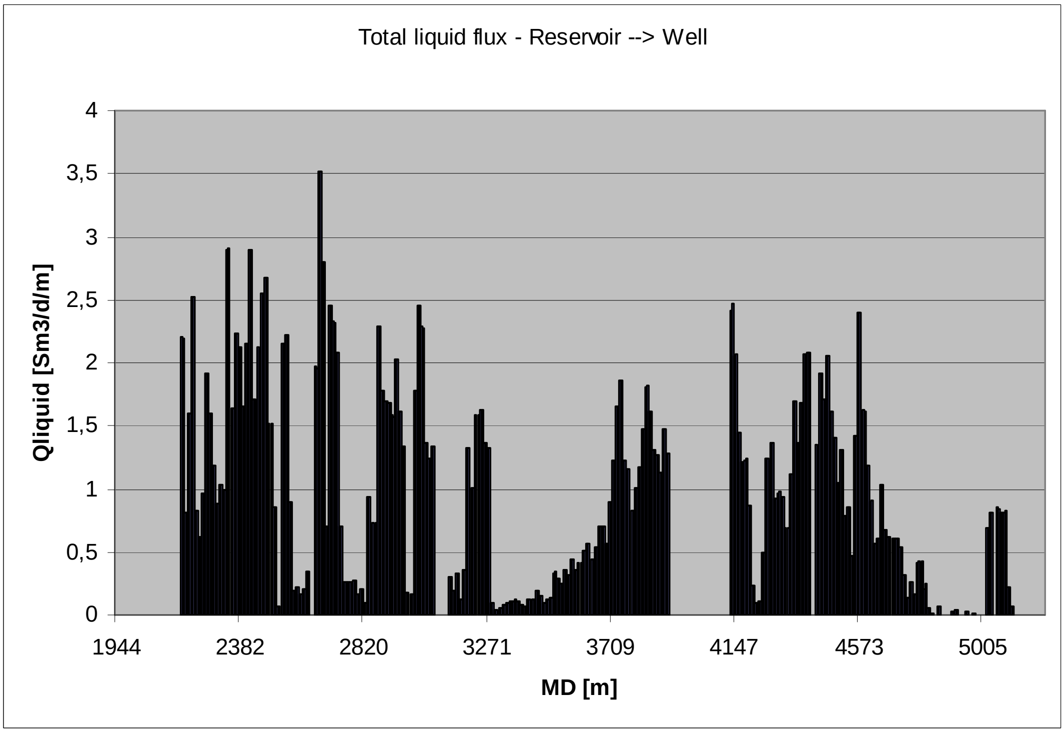

Figure 40: Total liquid flux into BY1H.

It is seen that the influx of liquid is highest closer to the heel of the branch. This is also the part with the highest WC. No influx is seen in areas with blank pipes, and the interval with lower permeability has less influx. The highest influx in Figure 40 is found to be 3,5 Sm^3/d/m near 2700 m MD.

8.2.3. Pressures in BY2H

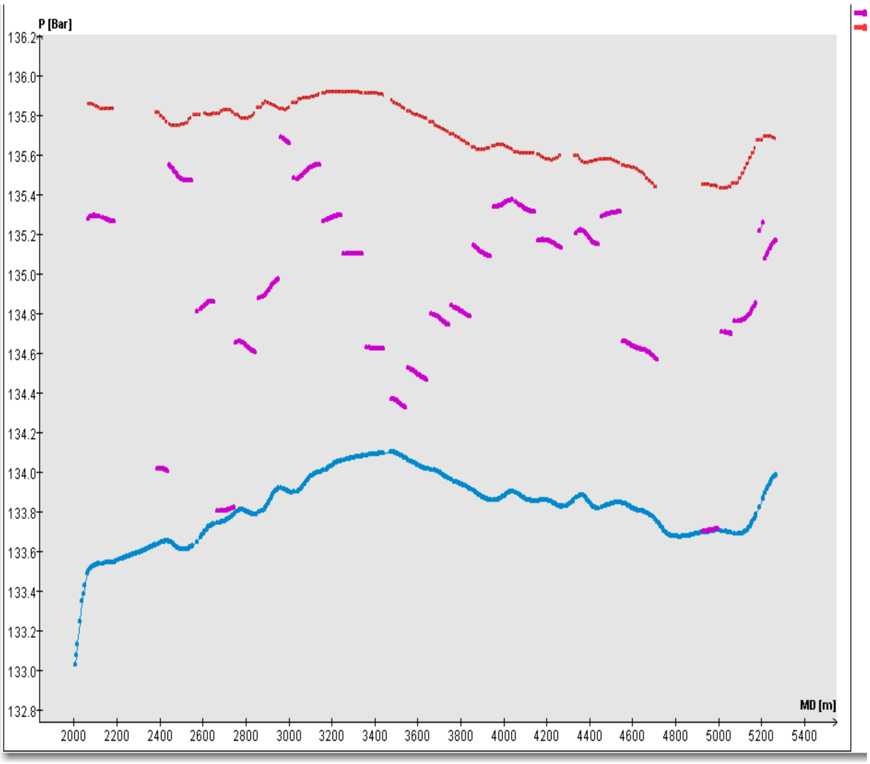

Figure 41: Different pressures in BY2H.

As for BY1H, in Figure 41 the red values represent the reservoir pressure, the pink are the annulus pressure and the blue give the tubing pressure. It is seen that the reservoir pressure varies more in this branch and so does the tubing pressure. It must be remembered that the reservoir pressure in this branch is not imported from the reservoir model, but calculated as the difference in hydrostatic oil column from the gauge. Especially in the middle section of the branch is the annulus pressure found to be low, and this is an area with low permeability.

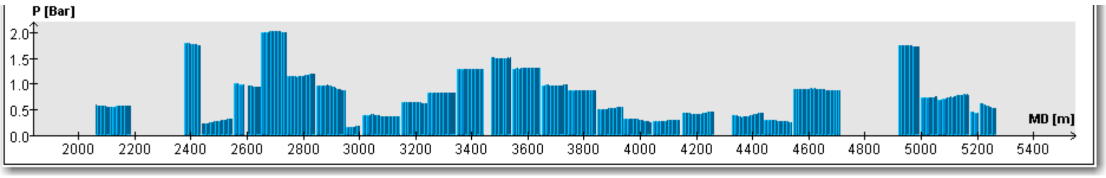

Figure 42: Drawdown in BY2H.

The drawdown seen in Figure 42 is very irregular. It is quite high in the toe section, it has a peak in the middle of the branch (3400 – 3600 m MD) and another top around 2400 m MD. This behaviour can be expected when considering the horizontal permeabilities.

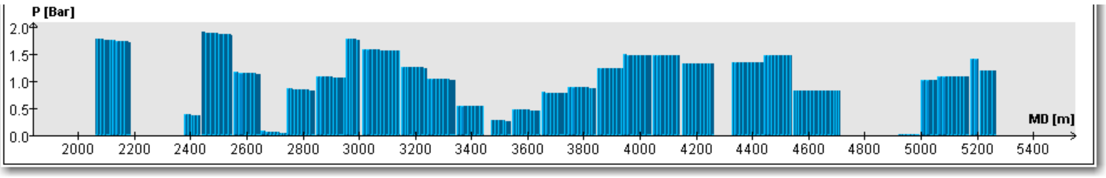

Figure 43: Pressure drop across completion in BY2H.

In the middle section of BY2H it is seen from the simulation that the pressure drop across the completion (Figure 43) has the opposite trend as the drawdown has in Figure 42 above. These results can be expected by the same argument as given for the drawdown. The variation between lowest and highest pressure drop in this branch is about 1,5 bar (from 0,5 to 2 bar).

8.2.4. Flow Rates in BY2H

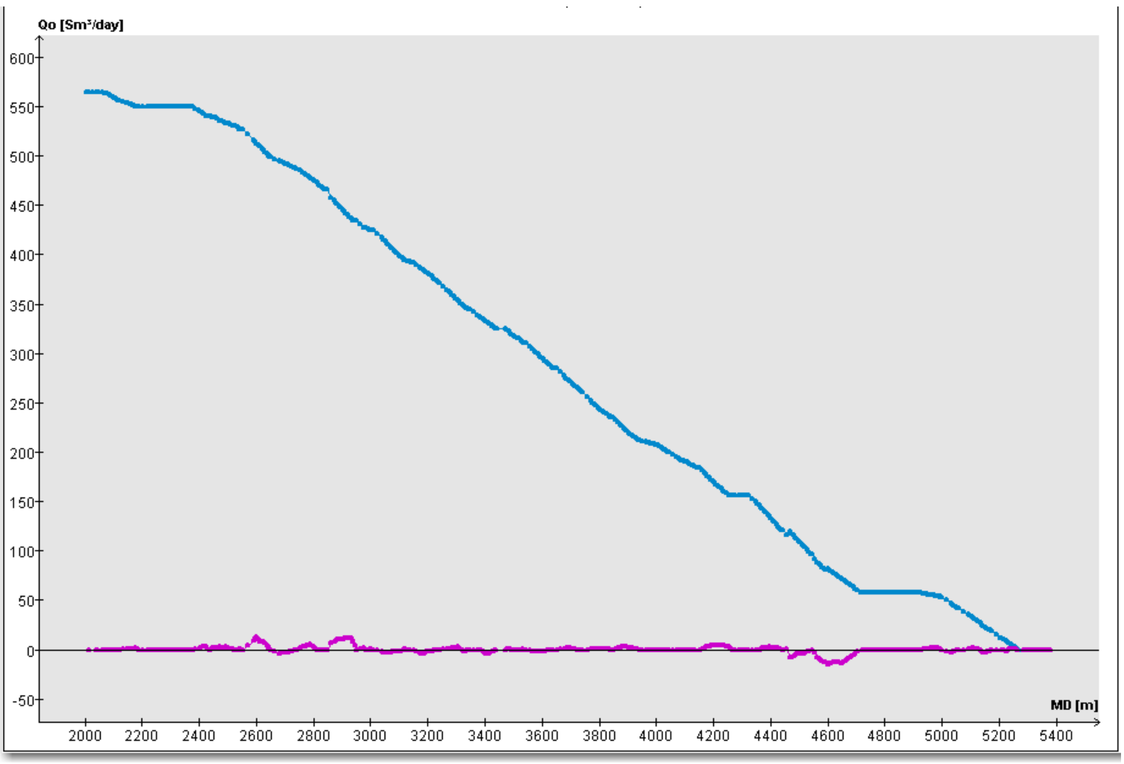

Figure 44: Cumulative oil flow rate in BY2H.

Except from the plateau in the interval from 4700 – 5100 m MD, a section with blank pipes, the oil inflow in Figure 41 seems linear. This is expected from the RCP valves.

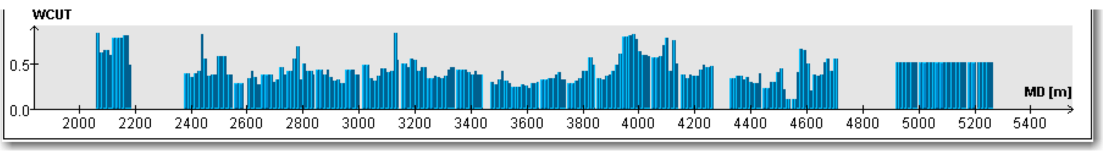

Figure 45: WC in BY2H.

The WC is found to have two sections where it is elevated; about 100 meters close to the heel section (2100 to 2200 m MD) and around 4000 m MD. The reason for this is given in the water flowing fractions implemented, which are highest in the same areas as in Figure 45.

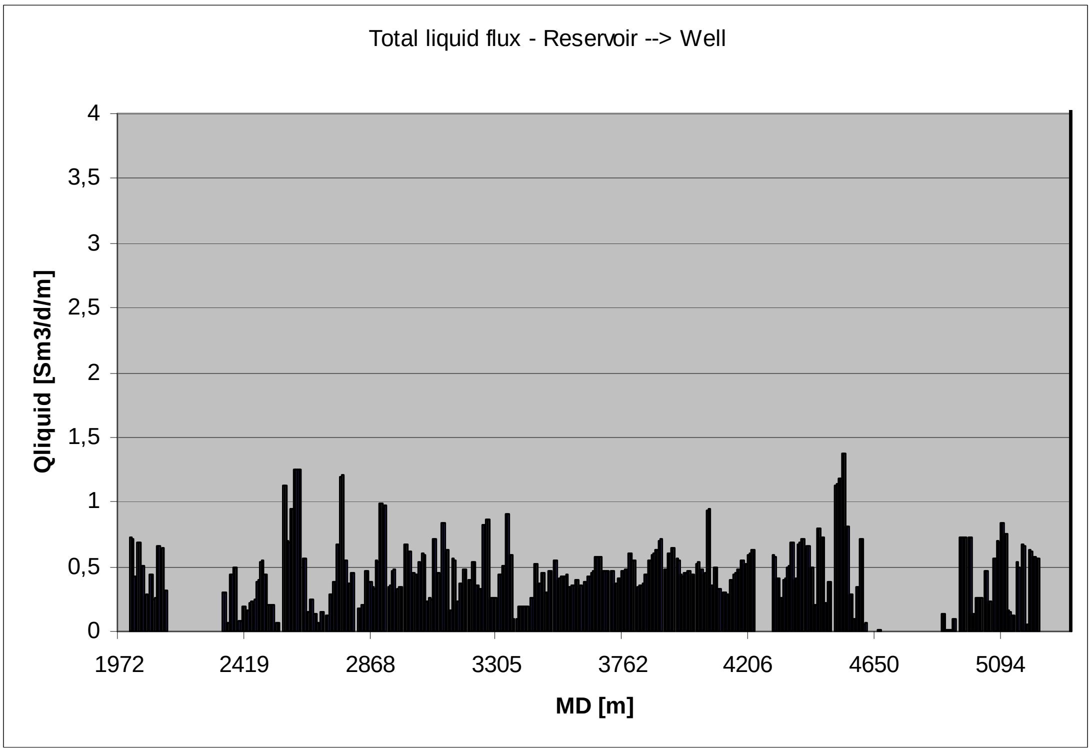

Figure 46: Total liquid flux into BY2H.

The liquid influx from the reservoir into BY2H is quite stable except from two peaks close to 2650 and 4550 m MD. These follow the argument given for Figure 45 above regarding the water saturation. The highest total influx is seen to be 1,25 $Sm^3/d/m$ at 2700 m MD.

In the Figures in the two following sections of the thesis the blue values represent the parameter in the relevant branch when producing from both at the same time (commingled) while the pink values indicate the same parameter when only producing from that particular branch.

8.3. Comparison of BY1H in Commingled and Single Production

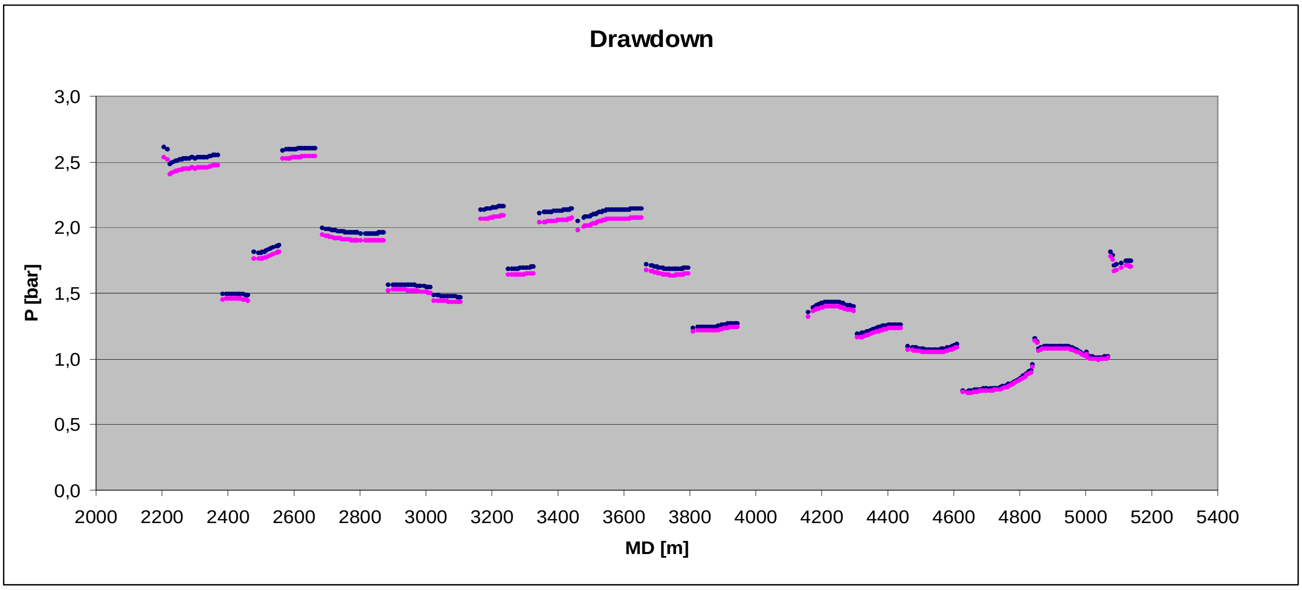

Figure 47: Comparison of drawdown in BY1H in commingled and single production.

The two sets of results (blue and pink) in Figure 47 are comparable, and they seem to be most alike close to the toe section. The drawdown when having a commingled production is marginally larger than when the well is only producing from the ICD branch. These findings seem to also be valid in the same comparison of the pressure drops across completion seen in Figure 48 below.

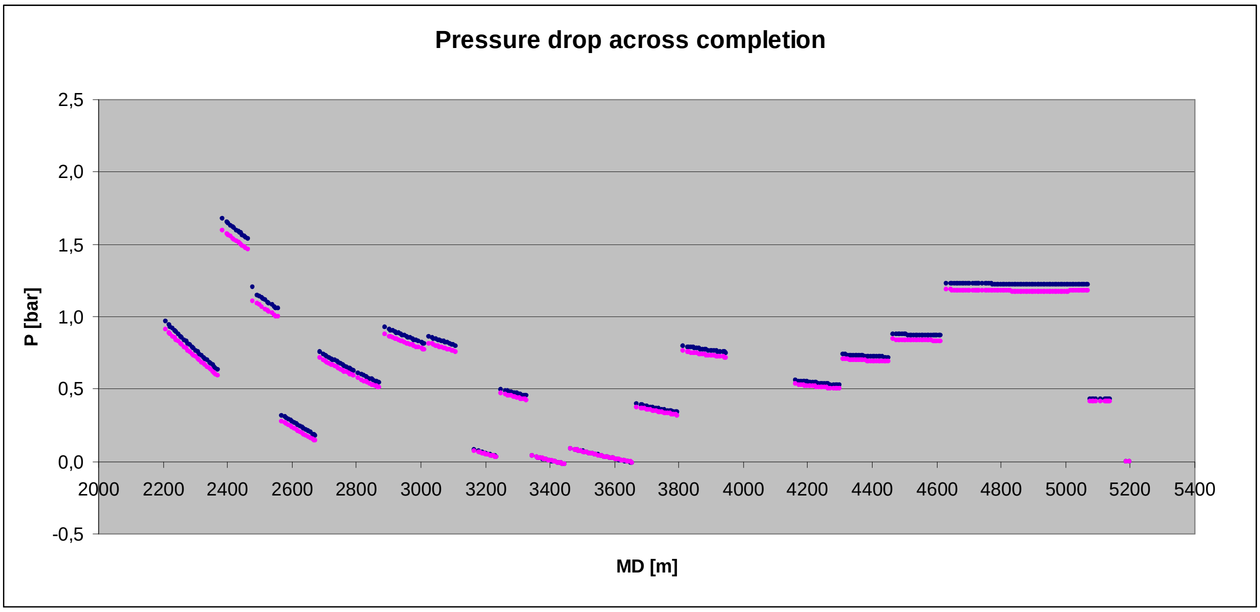

Figure 48: Comparison of pressure drop in completion in BY1H in commingled and single production.

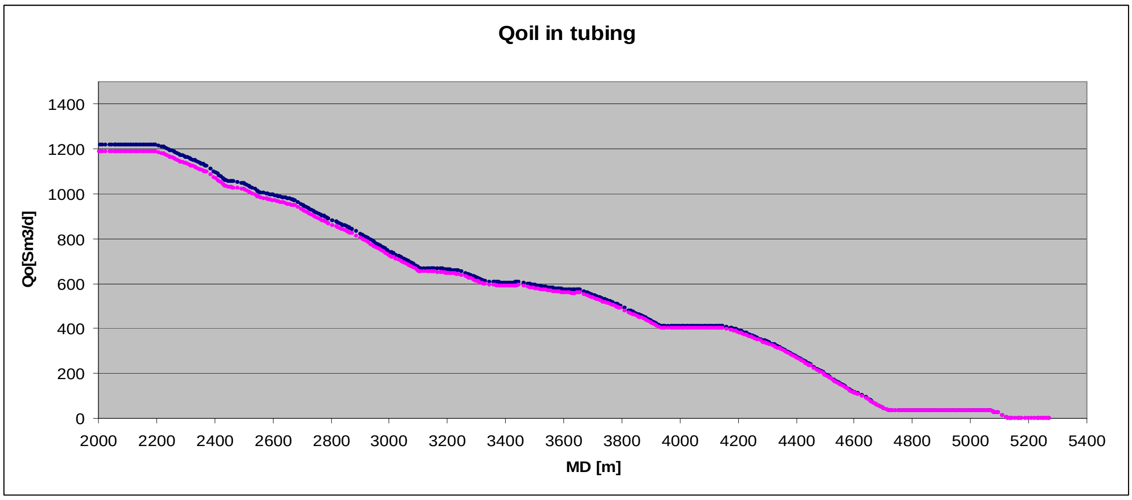

Figure 49: Comparison of cumulative oil flow rate in BY1H in commingled and single production.

From Figure 49 the cumulative production of oil obtained in BY1H appears to be slightly higher when producing from BY2H simultaneously. There is no reason found why this should be expected.

8.4. Comparison of BY2H in Commingled and Single Production

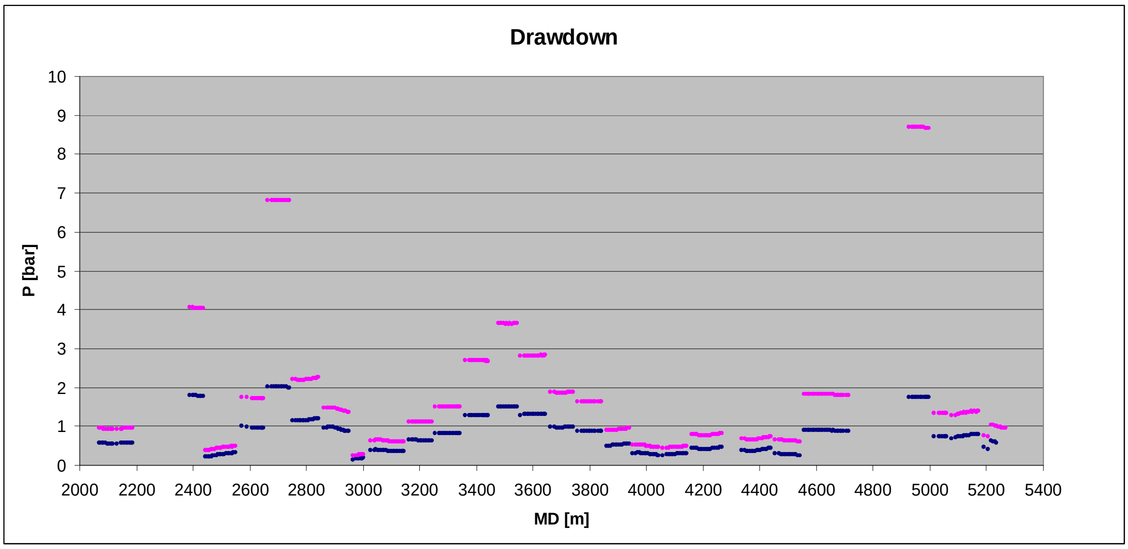

Figure 50: Comparison of drawdown in BY2H in commingled and single production.

When having BY1H closed, hence only producing from BY2H, Figure 50 indicate that the pressure drawdown is always larger than when producing from both branches simultaneously. It seems that the difference between the two scenarios is biggest at 5000 m MD, at 3500 m MD and at 2700 and 2400 m MD. These are areas with low horizontal permeability, which will according to the PI equation presented earlier at a given flow rate provide a higher pressure drop.

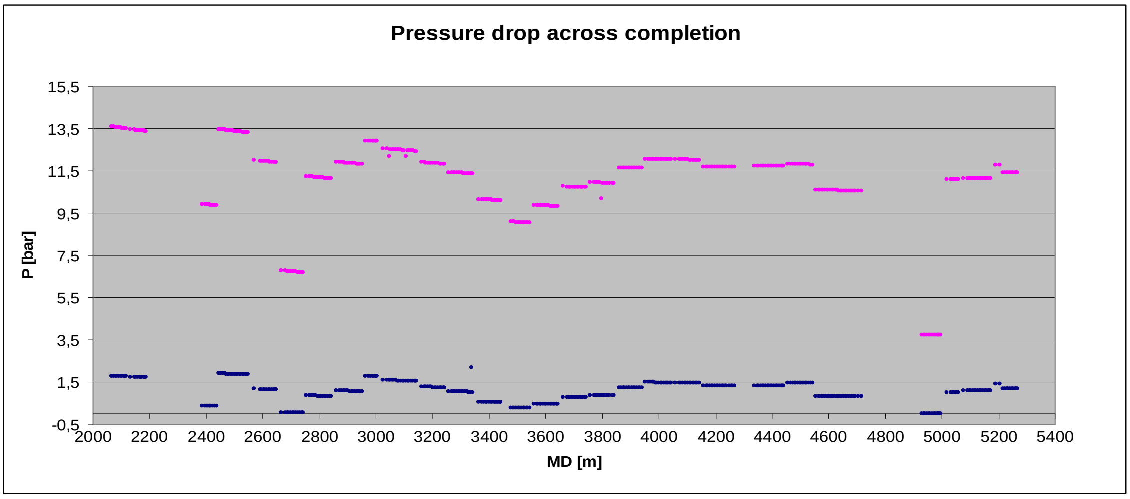

Figure 51: Comparison of pressure drop in completion in BY2H in commingled and single production.

The pressure drop across the completion is much larger when only producing the well from BY2H. At the same locations as discussed above, here are the points where the difference now appears to be the smallest. In other locations of the well the difference in pressure drop seem constant.

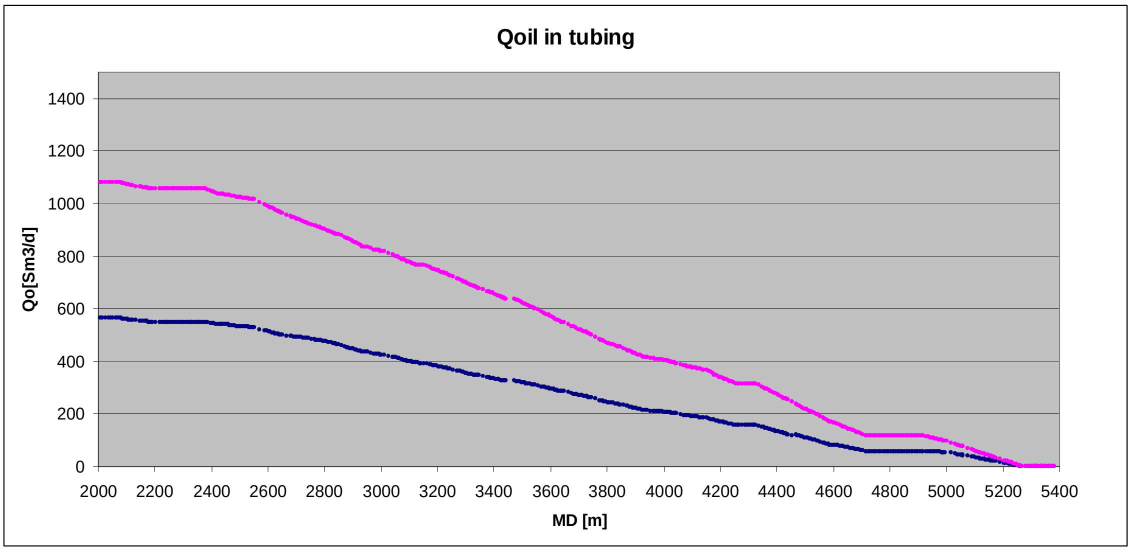

Figure 52: Comparison of cumulative oil flow rate in BY1H in commingled and single production.

The simulations in Figure 52 indicate an increase in cumulative oil rate of approximately 500 Sm^3/d (1100 vs. 570 Sm^3/d) when producing from BY2H alone, which is an increase of over 90 %. Apparently when allowing the well to produce only from the RCP branch, the pressure drop across the completion is of a size that nearly doubles the cumulative oil flow rate.

8.5 Comparison of Production Performance and Simulation Results

Having tuned the NETool model to fit the tests chosen for matching makes it valid for control. If the simulation results of other tests also fit well in the model, it can be argued that the model should be more widely accepted because it now shows to fit other data as well. All except the commingled production test performed on the 11th of October 2010 were investigated. It was discarded due to lack of water rate measurements.

For the tests having a GOR larger than the solution GOR, an amount of free gas was added in the model as a gas fraction giving a GOR result close to the test value. The simulations are performed with respect to the test dates; the earliest test is simulated first. In this way one may discover trends as the well develops. The three different test conditions (commingled production and single testing of each branch) are also presented separately.

8.5.1 Boundary Condition: Q_{liquid}, Commingled Tests

Parameter	Control 1	Control 2	Control 3	Control 4	Control 5	Control 6
Q_{liquid} [Sm^3/d]	3000	2249,3	2870,4	2853,6	2985,6	2556
Q_{oil} [Sm^3/d]	1632,7	1136,2	1429,9	1324,4	1385,6	935,8
Q_{water} [Sm^3/d]	1367,3	1113,1	1440,5	1529,2	1600	1620,2
WC [%]	45,6	49,5	50,2	53,6	53,6	63,4
Q_{gas}[Sm^3/d]	78357,2	83282,4	113774,7	143045,3	149300	208200,4
GOR [Sm^3/Sm^3]	48	73,3	79,6	108	107,8	222,5
BHP	133,02	134,125	133,169	133,155	132,897	133,574

Table 25: NETool simulation results of controlling commingled test values with boundary condition Qliquid.

The different simulation results from commingled tests are given in Table 25, while the deviation between model and test is given in Table 26.

BHP production test [bar]	BHP simulation modell [bar]	Discrepancy [%]
132,026	133,02	1,01
133,104	134,125	1,01
131,348	133,169	1,01
130,661	133,155	1,02
130,395	132,897	1,02

130,778	133,57	1,02

Table 26: Difference in values of BHP when using Qliquid from commingled tests as the boundary condition.

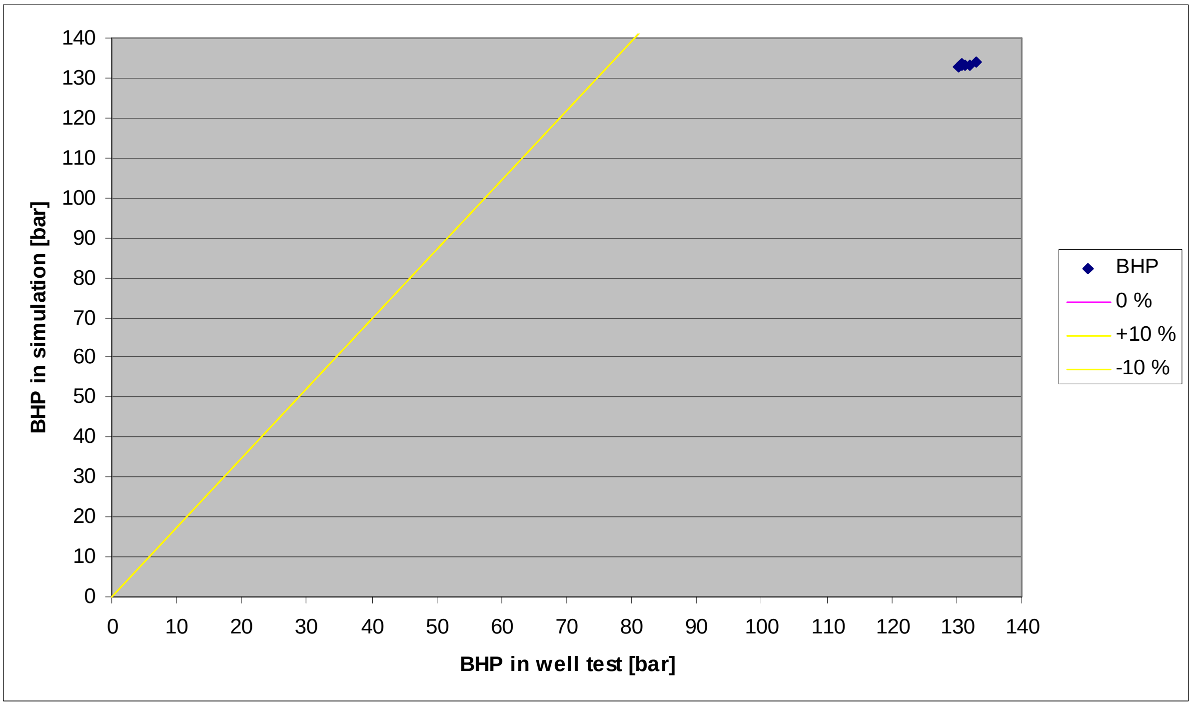

Figure 53: Discrepancy in simulated values in compared to values from commingled tests when using Qliquid as the boundary condition.

Figure 53 show little deviation between BHP from test and from simulation model.

8.5.2. Boundary Condition: Q_{liquid}, Single Tests BY1H

Parameter	**Control 1**	**Control 2**	**Control 3**
Q_{liquid} [Sm^3/d]	1795,2	1728	1713,6
Q_{oil} [Sm^3/d]	979,8	900,9	792,8
Q_{water} [Sm^3/d]	815,4	827,1	920,8
WC [%]	45,4	47,9	53,7
Q_{gas}[Sm^3/d]	47213,3	57960,2	87581,8
GOR [Sm^3/Sm^3]	48,2	64,3	110,5
BHP	133,743	133,891	133,885

Table 27: NETool simulation results of controlling single test values from BY1H with boundary condition Qliquid.

BHP production test [bar]	BHP simulation model [bar]	Discrepancy [%]
132,027	133,743	1,30
131,346	133,891	1,94
130,396	133,885	2,68

Table 28: Difference in values of BHP when using Q_{liquid} from single tests of BY1H as the boundary condition.

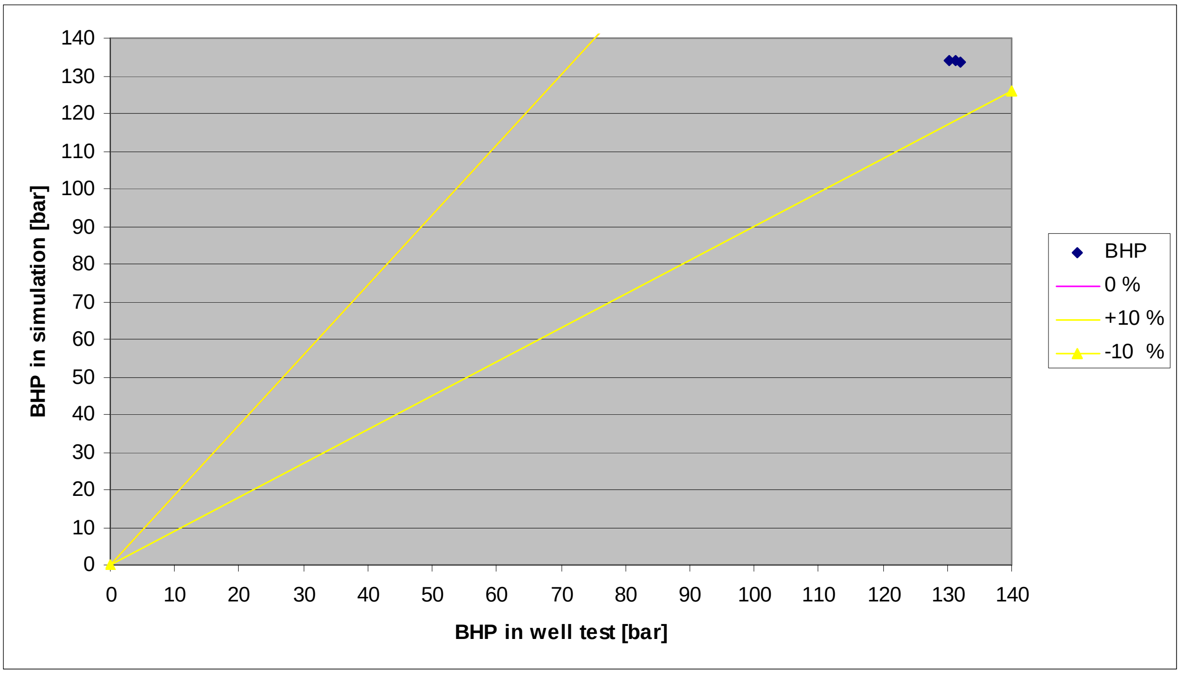

Figure 54: Discrepancy in simulated values in compared to values from single tests of BY1H when using Qliquid as the boundary condition.

8.5.3. Boundary condition: Q_{liquid}, single tests BY2H

The discrepancy analysis was not possible to perform in this branch because the numerical solver did not converge. “LU decomposition failed. Solver status: 3.” What does this mean? Several attempts were made to reconsider parameters and settings to at least have the simulation running but, this was not succeeded.

9. Pressure Drop Estimates

The following calculations in this Chapter are based on the equations given in Chapter 6.

9.1. ΔP_F Estimates

9.1.1. Results for BY1H in Commingled Production Tests

Start [D.M.Y hh.mm]	**Stopp [D.M.Y hh.mm]**	**ID [in.]**	**A [m²]**	**U_{mix} [m/s]**	**ρ_{mix} [cP]**	**μ_{mix} [cP]**	**Re**	**fm**	**L [m]**	**ΔP_F [bar]**
12.05.2011 06:03	12.05.2011 11:04	5,291	0,01419	3,88	710,53	0,98	376759	0,0035	79	0,1090
31.03.2011 11:00	01.04.2011 05:30	5,291	0,01419	1,78	649,15	1,56	99417	0,0045	79	0,0271
17.03.2011 11:10	17.03.2011 17:00	5,291	0,01419	3,14	785,83	1,14	291751	0,0036	79	0,0830
08.02.2011 08:10	09.02.2011 21:50	5,291	0,01419	2,44	765,91	1,05	238570	0,0038	79	0,0507
15.01.2011 10:55	15.01.2011 20:21	5,291	0,01419	3,16	756,30	1,06	302343	0,0036	79	0,0800
21.11.2010 02:00	22.11.2010 22:00	5,291	0,01419	3,38	711,55	0,97	334405	0,0035	79	0,0848
11.10.2010 15:00	12.10.2010 09:30	5,291	0,01419	3,56	708,39	0,96	354773	0,0035	79	0,0925
02.10.2010 19:00	03.10.2010 03:40	5,291	0,01419	3,70	605,39	0,79	382050	0,0035	79	0,0842

Table 29: Frictional pressure drops for BY1H in commingled production tests.

The frictional pressure drop in the ICD branch when producing from both is found to be below 0,1 bar for all except the first test according to Table 29.

9.1.2. Results for BY2H in Commingled Production Tests

Start [D.M.Y hh.mm]	**Stopp [D.M.Y hh.mm]**	**ID [in.]**	**A [m²]**	**U_{mix} [m/s]**	**ρ_{mix} [cP]**	**μ_{mix} [cP]**	**Re**	**fm**	**L [m]**	**ΔP_F [bar]**
12.05.2011 06:03	12.05.2011 11:04	5,291	0,01419	3,88	710,53	0,98	376759	0,0035	129,7	0,1790
31.03.2011	01.04.2011	5,291	0,01419	1,78	649,15	1,56	99417	0,0045	129,7	0,0445

11:00	05:30									
17.03.2011 11:10	17.03.2011 17:00	5,291	0,01419	3,14	785,83	1,14	291751	0,0036	129,7	0,1363
08.02.2011 08:10	09.02.2011 21:50	5,291	0,01419	2,44	765,91	1,05	238570	0,0038	129,7	0,0833
15.01.2011 10:55	15.01.2011 20:21	5,291	0,01419	3,16	756,30	1,06	302343	0,0036	129,7	0,1313
21.11.2010 02:00	22.11.2010 22:00	5,291	0,01419	3,38	711,55	0,97	334405	0,0035	129,7	0,1393
11.10.2010 15:00	12.10.2010 09:30	5,291	0,01419	3,56	708,39	0,96	354773	0,0035	129,7	0,1519
02.10.2010 19:00	03.10.2010 03:40	5,291	0,01419	3,70	605,39	0,79	382050	0,0035	129,7	0,1383

Table 30: Frictional pressure drops for BY2H in commingled production tests.

Considering Table 29 and 30, it is seen that when producing from both branches the frictional pressure drop is bigger for RCP valves than ICD valves, but this is explained by the different lengths the calculations are based upon.

9.1.3. Results for Single Tests of BY1H

Start	**Stopp**	**ID**	**A**	$\mathbf{U_{mix}}$	$\boldsymbol{\rho_{mix}}$	$\boldsymbol{\mu_{mix}}$	**Re**	**fm**	**L**	$\mathbf{\Delta P_F}$
[D.M.Y hh.mm]	**[D.M.Y hh.mm]**	**[in.]**	**[m^2]**	**[m/s]**	**[cP]**	**[cP]**			**[m]**	**[bar]**
03.10.10 11:00	03.10.10 21:00	5,291	0,01419	2,17	829,74	1,01	238845	0,00389	79	0,0449
21.11.10 02:01	22.11.10 22:01	5,291	0,01419	1,87	793,34	1,06	188253	0,00406	79	0,0332
08.02.11 08:12	09.02.11 21:50	5,291	0,01419	1,78	805,00	1,05	182361	0,00408	79	0,0305
31.03.11 11:01	01.04.11 05:30	5,291	0,01419	1,96	737,52	0,92	210925	0,00398	79	0,0332

Table 31: Frictional pressure drops for single tests BY1H.

9.1.4. Results for Single Tests of BY2H

Start	**Stopp**	**ID**	**A**	$\mathbf{U_{mix}}$	$\boldsymbol{\rho_{mix}}$	$\boldsymbol{\mu_{mix}}$	**Re**	**fm**	**L**	$\mathbf{\Delta P_F}$
[D.M.Y hh.mm]	**[D.M.Y hh.mm]**	**[in.]**	**[m^2]**	**[m/s]**	**[cP]**	**[cP]**			**[m]**	**[bar]**
04.10.10	04.10.10	5,291	0,01419	2,16	743,91	1,26	171464	0,0041	129,7	0,0694

00:00	07:30									
22.11.10 12:22	22.11.10 17:26	5,291	0,01419	1,41	710,44	1,14	118066	0,0044	129,7	0,0301
11.02.11 01:10	11.02.11 07:30	5,291	0,01419	1,28	689,37	1,07	110647	0,0045	129,7	0,0244
02.04.11 18:00	02.04.11 23:00	5,291	0,01419	1,49	669,12	0,99	135415	0,0043	129,7	0,0311

Table 32: Frictional pressure drops for single tests BY2H.

Seen in Table 31 and 32 above, the frictional pressure drops could be neglected in further calculations if wanted, as it is in the range of 30-70 mBar for both branches.

9.2. ΔP_{PE} Estimates

9.2.1. Results for Single Tests of BY1H

Start	**Stopp**	**ID**	**A**	**ρ_{mix}**	**L**	**ΔP_{PE}**
[D.M.Y hh.mm]	**[D.M.Y hh.mm]**	**[in.]**	**[m^2]**	**[cP]**	**[m]**	**[bar]**
03.10.10 11:00	03.10.10 21:00	5,291	0,01419	829,74	26,5	2,16
21.11.10 02:01	22.11.10 22:01	5,291	0,01419	793,34	26,5	2,06
08.02.11 08:12	09.02.11 21:50	5,291	0,01419	805,00	26,5	2,09
31.03.11 11:01	01.04.11 05:30	5,291	0,01419	737,52	26,5	1,92

Table 33: Pressure drop due to vertical distance between gauge and top screen for single tests BY1H.

9.2.1. Results for Single Tests of BY2H

Start	**Stopp**	**ID**	**A**	**ρ_{mix}**	**ΔZ single gauge**	**ΔP_{PE}**
[D.M.Y hh.mm]	**[D.M.Y hh.mm]**	**[in.]**	**[m^2]**	**[cP]**	**[m]**	**[bar]**
04.10.10 00:00	04.10.10 07:30	5,291	0,01419	743,91	31	2,26
22.11.10 12:22	22.11.10 17:26	5,291	0,01419	710,44	31	2,16

11.02.11 01:10	11.02.11 07:30	5,291	0,01419	689,37	31	2,10
02.04.11 18:00	02.04.11 23:00	5,291	0,01419	669,12	31	2,03

Table 34: Pressure drop due to vertical distance between gauge and top screen for single tests BY2H.

Table 33 and 34 above show the pressure drops in the tests due to the vertical distance between top screen in each branch and the relevant gauge. This contribution is found to be larger than the term related to friction, also varying for the two different branches because the respective gauges are found in at different locations.

9.3. PI Calculations

Parameters given in Table 17 that are not calculated in the following paragraph are based on experience within the Troll production technology group and verified by Martin Halvorsen. B_o and μ_o are found from the PVT data in Appendix B, r_w is obtained from [14].

9.3.1. Calculated Input Parameters

Production Lengths and Permeabilities

The production length (L_p) is just the sum of the lengths of screens placed in the well. Horizontal permeability is estimated by averaging the values given in the open hole logs for the depths where the screens are located, given in Table 35 and Table 36 below. In order to take into account the different lengths of the intervals, the total sum of the permeabilities for each interval was eventually divided by the total length of screens.

Screen			**Alt. Screen/Blank**			**Avg. κ_H in interval**	**κ_H**
From [m]	**To [m]**	**Length [m]**	**From [m]**	**To [m]**	**Length [m]**	**[D]**	**[D*m]**
2197	3097	900				5,337	4803,6
3156	3938	782				3,170	2478,9
4149	4730	581				7,748	4501,3
5090	5130	40				2,688	107,5
5170	5200	30				5,489	164,6
						7,519	150,3
			5070	5090	20	5,337	4803,6
Total permeability [Dm]							**12206,51**
Total length [m]							**2333**
Average permeability [D/mD]							**5,2321/5232**

Table 35: Producing well length and average permeability for branch BY1H.

Screen			Alt. Screen/Blank			Avg. κ_H in interval	κ_H
From [m]	**To [m]**	**Length [m]**	**From [m]**	**To [m]**	**Length [m]**	**[D]**	**[D*m]**
2003,5	2190	186,5				3,487	650,3
2375	2440	65				2,888	187,7
2550	2960	410				6,870	2816,8
3010	4275	1265				6,000	7589,8
4330	4720	390				8,035	3133,6
4920	5333	413				3,476	1435,7
			2960	3010	50	18,169	454,2
			2440	2550	110	6,374	350,5
Total permeability [Dm]							**16619,05**
Total length [m]							**2809,5**
Average permeability [D/mD]							**5,9153/5915**

Table 36: Producing well length and average permeability for branch BY2H.

To check the dependency of PI on some of the different parameters, there have been developed 4 cases for each of the branches. The most realistic case was chosen as a basis for the pressure drop calculations, seen in Table 17. In addition to the four cases based on the Goode and Kuchuk equation presented earlier, there is performed another PI calculation case referred to as "Humberto". This is developed with respect to [33]. Since it is not emphasized in this thesis it will not be further discussed.

9.3.2. Sensitivities BY1H – The Well with ICD Valves

Basic input parameters	Case 1	Case 2	Case 3	Case 4	Humberto	Unit
Formation thickness (h)	100	75	50	20	100	m
Wellbore radius (r_w)	0,10795	0,10795	0,10795	0,10795	0,10795	m
Well length perforated (L_p)	2333	2333	2333	2333	2333	m
Short intervals? (0=no, 1=yes)	0	0	0	0		
Well deviation (theta)	90,0	90,0	90,0	90,0		deg
Well location (z_w)	50	37,5	25	10		m
Skin along the well (damage)	1	1	1	0		
Reservoir length along well (x_e)	5600	4200	3500	3000	4000	m
Reservoir width across well (y_e)	2000	1000	500	250	1000	m
Well location along reservoir (x_w)	2333	2100	1750	1500		m
Well location across reservoir (y_w)	1000	500	250	125		m
Horizontal permeability (κ_H)	5232	5232	5232	5232	5232	mD

κ_V/ κ_H ratio	0,6	0,6	0,6	0,6		
Formation volume factor (B)	1,14	1,14	1,14	1,14	1,14	Rm^3/Sm^3
Viscosity (μ)	2,07	2,07	2,07	2,07	2,07	cP
Main result						
Productivity index (PSS)	**8671,7**	**9962,9**	**8864,4**	**5850,6**	**11456,75**	Sm^3/d/bar
	Goode&Kuchuk				**Humberto**	

Table 37: PSS PI for different scenarios BY1H.

9.3.3. Sensitivities BY2H – The Well with RCP Valves

Basic input parameters	**Case 1**	**Case 2**	**Case 3**	**Case 4**	**Humberto**	**Unit**
Formation thickness (h)	100	75	50	20	100	m
Wellbore radius (r_w)	0,10795	0,10795	0,10795	0,10795	0,10795	m
Well length perforated (L_p)	2809,5	2809,5	2809,5	2809,5	2809,5	m
Short intervals? (0=no, 1=yes)	0	0	0	0		
Well deviation (theta)	90,0	90,0	90,0	90,0		deg
Well location (z_w)	50	37,5	25	10		m
Skin along the well (damage)	1	1	1	0		
Reservoir length along well (x_e)	5600	4200	3500	3000	4000	m
Reservoir width across well (y_e)	2000	1000	500	250	1000	m
Well location along reservoir (x_w)	2809,5	2100	1750	1500		m
Well location across reservoir (y_w)	1000	500	250	125		m
Horizontal permeability (κ_H)	5915	5915	5915	5915	5915	mD
κ_V/ κ_H ratio	0,6	0,6	0,6	0,6		
Formation volume factor (B)	1,14	1,14	1,14	1,14	1,14	Rm^3/Sm^3
Viscosity (μ)	2,07	2,07	2,07	2,07	2,07	cP
Main result						
Productivity index (PSS)	**13537,8**	**16131,6**	**18595,8**	**25646,3**	**15580,61**	Sm^3/d/bar
	Goode&Kuchuk				**Humberto**	

Table 38: PSS PI for different scenarios BY2H.

9.4. ΔP_{fm} and ΔP_c Estimates Based on PI Calculations

9.4.1. Depletion Evaluation

The shut in pressures (SIP) measured must be corrected for the depletion of the field (in addition to hydrostatic column) when performing the calculations of pressure drop through formation and completion. When a branch is shut-in over time the pressure builds up to a stable value, and this value will represent the reservoir pressure at that instant. This was investigated in BY2H. The res. pressure is assumed to be equal in both branches, so this investigation is also valid for BY1H. An example of a period of shut in is shown in Figure 55 representing the pressure at the time of the first single test of BY1H being performed in October 2010.

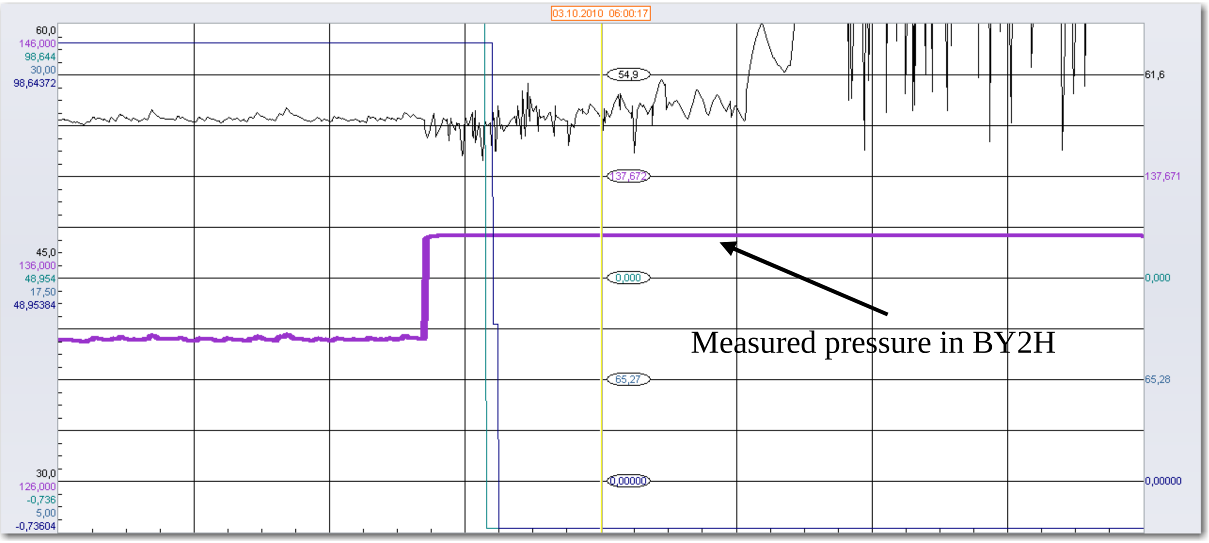

Figure 55: First measured SIP in BY2H.

Three different SIPs given below were plotted to investigate the depletion.

Date [DD.MM.YYYY]	SIP [bar]
03.10.2010	137,67
16.12.2010	137,233
15.02.2011	136,914

Table 39: SIP in BY2H.

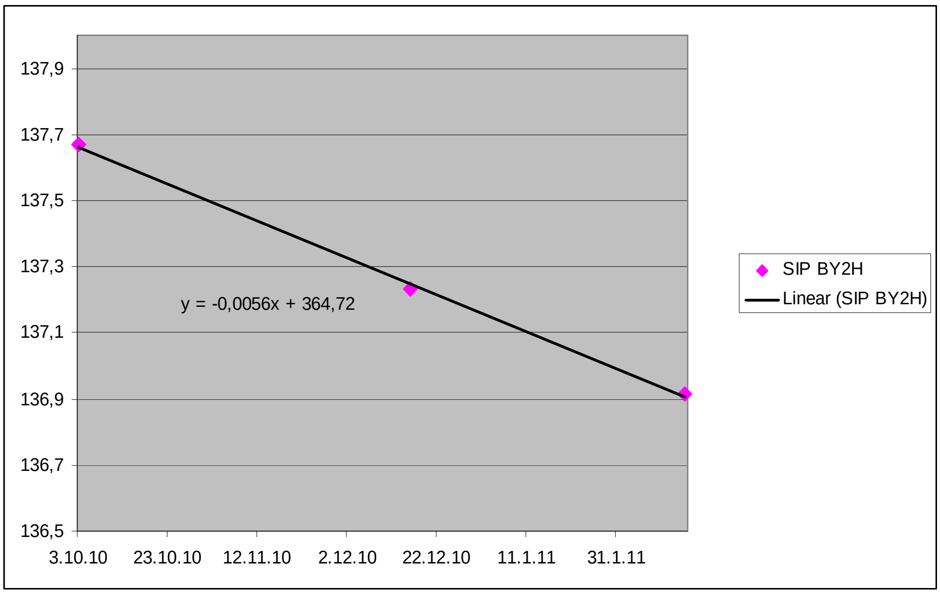

Figure 56: Depletion investigation from SIP BY2H.

Depletion [bar/day]	0,0056
Depletion [bar/year]	2,04

Table 40: Estimated depletion.

The above calculation assumes a year as 365 days, and gives a depletion of approximately ***2 bar pr. year.*** This is in accordance with the general experience in wells located in the Sognefjorden Formation [2] and is used in the following investigations.

It is important to have in mind that the pressure measurements in BY1H are assumed to be incorrect due to a problem with the sensor tube from the dual gauge and down to the S-FCV. The calculations performed for BY1H and the ICD valve can therefore only be taken as indicative and highly uncertain. Of this reason they will not be evaluated in the same depth as the results for BY2H will be.

9.4.2. Results for BY1H in commingled tests

Start	**Stopp**	**DHG Y1 corrected**	**SIP corrected**	**ΔP**	**PI**	**Q_{liquid}**	**ΔP_{fm}**	**ΔP_C**	**GOR**
[D.M.Y hh.mm]	**[D.M.Y hh.mm]**	**[Bar]**	**[Bar]**	**[Bar]**	**[Sm³/d/bar]**	**[m³/d]**	**[Bar]**	**[Bar]**	**[Sm³/ Sm³]**
02.10.2010 19:00	03.10.2010 03:40	136,99	139,27	2,28	8671,7	3273,4	0,38	1,90	109,0
11.10.2010 15:00	12.10.2010 09:30	136,85	139,06	2,21	8671,7	1437,6	0,17	2,05	53,5
21.11.2010 02:00	22.11.2010 22:00	136,56	139,19	2,64	8671,7	3000,0	0,35	2,29	56,9
15.01.2011 10:55	15.01.2011 20:21	136,88	138,84	1,96	8671,7	2249,3	0,26	1,70	75,8
08.02.2011 08:10	09.02.2011 21:50	136,78	138,68	1,90	8671,7	2870,4	0,33	1,57	78,0
17.03.2011 11:10	17.03.2011 17:00	136,59	138,36	1,77	8671,7	2853,6	0,33	1,44	112,3
31.03.2011 11:00	01.04.2011 05:30	136,57	138,28	1,70	8671,7	2985,6	0,34	1,36	116,3
12.05.2011 06:03	12.05.2011 11:04	136,02	137,78	1,76	8671,7	2556,0	0,29	1,46	211,9

Table 41: Pressure drop evaluations for BY1H in commingled tests.

In Table 41 the total pressure drop over the ICD valves are found to be higher than the pressure drop across the completion due to the high PI calculated in Table 37.

9.4.3. Results for BY2H in commingled tests

Start	**Stopp**	**DHG Y2 corrected**	**SIP corrected**	**ΔP**	**PI**	$\mathbf{Q_{liquid}}$	$\mathbf{\Delta P_{fm}}$	$\mathbf{\Delta P_C}$	**GOR**
[D.M.Y hh.mm]	**[D.M.Y hh.mm]**	**[Bar]**	**[Bar]**	**[Bar]**	**[Sm^3/d/bar]**	**[m^3/d]**	**[Bar]**	**[Bar]**	**[Sm^3/ Sm^3]**
02.10.2010 19:00	03.10.2010 03:40	135,88	139,83	3,95	13538,5	3273,4	0,24	3,71	109,0
11.10.2010 15:00	12.10.2010 09:30	134,69	139,60	4,91	13538,5	1437,6	0,11	4,80	53,5
21.11.2010 02:00	22.11.2010 22:00	136,35	139,79	3,44	13538,5	3000,0	0,22	3,22	56,9
15.01.2011 10:55	15.01.2011 20:21	137,13	139,43	2,30	13538,5	2249,3	0,17	2,13	75,8
08.02.2011 08:10	09.02.2011 21:50	135,49	139,27	3,78	13538,5	2870,4	0,21	3,56	78,0
17.03.2011 11:10	17.03.2011 17:00	135,11	138,93	3,82	13538,5	2853,6	0,21	3,61	112,3
31.03.2011 11:00	01.04.2011 05:30	135,19	138,84	3,65	13538,5	2985,6	0,22	3,43	116,3
12.05.2011 06:03	12.05.2011 11:04	135,06	138,30	3,24	13538,5	2556,0	0,19	3,05	211,9

Table 42: Pressure drop evaluations for BY2H in commingled tests.

As the well matures, the total drawdown seen in BY2H in Table 42 is decreasing. Still the PI is so high that the pressure drop across sandface is accordingly low and the main contribution to the drawdown is seen across the RCP valves.

9.4.4. Results for single tests of BY1H

Start	**Stopp**	**DHG Y1 corrected**	**SIP corrected**	**ΔP**	**PI**	$\mathbf{Q_{liquid}}$	$\mathbf{\Delta P_{fm}}$	$\mathbf{\Delta P_C}$	**GOR**
[D.M.Y hh.mm]	**[D.M.Y hh.mm]**	**[Bar]**	**[Bar]**	**[Bar]**	**[Sm^3/d/bar]**	**[m^3/d]**	**[Bar]**	**[Bar]**	**[Sm^3/ Sm^3]**
03.10.2010 11:00	03.10.2010 21:00	133,99	139,58	5,58	8671,7	2177,0	0,25	5,33	57,3
21.11.2010 02:01	22.11.2010 22:01	136,47	139,22	2,74	8671,7	1795,2	0,21	2,54	64,6
08.02.2011	09.02.2011	136,81	138,81	2,00	8671,7	1728,0	0,20	1,80	61,3

08:12	21:50								
31.03.2011 11:01	01.04.2011 05:30	136,53	138,36	1,83	8671,7	1713,6	0,20	1,63	114,0

Table 43: Pressure drop evaluations for single tests BY1H.

In table 43 the trend of the pressure distribution is that the main pressure drop is seen across the completion.

9.4.5. Results for single tests of BY2H

Start	**Stopp**	**DHG Y2 corrected**	**SIP corrected**	**ΔP**	**PI**	**Q_{liquid}**	**ΔP_{fm}**	**ΔP_C**	**GOR**
[D.M.Y hh.mm]	**[D.M.Y hh.mm]**	**[Bar]**	**[Bar]**	**[Bar]**	**[Sm^3/d/bar]**	**[m^3/d]**	**[Bar]**	**[Bar]**	**[Sm^3/ Sm^3]**
04.10.10 00:00	04.10.10 07:30	131,50	139,93	8,43	13538,5	1968,5	0,15	8,28	56,0
22.11.10 12:22	22.11.10 17:26	136,27	139,56	3,29	13538,5	1205,0	0,09	3,20	80,9
11.02.11 01:10	11.02.11 07:30	136,13	139,05	2,92	13538,5	1053,6	0,08	2,85	98,2
02.04.11 18:00	02.04.11 23:00	135,03	138,71	3,69	13538,5	1180,8	0,09	3,60	121,0

Table 44: Pressure drop evaluations for single tests BY2H.

Table 44 shows the pressure drop distribution for single tests of BY2H. The results obtained support the findings in Table 42 that the pressure drops across the valves exceeds the pressure drops across the formation due to the high PI.

10. Evaluation of Inflow Control Technologies

10.1. Well Test Analysis – Measured Production Performance

It is advantageous to perform an evaluation of the production tests since these give the production performance of the well at that time. There is a lot of material available on each of the 15 well tests, but for this thesis the relevant parameters are:

- GOR – how much gas is being produced and has there been a GBT?
- WC – how much water is produced compared to oil, and is this changing?

For sections 10.1 to 10.3 the first test (Test number 1) marked in gray was used for development of the NETool simulation model presented in the previous chapter.

10.2. Commingled Production Tests

Test number	WC [%]	GOR [Sm^3/Sm^3]
1	51,0	109,0 [6]
2	1,1 [7]	53,5
3	49,1	56,9
4	52,4	75,8
5	50,9	78,0
6	52,3	112,3
7	52,8	116,3
8	53,0	211,9 [8]

Table 45: Development of water cut and gas-oil ratios over time in all well tests.

We see from Table 45 above that the WC has slightly increased since start up, but the difference is insignificant for the evaluations performed in this thesis. Considering the GOR values in the same Table indicates that the well has probably not had a massive GBT yet. The solution GOR is found to be 48 Sm^3/Sm^3 from Appendix B, and the test show values close to this.

[6] Assumed to be incorrect and more likely to have a value of 45-55 Sm^3/Sm^3. Since this is a test performed just as the well went into production, it may be contaminated in some way

[7] Not a valid measurement, no water rate measured at this test. Test discarded in later NETool simulations.

[8] This value is still being investigated as this thesis is completed, expected to be too high due to an error in the estimated RGL. It was recommended to be assumed correct until further notice was given

10.3. Single Tests BY1H

The WC varies slightly in this branch, while the GOR is increasing. The last value in Table 46 indicates a possible GBT.

Test number	WC [%]	GOR [Sm^3/Sm^3]
1	60,9	57,3
2	54,7	64,6
2	56,2	61,3
4	58,3	114,0

Table 46: Development of water cut and gas-oil ratios over time in single tests on BY1H.

10.4. Single Tests BY2H

As for BY1H the GOR is increasing in this branch too. This is also the case for the WC and is presented in Table 47:

Test number	WC [%]	GOR [Sm^3/Sm^3]
1	36,3	56,0
2	40,2	80,9
2	42,1	98,2
4	45,2	121,0

Table 47: Development of water cut and gas-oil ratios over time in single tests on BY2H.

10.5. Investigation of Number of Valves Filled

As mentioned in Chapter 4.5. one way to study the performance of the valves is to calculate the number of valves that are filled with the respective fluid in each test. The number of valves with gas is calculated based on a constant B_g at a pressure of 139 bar, and is expected to be slightly overestimated. This analysis is performed on all the single tests of BY2H. It was suggested by the Troll Production Technology group to only consider this branch since the calculations for BY1H are most likely incorrect as mentioned earlier.

10.5.1. Number of RCP Valves in BY2H

Start	DHG Y2 corrected	ΔP	Q_g	Q_g	$\#RCP_{gas}$	$\#RCP_{liquid}$	$\# RCP_{total}$	Q_w
[DD.MM.YY]	[bar]	[bar]	[Sm3/d]	[Am^3/d]				[Am^3/d]
04.10.10	131,5	8,28	70164	21,0	23,4	228,1	251,6	8,6
22.11.10	136,27	3,20	58320	16,5	24,7	177,1	201,8	6,8
11.02.11	136,13	2,85	59952	16,0	26,2	159,5	185,7	6,6
02.04.11	135,03	3,06	78288	17,0	32,2	168,5	200,7	7,0

Table 48: Calculation of minimum filled RCP valves in BY2H.

The resulting number of valves is plotted against the total number of valves in the well in Figure 57 below.

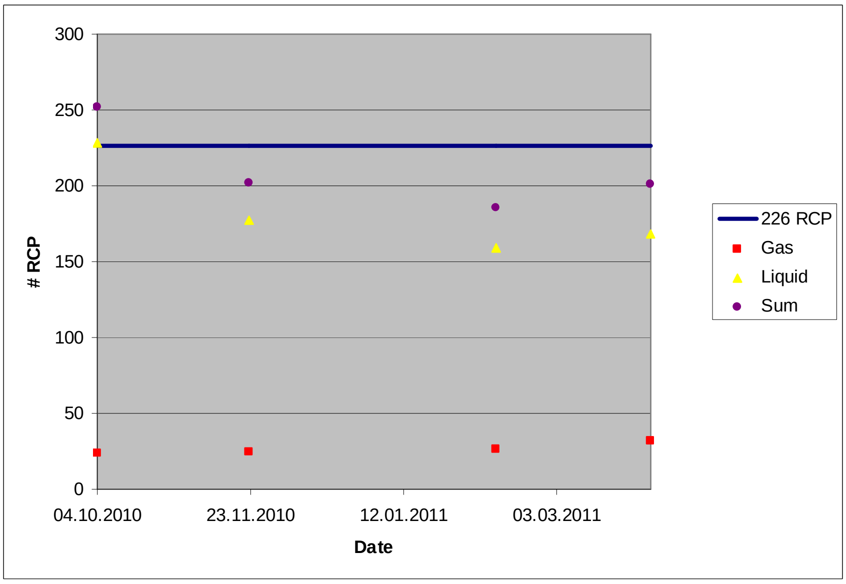

Figure 57: Number of RCP valves filled with gas and/or liquid in single tests.

It is seen that the minimum number of filled valves are less than the total available in the well.

10.5.2. Position of Single Tests With Respect to Pressure Drop Curves in BY2H

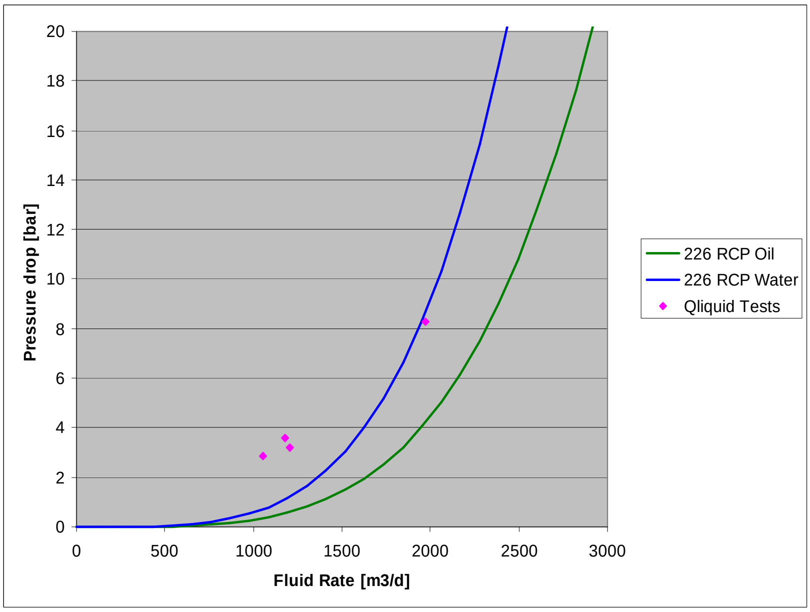

Figure 58: Pressure drop in tests in relation to pressure drop curve for BY2H.

Figure 58 shows the liquid flow rates from the single tests of BY2H in relation to the characteristics for the oil and gas for 226 RCP valves. It is seen that only one of the tests are performed with no gas present since it is situated on the blue line. A test value to the left in the chart indicates a higher GOR, thus more gas present.

11. Uncertainties

11.1. Uncertainties in the NETool^{TM} Model

It is expected that there are a lot of uncertainty related to the use of simulators to represent the real world. NETool simulates an instant in time at static conditions whereas the reality is both dynamic and more complex than the simulator. Accepting this, it is important to determine which parameters that have the largest uncertainty and will in reality have a range of valid values rather than only one correct number. There are a lot of personal evaluations when creating a model, making it hard to quantify the uncertainty in the data entries. Then it must be evaluated if the certain parameter can give rise to possible discrepancies in the results.

11.1.1. The Reservoir Model

The NETool simulations in this thesis are based on a reservoir model developed by Svend Magnus Pettersen on behalf of Statoil ASA. Usually, the model is the result of a single history match which is conditioned to production data. This is then used as a tool for investigating future production profiles. These forecasts will be linked to an uncertainty, usually not quantified, due to the non-uniqueness of the history match [32]. The reservoir models are updated continuously as more history data becomes available, but still they are not perfect. The model used in this thesis was updated earlier in 2011.

It is also seen that the interval between approximately 3900 and 4100 m MD does not contain any information. The reason for this is not quite clear, but it is probably due to a fault. BY1H is completed with blank pipes in this area and according to permeability data (Appendix G) the lack of res. data does not affect the total result much. It might cause a bigger problem when considering BY2H where the permeability data (Appendix H) are more promising and the completion type is RCP valves.

The uncertainties in TVD of OWC and GOC can also be a source of error in the simulations in NETool, but is difficult to quantify.

11.1.2. Trajectory and Completion

The trajectory of the well is not set in stone, nor is the tally. This was experienced by the author as there was a lot of inconsistency between documents obtained from different sources. It was quite difficult to determine which one was most reliable, especially when there was a lot of debate on whether the distance from the RKB to MSL was 25 or 35,5 meters, which one would assume was easy to figure out. After some debate on the possibility of different distances RKB to MSL for drilling and production facilities, the value 25 meters was chosen.

This discussion shows that the trajectory, the very first parameter given into the res. model in NETool, is not assured to be correct.

Another issue in the same category is the depths of the completions. The depths given in tallys and completion diagrams provided were not the same, and it was difficult to determine which was most reliable. This problem may be linked to the consideration in the previous section, or there may be other reasons, i.e. rat holes before installing completion to mention one. The depths in the tallys were found to be the most realistic ones.

Another concern is that it is customary in Statoil ASA to have an acceptable packer interval of + or – 5 meters, and the setting depth is not verified for all of them. This gives an additional possible source of error in the tally.

11.1.3. Reservoir Parameters

The pressure drop method assumed is a homogeneous model of a single phase flow correlation using average properties of the phases present in that section of the well. It is not accurate, but it is given as the best correlation for producing sections of the well.

The mobility is set to be related to flowing fractions since we have a log for the water saturation. It must be remembered that this represents the saturation before production, and will change over time. This is one of the reasons why the first production test was chosen for matching in NETool.

The PI model is very sensitive to what pressure is used, and also to other manually entered parameters. The NETool User Guide emphasizes *rough* estimates of flow rates, which could be a possible explanation of why the simulations run with different boundary conditions did not give the same deviations. The error could also indicate a problem with the algorithm that the NETool calculations are based on.

11.1.4. Uncertainties in the Production Well Tests

Unfortunately it is not only the computer simulations that have uncertainties linked to them; also the results obtained from physically performed tests cannot be taken for granted. First of all the test equipment may not be in satisfactory condition. An example of this is the sensor tube measuring the pressures in BY1H which is assumed to be partially plugged; basically giving unrepresentative pressures in this branch. Secondly there are comments given on tests that suggest problems with achieving a steady state production, trouble with measuring the water rate and loss of data servers. Thirdly the gas rates are often corrected for the Gas cap gas lift (GKGL), which is estimates based on the characteristics of the valves and measured pressure drops. Martin Halvorsen states that the error in the measured rates on the test separator is within the range of ± 5-10 %.

All the above mentioned factors affect the quality of the test and give sources to error in the results obtained. This is not only relevant when comparing them with the NETool simulations, but also in relation to the theoretical pressure drop calculations performed in Chapter 9. The measured pressures and flow rates from the production tests are the foundation for the calculations on the total pressure drop of the well, and if these are incorrect so will the performance evaluation of the valves be as well.

12. Conclusion

Based on experimental data different equations have been developed expressing the theoretical performance of the ICD valves and the RCP valves. It is seen in Figure 17 that the RCP is expected to restrict the production of gas better than the ICD valve for a given pressure drop. This would be beneficial for this well. On the other hand, the ICD valve is seen to deliver a higher oil rate than the RCP valve at the same pressure drop. This forms a dilemma; if choosing a completion with the ICD principle, could the gas production rates become so high that the pressure drop must be reduced enough to make it more profitable to complete with the RCP valve instead?

It can be concluded that the simulation model developed in this thesis is satisfactory, at least for the periods it is simulating. The trend of increased discrepancy between simulations and measured performance indicates that the model is best for simulating conditions closer in time to the test that is matched. This is to be expected since the simulator represents a given moment in time, a snap shot, and not a dynamic development. If this model is to be used further it is recommended to improve the method of matching the GOR. Also one should attempt to update the res. model by importing restart files simulating the field at a later stage.

It is seen that the PI calculation for both branches give very high results; in BY1H it is calculated to over 8600 $Sm^3/d/bar$, while it was found to be over 13000 $Sm^3/d/bar$ in BY2H. This implies that the pressure drops across the formation will be small and following the pressure drop across the completion is the largest contributor to the drawdown. This result is also backed up by the NETool simulations performed.

From simulations it is also suggested that the inflow profile is more even for the RCP completion than for the ICD. Another point of interest is that running BY2H alone appears to nearly double the oil production. This effect was not found in BY1H, and a reasonable explanation for this phenomenon was not discovered. Apart from in this last discussion can the results from the simulations often be explained by the completion, the permeability or the water saturation implemented by the author. This implies that in order to obtain the best possible match when making the model, it will be advantageous with some experience regarding the well in question to ensure the most reasonable choice of parameter conditions.

As seen in Chapter 11 there is a lot of uncertainty in both simulations and calculations relevant for this thesis. One important factor is the assumed error in measurements of BHP in BY1H. Of this reason it is not possible to draw any conclusions on the performance of the ICD valves. Still it can be said that the performed analysis indicate

There have not been performed that many tests in this well yet, of the simple fact that it is new. It would have been exiting to continue this investigation, especially since the well has not had a massive GBT yet and the conditions for analyzing the restriction of gas have not been optimal. It would be very interesting to see how the well continues to develop and if clearer results may be obtained regarding the different performances of the two inflow control technologies.

13. References

[1] K. H. Henriksen *et al.*, "Case Study: The Application of Inflow Control Devices in the Troll Oil Field", in: *Annual Conf. and Exhibition*, Vienna, Austria: June 12–15 2006. SPE Paper 100308.

[2] M. Halvorsen, *Troll Q-21BYH Experiences from the first RCP completed well,* Statoil ASA, unpublished.

[3] Statoil ASA, *31/2 P-13 BY1H/BY2H DG-2 Request for Approval*, Statoil ASA, unpublished.

[4] O. M. Nævdal *et al.*, "Troll B – fremtidig feltutvikling", in: *Statoil ASA Troll B Plattformsamling,* Sandefjord, Norway: November 16 2010.

[5] Statoil ASA. (2007, Sept. 21, updated 2011, Jan. 31). *Troll-feltet* [Online] [downloaded 2.2.2011]. Available:http://www.statoil.com/no/OurOperations/ExplorationProd/ncs/troll/Pages/default.aspx

[6] EnergiLink. T. Haugstad (Edt.) (2008). *Troll-feltet*. [Online] [downloaded 2.2.2011]. Available:http://energilink.tu.no/leksikon/troll-feltet.aspx

[7] Oljedirektoratet (2010, June 29). "Troll" in: *Faktaheftet* [Online] [downloaded 26.4.2011] Available:http://www.npd.no/publikasjoner/faktahefter/fakta-2010/kap-11/troll/

[8] Statoil ASA. (2007, Sept. 29, updated 2011, Jan. 31). *Troll Gass* [Online] [downloaded 2.2.2011]. Available:http://www.statoil.com/no/OurOperations/ExplorationProd/ncs/troll/Pages/TrollGas.aspx

[9] Econ Analyse. (2006, May 8). "Troll Olje. Verdiskaping og teknologiutvikling" in: *ECON-rapport nr. 2006-022*, Prosjekt nr. 47300. ISSN: 0803-5113.

[10] Statoil ASA. (2007, Sept. 29, updated 2011, Jan. 31). *Troll Olje* [Online] [downloaded 2.2.2011]. Available:http://www.statoil.com/no/OurOperations/ExplorationProd/ncs/troll/Pages/TrollOil.aspx

[11] G. H. Tonning, K. A. Nilsen (verified) and C. Hatland (approved), *Oppstartsprogram for P-13 BYH,* Statoil ASA, unpublished, [Last updated 22.9.2009].

[12] Statoil ASA. (Unknown). *Casing Programme of Well X.* Statoil ASA, [Online, internal access only] [downloaded 2.4.2011].

[13] ExproSoft AS. (Updated 2009, Aug. 13). [Online] [downloaded 15.2.2011]. Available:http://www.exprobase.com/Default.aspx?page=477

[14] A. Smith, A. Amd, (verified), A. Midttun, (approved), *Well X BY1H Screen Tally Mainbore As Run.* Statoil ASA , unpublished.

[15] L. Ulvedal, K. O. Leite, (verified), B. Gil, (approved), *Well X BY2H Screen Tally As Run.* Statoil ASA , unpublished.

[16] V. Mathiesen. (2009, April 24) *RCP Implementation in Eclipse*, Statoil ASA, unpublished, [Last updated 28.4.2009].

[17] efluids bicycle aerodynamics. *Bernoullis Equation*, [Online] [downloaded 11.06.2011].
Available:http://www.efluids.com/efluids/bicycle/bicycle_pages/Bernoulli.jsp

[18] OilGasGlossary.com. (2011). *Production test definition* [Online] [downloaded 10.6.2011].
Available :http://oilgasglossary.com/production-test.html

[19] E. Skagseth and H. M. Gundersen, *Geologi og formasjonsevaluering*, Ch. 8. Brønntesting. [Online] [downloaded 26.5.2011].
Available:http://vvi.no/interactive/index.php?module=ContentExpress&func=display&ceid=110

[20] R. Cramer *et al.*, "Well-Test Optimization and Automation", in: *Intelligent Energy Conf. and Exhibition*, Amsterdam, The Netherlands: April 11–13 2006. SPE paper 99971 [Online] [downloaded 26.5.2011] .
Available:http://www.onepetro.org/mslib/servlet/onepetropreview?id=SPE-99971-MS&soc=SPE

[21] Schlumberger. (2010). Test separator. [Online] [downloaded 26.5.2011].
Available:http://www.glossary.oilfield.slb.com/Display.cfm?Term=test%20separator

[22] Heriot-Watt University, *Production Technology II.* Heriot-Watt University. Edinburgh, Scotland: [Online] [downloaded 29.03.2011].
Available:http://www.4shared.com/get/woH9768T/Heriot_Watt_University_-_Produ.html;jsessionid=A5CC1B716C0738497C61EB251F164BDC.dc323

[23] L. Larsen and F. Ahmadhadi, (update), *Productivity indices for vertical and deviated wells in closed rectangular reservoirs (PSS).* Statoil ASA, unpublished.

[24] P. A. Goode and F. J. Kuchuk, "Inflow Performance of Horizontal Wells" in: *SPE Reservoir Engineering*, August 1991. SPE Paper: 21460.

[25] H. Devold, *Oil and gas production handbook. An introduction to oil and gas production.* ABB ATPA Oil and Gas, Oslo, Norway: 2006, pp. 43-45 [Online] [downloaded 27.5.2011].
Available:http://www.scribd.com/doc/56429313/44/Separation

[26] M. Halvorsen, (2011 May 27) *Brønntester* [Online]. Available e-mail: NKAS@statoilhydro.com Message: Brønntester

[27] Schlumberger. (2010). Pressure drawdown. [Online] [downloaded 29.5.2011].
Available:http://www.glossary.oilfield.slb.com/Display.cfm?Term=pressure%20drawdown

[28] Schlumberger. (2010). Productivity index (PI). [Online] [downloaded 2.6.2011].

Available:http://www.glossary.oilfield.slb.com/Display.cfm?Term=productivity%20index%20(PI)

[29] S. M. Pettersen (2011 April 19) *TVD Position of Gauges* [Online]. Available e-mail: NKAS@statoilhydro.com Message: Re: Permeability for Well X

[30] F. Ahmadhadi, *Final Completion P-13 BY1*, Statoil ASA, unpublished.

[31] F. Ahmadhadi, *Final Completion P-13 BY2H,* Statoil ASA, unpublished.

[32] M. Christie et al. “Prediction under Uncertainty in Reservoir Modeling”, in *European Conf. on the Mathematics of Oil Recovery*, Freiberg, Germany: September 3–6 2002 [Online] [Downloaded 30.05.2011].

[33] F. H. Escobar and M. Montealegre, “A More Accurate Correlation for the Productivity Index of Horizontal Wells”, in *J. Eng. Applied Sciences 3*: 70-78, 2008 © Medwell Journals. ISSN: 1816-949X [Online] [downloaded 01.06.2011]. Available:http://docsdrive.com/pdfs/medwelljournals/jeasci/2008/70-78.pdf

14. Appendices

Appendix A: Constants and Conversion Factors

1 inch = 0, 0254 m

1 lb = 0, 45359 kg

1 ft = 0, 3048 m

1 bbl = 5,615 ft^3 = 0, 15898 m^3

Appendix B: PVT Data

Parameter	Troll Conditions
T [deg C]	68
P [bar g]	139,36
P_b [bar g]	158,004
GOR [Sm^3/Sm^3]	50,13
ñ$_o$ [kg/m^3]	817,71
ì$_o$ [cP]	2,07
B_o [m^3/Sm^3]	1,14
C_o [bar^{-1}]	0,0009952
ñ$_g$ [kg/m^3]	122,977
ì$_g$ [cP]	0,017027
B_g [m^3/Sm^3]	0,0070016
C_g [bar^{-1}]	0,81608
ñ$_w$ [kg/m^3]	1017,83
ì$_w$ [cP]	0,50176
B_w [m^3/Sm^3]	1,0169
C_w [bar^{-1}]	6,40E-05

Table 49: PVT data at Troll.

Appendix C: PI Model in NETool

PI Models Available

1. steady state
2. semi-steady state

Vertical wells use standard radial Darcy flow equations. Horizontal wells use Joshi for steady state flow, and Babu and Odeh for semi-steady state flow. Deviated wells use a transformation of both the vertical and horizontal formulations.

For this thesis, the Babu and Odeh model is applied. It assumes a rectangular shaped reservoir with a horizontal well parallel to the sides and a semi-steady state assumption with no-flow boundaries, giving flow rates as:

$$Q = PI \cdot (P_{av} - P_w) \quad \text{.......} \quad (24)$$

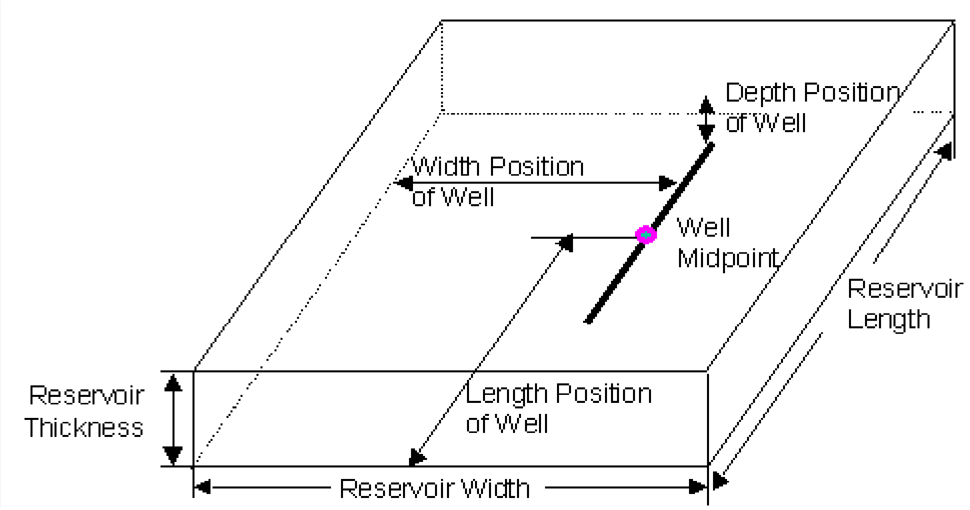

Figure 59: The Babu & Odeh PI model assumptions.

This model can handle cases where the well is not at the centre of the box reservoir, but having a well close to the boundaries will give low predications of the flow rates (tech manual).

The reservoir performance is represented by utilizing local PIs according to the permeability variations along the well trajectory. Defining the total PI for the well is also an option. If enabled, the local PIs are estimated and scaled proportionally to the local reservoir properties to fit the total well PI. In order to get the PI modelling correct, it is crucial to supply a consistent set of reservoir pressures and boundaries.

Appendix D: Mobility and Transmissibility in NETool

The mobility controls how the fluid properties and fluid-rock interactions affect the production, and is used in the basic equation for inflow of each phase according to equation 25 below:

$$Q_{phase} = \lambda_{phase} \cdot T \cdot \Delta P \quad \text{(25)}$$

Where

$$\lambda_{phase} = \frac{K_{r,phase}}{\mu_{phase}} \quad \text{(26)}$$

In NETool the mobilities may be defines in three different ways:

1. Saturations and relative permeability
2. Fractional Flow
3. Manual import of mobility

Another variable found in equation (25) is the transmissibility. It controls the inflow calculation from the reservoir into the well. It reflects the reservoir drainage geometry and conditions, the well geometry and the permeability. There are three different ways to identify this parameter:

1. From PI model
2. Manual T_A & T_B, allowing manually import of skin or calculation by NETool Skin Module
3. Manual

Transmissibility is a value that is not linked directly to the res. model, so it may be advantageous to enter it manually. An issue with this choice is that you then are not allowed to manually enter permeability and may not perform sensitivities based on this.

Appendix E: Completion BY1H NETool

Top MD [m]	Seg. length [m]	Top TVD [m]	Completion
1978.05	11.97	1548.78	Cemented blank pipe
1990.02	12.0	1549.83	Packer
2002.02	3.6415	1552.21	Packer
2005.67	8.46	1553.01	Packer
2014.13	12.0	1554.07	Tubing Plug/Choke
2026.13	12.0	1555.37	Packer
2038.13	17.84	1556.42	Blank pipe
2055.97	6.16	1557.58	Blank pipe
2062.13	12.0	1557.89	Blank pipe
2074.13	12.0001	1558.4	Blank pipe
2086.13	12.0	1558.76	Blank pipe
2098.13	12.0	1558.98	Blank pipe
2110.13	12.0	1559.08	Blank pipe
2122.13	12.0	1559.12	Blank pipe
2134.13	12.0	1559.12	Blank pipe
2146.13	12.0	1559.08	Blank pipe
2158.13	15.01	1559.0	Blank pipe
2173.14	8.99	1558.8	Blank pipe
2182.13	12.0	1558.63	Blank pipe
2194.13	2.52	1558.39	Packer
2196.65	21.48	1558.34	ICD — Baker Spiral ICD, Troll
2218.13	12.0	1557.95	ICD — Baker Spiral ICD, Troll
2230.13	12.0	1557.78	ICD — Baker Spiral ICD, Troll
2242.13	12.0	1557.64	ICD — Baker Spiral ICD, Troll
2254.13	12.0	1557.53	ICD — Baker Spiral ICD, Troll
2266.13	12.0	1557.44	ICD — Baker Spiral ICD, Troll
2278.13	12.0	1557.38	ICD — Baker Spiral ICD, Troll
2290.13	12.0	1557.36	ICD — Baker Spiral ICD, Troll
2302.13	12.0	1557.37	ICD — Baker Spiral ICD, Troll
2314.13	12.0	1557.36	ICD — Baker Spiral ICD, Troll
2326.13	12.0	1557.33	ICD — Baker Spiral ICD, Troll
2338.13	12.0	1557.28	ICD — Baker Spiral ICD, Troll

2350.13	10.35	1557.2	ICD — Baker Spiral ICD, Troll
2360.48	8.65	1557.13	ICD — Baker Spiral ICD, Troll
2369.13	2.98	1557.08	Packer
2372.11	26.02	1557.07	ICD — Baker Spiral ICD, Troll
2398.13	12.0	1556.99	ICD — Baker Spiral ICD, Troll
2410.13	12.0	1556.97	ICD — Baker Spiral ICD, Troll
2422.13	12.0	1556.98	ICD — Baker Spiral ICD, Troll
2434.13	7.59	1556.99	ICD — Baker Spiral ICD, Troll
2441.72	11.74	1557.01	ICD — Baker Spiral ICD, Troll
2453.46	9.67	1557.06	ICD — Baker Spiral ICD, Troll
2463.13	2.6	1557.14	Packer
2465.73	28.4	1557.16	ICD — Baker Spiral ICD, Troll
2494.13	12.0	1557.32	ICD — Baker Spiral ICD, Troll
2506.13	12.0	1557.28	ICD — Baker Spiral ICD, Troll
2518.13	12.0	1557.16	ICD — Baker Spiral ICD, Troll
2530.13	17.15	1556.98	ICD — Baker Spiral ICD, Troll
2547.28	9.64	1556.76	ICD — Baker Spiral ICD, Troll
2556.92	2.0	1556.68	Packer
2558.92	19.21	1556.67	ICD — Baker Spiral ICD, Troll
2578.13	12.0	1556.6	ICD — Baker Spiral ICD, Troll
2590.13	12.0	1556.58	ICD — Baker Spiral ICD, Troll
2602.13	12.0	1556.56	ICD — Baker Spiral ICD, Troll
2614.13	12.0	1556.51	ICD — Baker Spiral ICD, Troll
2626.13	12.0	1556.46	ICD — Baker Spiral ICD, Troll
2638.13	12.0	1556.44	ICD — Baker Spiral ICD, Troll
2650.13	14.16	1556.44	ICD — Baker Spiral ICD, Troll
2664.29	8.84	1556.47	ICD — Baker Spiral ICD, Troll
2673.13	2.85	1556.51	Packer
2675.98	22.15	1556.53	ICD — Baker Spiral ICD, Troll
2698.13	12.0	1556.67	ICD — Baker Spiral ICD, Troll
2710.13	12.0	1556.76	ICD — Baker Spiral ICD, Troll
2722.13	12.0	1556.83	ICD — Baker Spiral ICD, Troll
2734.13	12.0	1556.89	ICD — Baker Spiral ICD, Troll
2746.13	12.0	1556.94	ICD — Baker Spiral ICD, Troll
2758.13	12.0	1556.98	ICD — Baker Spiral ICD, Troll

2770.13	10.95	1557.02	ICD — Baker Spiral ICD, Troll
2781.08	9.05	1557.05	ICD — Baker Spiral ICD, Troll
2790.13	2.57	1557.07	ICD — Baker Spiral ICD, Troll
2792.7	25.43	1557.07	ICD — Baker Spiral ICD, Troll
2818.13	12.0	1557.12	ICD — Baker Spiral ICD, Troll
2830.13	12.0	1557.13	ICD — Baker Spiral ICD, Troll
2842.13	12.0	1557.12	ICD — Baker Spiral ICD, Troll
2854.13	8.77	1557.09	ICD — Baker Spiral ICD, Troll
2862.9	9.23	1557.07	ICD — Baker Spiral ICD, Troll
2872.13	2.37	1557.04	Packer
2874.5	27.63	1557.03	ICD — Baker Spiral ICD, Troll
2902.13	12.0	1556.97	ICD — Baker Spiral ICD, Troll
2914.13	12.0	1556.97	ICD — Baker Spiral ICD, Troll
2926.13	12.0	1556.97	ICD — Baker Spiral ICD, Troll
2938.13	12.0	1556.98	ICD — Baker Spiral ICD, Troll
2950.13	12.0	1557.0	ICD — Baker Spiral ICD, Troll
2962.13	12.0	1557.03	ICD — Baker Spiral ICD, Troll
2974.13	12.004	1557.06	ICD — Baker Spiral ICD, Troll
2986.13	16.93	1557.11	ICD — Baker Spiral ICD, Troll
3003.06	9.7	1557.18	ICD — Baker Spiral ICD, Troll
3012.76	2.49	1557.21	Packer
3015.25	19.51	1557.22	ICD — Baker Spiral ICD, Troll
3034.76	12.0	1557.27	ICD — Baker Spiral ICD, Troll
3046.76	12.0	1557.29	ICD — Baker Spiral ICD, Troll
3058.76	12.0	1557.32	ICD — Baker Spiral ICD, Troll
3070.76	12.0	1557.34	ICD — Baker Spiral ICD, Troll
3082.76	14.38	1557.36	ICD — Baker Spiral ICD, Troll
3097.14	9.62	1557.39	ICD — Baker Spiral ICD, Troll
3106.76	2.12	1557.42	Packer
3108.88	21.88	1557.43	Blank pipe
3130.76	13.24	1557.51	Blank pipe
3144.0	8.76	1557.56	Blank pipe
3152.76	2.87	1557.58	Packer
3155.63	23.13	1557.59	ICD — Baker Spiral ICD, Troll
3178.76	12.0	1557.57	ICD — Baker Spiral ICD, Troll

3190.76	12.0	1557.52	ICD — Baker Spiral ICD, Troll
3202.76	12.0	1557.45	ICD — Baker Spiral ICD, Troll
3214.76	11.14	1557.38	ICD — Baker Spiral ICD, Troll
3225.9	8.86	1557.33	ICD — Baker Spiral ICD, Troll
3234.76	2.62	1557.3	Packer
3237.38	25.38	1557.3	ICD — Baker Spiral ICD, Troll
3262.76	12.0	1557.31	ICD — Baker Spiral ICD, Troll
3274.76	12.0	1557.3	ICD — Baker Spiral ICD, Troll
3286.76	12.0	1557.27	ICD — Baker Spiral ICD, Troll
3298.76	12.0	1557.24	ICD — Baker Spiral ICD, Troll
3310.76	8.4	1557.2	ICD — Baker Spiral ICD, Troll
3319.16	8.6	1557.17	ICD — Baker Spiral ICD, Troll
3327.76	2.89	1557.13	Packer
3330.65	28.11	1557.12	ICD — Baker Spiral ICD, Troll
3358.76	12.0	1557.03	ICD — Baker Spiral ICD, Troll
3370.76	12.0	1556.99	ICD — Baker Spiral ICD, Troll
3382.76	12.0	1556.96	ICD — Baker Spiral ICD, Troll
3394.76	12.0	1556.92	ICD — Baker Spiral ICD, Troll
3406.76	12.0	1556.88	ICD — Baker Spiral ICD, Troll
3418.76	12.0	1556.85	ICD — Baker Spiral ICD, Troll
3430.76	5.0	1556.82	ICD — Baker Spiral ICD, Troll
3435.76	9.0	1556.79	ICD — Baker Spiral ICD, Troll
3444.76	2.7	1556.7	Packer
3447.46	31.3	1556.66	ICD — Baker Spiral ICD, Troll
3478.76	12.0	1556.15	ICD — Baker Spiral ICD, Troll
3490.76	12.0	1555.93	ICD — Baker Spiral ICD, Troll
3502.76	12.0	1555.75	ICD — Baker Spiral ICD, Troll
3514.76	12.0	1555.59	ICD — Baker Spiral ICD, Troll
3526.76	12.0	1555.46	ICD — Baker Spiral ICD, Troll
3538.76	12.0	1555.36	ICD — Baker Spiral ICD, Troll
3550.76	12.0	1555.28	ICD — Baker Spiral ICD, Troll
3562.76	12.0	1555.26	ICD — Baker Spiral ICD, Troll
3574.76	12.0	1555.26	ICD — Baker Spiral ICD, Troll
3586.76	12.0	1555.25	ICD — Baker Spiral ICD, Troll
3598.76	12.0	1555.23	ICD — Baker Spiral ICD, Troll

3610.76	12.0	1555.21	ICD — Baker Spiral ICD, Troll
3622.76	12.0	1555.18	ICD — Baker Spiral ICD, Troll
3634.76	10.56	1555.15	ICD — Baker Spiral ICD, Troll
3645.32	9.44	1555.15	ICD — Baker Spiral ICD, Troll
3654.76	2.23	1555.18	Packer
3656.99	25.77	1555.18	ICD — Baker Spiral ICD, Troll
3682.76	12.0	1555.34	ICD — Baker Spiral ICD, Troll
3694.76	12.0	1555.44	ICD — Baker Spiral ICD, Troll
3706.76	12.0	1555.53	ICD — Baker Spiral ICD, Troll
3718.76	12.0	1555.6	ICD — Baker Spiral ICD, Troll
3730.76	12.0	1555.66	ICD — Baker Spiral ICD, Troll
3742.76	12.0	1555.69	ICD — Baker Spiral ICD, Troll
3754.76	12.0	1555.69	ICD — Baker Spiral ICD, Troll
3766.76	12.0	1555.67	ICD — Baker Spiral ICD, Troll
3778.76	6.94	1555.62	ICD — Baker Spiral ICD, Troll
3785.7	9.06	1555.58	ICD — Baker Spiral ICD, Troll
3794.76	2.64	1555.52	Packer
3797.4	29.36	1555.51	ICD — Baker Spiral ICD, Troll
3826.76	12.0	1555.38	ICD — Baker Spiral ICD, Troll
3838.76	12.0	1555.37	ICD — Baker Spiral ICD, Troll
3850.76	12.0	1555.38	ICD — Baker Spiral ICD, Troll
3862.76	12.0	1555.4	ICD — Baker Spiral ICD, Troll
3874.76	12.0	1555.38	ICD — Baker Spiral ICD, Troll
3886.76	12.0	1555.32	ICD — Baker Spiral ICD, Troll
3898.76	12.0	1555.23	ICD — Baker Spiral ICD, Troll
3910.76	12.0	1555.15	ICD — Baker Spiral ICD, Troll
3922.76	14.74	1555.08	ICD — Baker Spiral ICD, Troll
3937.5	9.26	1555.04	Blank pipe
3946.76	2.49	1555.04	Packer
3949.25	21.51	1555.04	Blank pipe
3970.76	12.0	1554.98	Blank pipe
3982.76	12.0	1554.99	Blank pipe
3994.76	12.0	1555.13	Blank pipe
4006.76	12.0	1555.44	Blank pipe
4018.76	12.0	1555.91	Blank pipe

4030.76	12.0	1556.57	Blank pipe
4042.76	12.0	1557.22	Blank pipe
4054.76	12.0	1557.69	Blank pipe
4066.76	12.0	1558.0	Blank pipe
4078.76	12.0	1558.12	Blank pipe
4090.76	12.0	1558.05	Blank pipe
4102.76	12.0	1557.82	Blank pipe
4114.76	12.0	1557.43	Blank pipe
4126.76	9.69	1556.96	Blank pipe
4136.45	9.31	1556.53	Blank pipe
4145.76	2.43	1556.12	Packer
4148.19	26.57	1556.02	ICD — Baker Spiral ICD, Troll
4174.76	12.0	1555.18	ICD — Baker Spiral ICD, Troll
4186.76	12.0	1554.98	ICD — Baker Spiral ICD, Troll
4198.76	12.0	1554.85	ICD — Baker Spiral ICD, Troll
4210.76	12.0	1554.77	ICD — Baker Spiral ICD, Troll
4222.76	12.0	1554.72	ICD — Baker Spiral ICD, Troll
4234.76	12.0	1554.7	ICD — Baker Spiral ICD, Troll
4246.76	12.0	1554.72	ICD — Baker Spiral ICD, Troll
4258.76	12.0	1554.81	ICD — Baker Spiral ICD, Troll
4270.76	17.79	1554.93	ICD — Baker Spiral ICD, Troll
4288.55	9.21	1555.06	ICD — Baker Spiral ICD, Troll
4297.76	2.47	1555.1	Packer
4300.23	18.53	1555.11	ICD — Baker Spiral ICD, Troll
4318.76	12.0	1555.05	ICD — Baker Spiral ICD, Troll
4330.76	12.0	1554.95	ICD — Baker Spiral ICD, Troll
4342.76	12.0	1554.83	ICD — Baker Spiral ICD, Troll
4354.76	12.0	1554.69	ICD — Baker Spiral ICD, Troll
4366.76	12.0	1554.56	ICD — Baker Spiral ICD, Troll
4378.76	12.0	1554.44	ICD — Baker Spiral ICD, Troll
4390.76	12.0	1554.35	ICD — Baker Spiral ICD, Troll
4402.76	12.0	1554.29	ICD — Baker Spiral ICD, Troll
4414.76	12.0	1554.27	ICD — Baker Spiral ICD, Troll
4426.76	13.21	1554.27	ICD — Baker Spiral ICD, Troll
4439.97	8.79	1554.28	ICD — Baker Spiral ICD, Troll

4448.76	2.59	1554.3	Packer
4451.35	23.41	1554.3	ICD — Baker Spiral ICD, Troll
4474.76	12.0	1554.37	ICD — Baker Spiral ICD, Troll
4486.76	12.0	1554.42	ICD — Baker Spiral ICD, Troll
4498.76	12.0	1554.48	ICD — Baker Spiral ICD, Troll
4510.76	12.0	1554.53	ICD — Baker Spiral ICD, Troll
4522.76	12.0	1554.55	ICD — Baker Spiral ICD, Troll
4534.76	12.0	1554.56	ICD — Baker Spiral ICD, Troll
4546.76	12.0	1554.57	ICD — Baker Spiral ICD, Troll
4558.76	12.0	1554.56	ICD — Baker Spiral ICD, Troll
4570.76	12.0	1554.5	ICD — Baker Spiral ICD, Troll
4582.76	12.0	1554.41	ICD — Baker Spiral ICD, Troll
4594.76	7.82	1554.3	ICD — Baker Spiral ICD, Troll
4602.58	9.18	1554.22	ICD — Baker Spiral ICD, Troll
4611.76	2.44	1554.13	Packer
4614.2	28.56	1554.11	ICD — Baker Spiral ICD, Troll
4642.76	12.0	1553.9	ICD — Baker Spiral ICD, Troll
4654.76	12.0	1553.83	ICD — Baker Spiral ICD, Troll
4666.76	12.0	1553.75	ICD — Baker Spiral ICD, Troll
4678.76	12.0	1553.69	ICD — Baker Spiral ICD, Troll
4690.76	12.0	1553.66	ICD — Baker Spiral ICD, Troll
4702.76	16.8	1553.65	ICD — Baker Spiral ICD, Troll
4719.56	9.2	1553.61	Blank pipe
4728.76	2.54	1553.58	Blank pipe
4731.3	19.46	1553.57	Blank pipe
4750.76	12.0	1553.44	Blank pipe
4762.76	12.0	1553.32	Blank pipe
4774.76	12.0	1553.18	Blank pipe
4786.76	12.0	1553.01	Blank pipe
4798.76	12.0	1552.81	Blank pipe
4810.76	12.0	1552.58	Blank pipe
4822.76	12.0	1552.32	Blank pipe
4834.76	12.0	1552.03	Blank pipe
4846.76	12.0	1551.76	Blank pipe
4858.76	12.0	1551.54	Blank pipe

4870.76	12.0	1551.41	Blank pipe
4882.76	12.0	1551.33	Blank pipe
4894.76	12.0	1551.32	Blank pipe
4906.76	12.0	1551.33	Blank pipe
4918.76	12.0	1551.33	Blank pipe
4930.76	12.0	1551.31	Blank pipe
4942.76	12.0	1551.33	Blank pipe
4954.76	12.0	1551.41	Blank pipe
4966.76	12.0	1551.53	Blank pipe
4978.76	12.0	1551.7	Blank pipe
4990.76	12.0	1551.9	Blank pipe
5002.76	12.0	1552.07	Blank pipe
5014.76	12.0	1552.18	Blank pipe
5026.76	12.0	1552.25	Blank pipe
5038.76	12.0	1552.28	Blank pipe
5050.76	8.32	1552.27	Blank pipe
5059.08	9.68	1552.24	Blank pipe
5068.76	2.08	1552.15	Packer
5070.84	11.73	1552.13	ICD — Baker Spiral ICD, Troll
5082.57	11.75	1551.98	Blank pipe
5094.32	28.44	1551.78	ICD — Baker Spiral ICD, Troll
5122.76	6.66	1551.4	ICD — Baker Spiral ICD, Troll
5129.42	9.34	1551.4	Blank pipe
5138.76	2.3	1551.45	Packer
5141.06	23.49	1551.47	Blank pipe
5164.55	9.21	1551.9	Blank pipe
5173.76	2.52	1552.09	Packer
5176.28	23.35	1552.14	ICD — Baker Spiral ICD, Troll
5199.63	11.62	1552.42	Packer
5211.25	19.51	1552.45	Blank pipe
5230.76	12.0	1552.44	Blank pipe
5242.76	12.0	1552.47	Blank pipe
5254.76	12.0	1552.57	Blank pipe
5266.76	12.0	1552.77	Blank pipe
5278.76	7.02	1553.08	Blank pipe

Appendix F: Completion BY2H NETool

Top MD [m]	Seg. length [m]	Top TVD [m]	Completion
2005.67	8.47	1553.01	Cemented blank pipe
2014.14	12.0	1554.08	Tubing Plug/Choke
2026.14	12.0	1555.38	Packer
2038.14	12.0	1556.45	Blank pipe
2050.14	11.66	1557.27	Packer
2061.8	12.34	1557.87	ICD — Statoil Autonomous ICD
2074.14	12.0001	1558.1	ICD — Statoil Autonomous ICD
2086.14	12.0	1558.13	ICD — Statoil Autonomous ICD
2098.14	10.31	1558.14	ICD — Statoil Autonomous ICD
2108.45	10.15	1558.12	ICD — Statoil Autonomous ICD
2118.6	1.55	1558.09	Packer
2120.15	25.99	1558.09	ICD — Statoil Autonomous ICD
2146.14	12.0	1557.97	ICD — Statoil Autonomous ICD
2158.14	12.0	1557.89	ICD — Statoil Autonomous ICD
2170.14	8.27	1557.82	ICD — Statoil Autonomous ICD
2178.41	10.19	1557.79	Blank pipe
2188.6	1.42	1557.78	Packer
2190.02	28.12	1557.78	Blank pipe
2218.14	12.0	1557.76	Blank pipe
2230.14	12.0	1557.76	Blank pipe
2242.14	12.0	1557.76	Blank pipe
2254.14	12.0	1557.75	Blank pipe
2266.14	12.0	1557.74	Blank pipe
2278.14	12.0	1557.72	Blank pipe
2290.14	12.0	1557.7	Blank pipe
2302.14	12.0	1557.69	Blank pipe
2314.14	12.0	1557.68	Blank pipe
2326.14	12.0	1557.68	Blank pipe
2338.14	12.0	1557.68	Blank pipe
2350.14	12.0	1557.68	Blank pipe
2362.14	11.46	1557.69	Blank pipe
2373.6	3.82	1557.69	Packer

2377.42	20.72	1557.69	ICD — Statoil Autonomous ICD
2398.14	12.0	1557.7	ICD — Statoil Autonomous ICD
2410.14	13.88	1557.69	ICD — Statoil Autonomous ICD
2424.02	11.75	1557.65	Blank pipe
2435.77	2.83	1557.59	Packer
2438.6	8.86	1557.56	ICD — Statoil Autonomous ICD
2447.46	11.74	1557.48	Blank pipe
2459.2	11.59	1557.34	ICD — Statoil Autonomous ICD
2470.79	11.74	1557.15	Blank pipe
2482.53	11.7	1556.96	ICD — Statoil Autonomous ICD
2494.23	11.22	1556.81	Blank pipe
2505.45	11.68	1556.72	ICD — Statoil Autonomous ICD
2517.13	11.75	1556.66	Blank pipe
2528.88	11.69	1556.65	ICD — Statoil Autonomous ICD
2540.57	8.03	1556.68	Blank pipe
2548.6	3.71	1556.69	Packer
2552.31	37.83	1556.7	ICD — Statoil Autonomous ICD
2590.14	12.0	1556.99	ICD — Statoil Autonomous ICD
2602.14	12.0	1557.16	ICD — Statoil Autonomous ICD
2614.14	12.0	1557.3	ICD — Statoil Autonomous ICD
2626.14	12.0	1557.41	ICD — Statoil Autonomous ICD
2638.14	6.97	1557.45	ICD — Statoil Autonomous ICD
2645.11	3.49	1557.45	ICD — Statoil Autonomous ICD
2648.6	2.11	1557.45	Packer
2650.71	29.34	1557.44	ICD — Statoil Autonomous ICD
2680.05	12.0	1557.39	ICD — Statoil Autonomous ICD
2692.05	12.0	1557.38	ICD — Statoil Autonomous ICD
2704.05	12.0	1557.4	ICD — Statoil Autonomous ICD
2716.05	15.52	1557.43	ICD — Statoil Autonomous ICD
2731.57	10.94	1557.51	ICD — Statoil Autonomous ICD
2742.51	0.75	1557.58	Packer
2743.26	20.79	1557.59	ICD — Statoil Autonomous ICD
2764.05	12.0	1557.7	ICD — Statoil Autonomous ICD
2776.05	12.0	1557.71	ICD — Statoil Autonomous ICD
2788.05	12.0	1557.63	ICD — Statoil Autonomous ICD

2800.05	12.0	1557.51	ICD — Statoil Autonomous ICD
2812.05	12.0	1557.38	ICD — Statoil Autonomous ICD
2824.05	12.58	1557.25	ICD — Statoil Autonomous ICD
2836.63	5.88	1557.15	ICD — Statoil Autonomous ICD
2842.51	5.81	1557.13	Packer
2848.32	23.73	1557.13	ICD — Statoil Autonomous ICD
2872.05	12.0	1557.18	ICD — Statoil Autonomous ICD
2884.05	12.0	1557.25	ICD — Statoil Autonomous ICD
2896.05	12.0	1557.39	ICD — Statoil Autonomous ICD
2908.05	12.0	1557.62	ICD — Statoil Autonomous ICD
2920.05	12.0	1557.85	ICD — Statoil Autonomous ICD
2932.05	8.14	1558.04	ICD — Statoil Autonomous ICD
2940.19	11.32	1558.13	Blank pipe
2951.51	1.0	1558.2	Packer
2952.51	22.9	1558.2	ICD — Statoil Autonomous ICD
2975.41	11.764	1558.05	Blank pipe
2987.17	11.4	1557.93	ICD — Statoil Autonomous ICD
2998.57	3.94	1557.83	Blank pipe
3002.51	7.84	1557.79	Packer
3010.35	29.7	1557.73	ICD — Statoil Autonomous ICD
3040.05	12.0	1557.67	ICD — Statoil Autonomous ICD
3052.05	12.0	1557.75	ICD — Statoil Autonomous ICD
3064.05	12.0	1557.88	ICD — Statoil Autonomous ICD
3076.05	12.0	1558.04	ICD — Statoil Autonomous ICD
3088.05	12.0	1558.2	ICD — Statoil Autonomous ICD
3100.05	12.0	1558.32	ICD — Statoil Autonomous ICD
3112.05	12.0	1558.39	ICD — Statoil Autonomous ICD
3124.05	14.5	1558.43	ICD — Statoil Autonomous ICD
3138.55	3.96	1558.43	ICD — Statoil Autonomous ICD
3142.51	7.75	1558.43	Packer
3150.26	21.79	1558.43	ICD — Statoil Autonomous ICD
3172.05	12.0	1558.49	ICD — Statoil Autonomous ICD
3184.05	12.0	1558.54	ICD — Statoil Autonomous ICD
3196.05	12.0	1558.62	ICD — Statoil Autonomous ICD
3208.05	12.0	1558.69	ICD — Statoil Autonomous ICD

3220.05	11.84	1558.74	ICD — Statoil Autonomous ICD
3231.89	10.62	1558.77	ICD — Statoil Autonomous ICD
3242.51	1.06	1558.78	Packer
3243.57	24.48	1558.78	ICD — Statoil Autonomous ICD
3268.05	12.0	1558.79	ICD — Statoil Autonomous ICD
3280.05	12.0	1558.79	ICD — Statoil Autonomous ICD
3292.05	12.0	1558.79	ICD — Statoil Autonomous ICD
3304.05	12.0	1558.79	ICD — Statoil Autonomous ICD
3316.05	12.0	1558.78	ICD — Statoil Autonomous ICD
3328.05	8.36	1558.78	ICD — Statoil Autonomous ICD
3336.41	6.1	1558.78	ICD — Statoil Autonomous ICD
3342.51	5.48	1558.78	Packer
3347.99	28.06	1558.78	ICD — Statoil Autonomous ICD
3376.05	12.0	1558.77	ICD — Statoil Autonomous ICD
3388.05	12.0	1558.76	ICD — Statoil Autonomous ICD
3400.05	12.0	1558.74	ICD — Statoil Autonomous ICD
3412.05	12.0	1558.73	ICD — Statoil Autonomous ICD
3424.05	5.34	1558.72	ICD — Statoil Autonomous ICD
3429.39	10.12	1558.71	ICD — Statoil Autonomous ICD
3439.51	1.48	1558.7	ICD — Statoil Autonomous ICD
3440.99	31.06	1558.7	Packer
3472.05	12.0	1558.7	ICD — Statoil Autonomous ICD
3484.05	12.0	1558.66	ICD — Statoil Autonomous ICD
3496.05	12.0	1558.61	ICD — Statoil Autonomous ICD
3508.05	12.0	1558.52	ICD — Statoil Autonomous ICD
3520.05	13.88	1558.42	ICD — Statoil Autonomous ICD
3533.93	8.58	1558.28	ICD — Statoil Autonomous ICD
3542.51	3.03	1558.2	Packer
3545.54	22.51	1558.17	ICD — Statoil Autonomous ICD
3568.05	12.0	1557.97	ICD — Statoil Autonomous ICD
3580.05	12.0	1557.87	ICD — Statoil Autonomous ICD
3592.05	12.0	1557.77	ICD — Statoil Autonomous ICD
3604.05	12.0	1557.65	ICD — Statoil Autonomous ICD
3616.05	12.0	1557.55	ICD — Statoil Autonomous ICD
3628.05	10.65	1557.46	ICD — Statoil Autonomous ICD

3638.7	3.81	1557.39	ICD — Statoil Autonomous ICD
3642.51	7.79	1557.37	Packer
3650.3	25.75	1557.35	ICD — Statoil Autonomous ICD
3676.05	12.0	1557.26	ICD — Statoil Autonomous ICD
3688.05	12.0	1557.2	ICD — Statoil Autonomous ICD
3700.05	12.0	1557.11	ICD — Statoil Autonomous ICD
3712.05	12.0	1556.99	ICD — Statoil Autonomous ICD
3724.05	7.81	1556.86	ICD — Statoil Autonomous ICD
3731.86	10.65	1556.78	ICD — Statoil Autonomous ICD
3742.51	0.95	1556.68	Packer
3743.46	28.59	1556.67	ICD — Statoil Autonomous ICD
3772.05	12.0	1556.45	ICD — Statoil Autonomous ICD
3784.05	12.0	1556.39	ICD — Statoil Autonomous ICD
3796.05	12.0	1556.31	ICD — Statoil Autonomous ICD
3808.05	12.0	1556.22	ICD — Statoil Autonomous ICD
3820.05	16.75	1556.13	ICD — Statoil Autonomous ICD
3836.8	5.71	1555.99	ICD — Statoil Autonomous ICD
3842.51	5.89	1555.94	Packer
3848.4	19.65	1555.89	ICD — Statoil Autonomous ICD
3868.05	12.0	1555.71	ICD — Statoil Autonomous ICD
3880.05	12.0	1555.59	ICD — Statoil Autonomous ICD
3892.05	12.0	1555.48	ICD — Statoil Autonomous ICD
3904.05	12.0	1555.37	ICD — Statoil Autonomous ICD
3916.05	13.34	1555.28	ICD — Statoil Autonomous ICD
3929.39	10.12	1555.2	ICD — Statoil Autonomous ICD
3939.51	1.57	1555.16	Packer
3941.08	22.97	1555.15	ICD — Statoil Autonomous ICD
3964.05	12.0	1555.14	ICD — Statoil Autonomous ICD
3976.05	12.0	1555.18	ICD — Statoil Autonomous ICD
3988.05	12.0	1555.24	ICD — Statoil Autonomous ICD
4000.05	12.0	1555.33	ICD — Statoil Autonomous ICD
4012.05	12.0	1555.44	ICD — Statoil Autonomous ICD
4024.05	10.15	1555.51	ICD — Statoil Autonomous ICD
4034.2	8.31	1555.53	ICD — Statoil Autonomous ICD
4042.51	3.28	1555.53	Packer

4045.79	26.26	1555.52	ICD — Statoil Autonomous ICD
4072.05	12.0	1555.35	ICD — Statoil Autonomous ICD
4084.05	12.0	1555.23	ICD — Statoil Autonomous ICD
4096.05	12.0	1555.12	ICD — Statoil Autonomous ICD
4108.05	12.0	1555.02	ICD — Statoil Autonomous ICD
4120.05	12.0	1554.96	ICD — Statoil Autonomous ICD
4132.05	10.46	1554.93	ICD — Statoil Autonomous ICD
4142.51	8.3	1554.91	Packer
4150.81	17.24	1554.91	ICD — Statoil Autonomous ICD
4168.05	12.0	1554.92	ICD — Statoil Autonomous ICD
4180.05	12.0	1554.93	ICD — Statoil Autonomous ICD
4192.05	12.0	1554.92	ICD — Statoil Autonomous ICD
4204.05	12.0	1554.89	ICD — Statoil Autonomous ICD
4216.05	12.0	1554.85	ICD — Statoil Autonomous ICD
4228.05	12.0	1554.77	ICD — Statoil Autonomous ICD
4240.05	15.61	1554.68	ICD — Statoil Autonomous ICD
4255.66	10.85	1554.56	Blank pipe
4266.51	0.9	1554.51	Packer
4267.41	20.64	1554.5	Blank pipe
4288.05	12.0	1554.51	Blank pipe
4300.05	13.93	1554.58	Blank pipe
4313.98	8.53	1554.72	Blank pipe
4322.51	3.09	1554.81	Packer
4325.6	22.45	1554.84	ICD — Statoil Autonomous ICD
4348.05	12.0	1555.07	ICD — Statoil Autonomous ICD
4360.05	12.0	1555.13	ICD — Statoil Autonomous ICD
4372.05	12.0	1555.08	ICD — Statoil Autonomous ICD
4384.05	12.0	1554.93	ICD — Statoil Autonomous ICD
4396.05	12.0	1554.75	ICD — Statoil Autonomous ICD
4408.05	12.0	1554.56	ICD — Statoil Autonomous ICD
4420.05	12.0	1554.41	ICD — Statoil Autonomous ICD
4432.05	7.46	1554.34	ICD — Statoil Autonomous ICD
4439.51	1.93	1554.33	Packer
4441.44	26.61	1554.34	ICD — Statoil Autonomous ICD
4468.05	12.0	1554.42	ICD — Statoil Autonomous ICD

4480.05	12.0	1554.47	ICD — Statoil Autonomous ICD
4492.05	12.0	1554.52	ICD — Statoil Autonomous ICD
4504.05	12.0	1554.56	ICD — Statoil Autonomous ICD
4516.05	12.0	1554.59	ICD — Statoil Autonomous ICD
4528.05	14.46	1554.6	ICD — Statoil Autonomous ICD
4542.51	3.9	1554.6	Packer
4546.41	17.64	1554.59	ICD — Statoil Autonomous ICD
4564.05	12.0	1554.54	ICD — Statoil Autonomous ICD
4576.05	12.0	1554.47	ICD — Statoil Autonomous ICD
4588.05	12.0	1554.38	ICD — Statoil Autonomous ICD
4600.05	12.0	1554.29	ICD — Statoil Autonomous ICD
4612.05	12.0	1554.21	ICD — Statoil Autonomous ICD
4624.05	12.0	1554.14	ICD — Statoil Autonomous ICD
4636.05	12.0	1554.11	ICD — Statoil Autonomous ICD
4648.05	12.0	1554.08	ICD — Statoil Autonomous ICD
4660.05	12.0	1554.04	ICD — Statoil Autonomous ICD
4672.05	12.0	1553.96	ICD — Statoil Autonomous ICD
4684.05	12.0	1553.86	ICD — Statoil Autonomous ICD
4696.05	19.46	1553.75	ICD — Statoil Autonomous ICD
4715.51	5.08	1553.51	Packer
4720.59	11.46	1553.43	Blank pipe
4732.05	12.0	1553.24	Blank pipe
4744.05	12.0	1553.05	Blank pipe
4756.05	12.0	1552.88	Blank pipe
4768.05	12.0	1552.76	Blank pipe
4780.05	12.0	1552.69	Blank pipe
4792.05	12.0	1552.66	Blank pipe
4804.05	12.0	1552.66	Blank pipe
4816.05	12.0	1552.64	Blank pipe
4828.05	12.0	1552.64	Blank pipe
4840.05	12.0	1552.65	Blank pipe
4852.05	12.0	1552.67	Blank pipe
4864.05	12.0	1552.7	Blank pipe
4876.05	12.0	1552.73	Blank pipe
4888.05	12.0	1552.77	Blank pipe

4900.05	15.46	1552.8	Blank pipe
4915.51	4.14	1552.83	Packer
4919.65	16.4	1552.84	ICD — Statoil Autonomous ICD
4936.05	12.0	1552.87	ICD — Statoil Autonomous ICD
4948.05	12.0	1552.88	ICD — Statoil Autonomous ICD
4960.05	12.0	1552.91	ICD — Statoil Autonomous ICD
4972.05	12.0	1552.94	ICD — Statoil Autonomous ICD
4984.05	5.46	1552.96	ICD — Statoil Autonomous ICD
4989.51	7.0	1552.96	ICD — Statoil Autonomous ICD
4996.51	4.69	1552.96	Packer
5001.2	30.85	1552.96	ICD — Statoil Autonomous ICD
5032.05	12.0	1552.9	ICD — Statoil Autonomous ICD
5044.05	12.0	1552.87	ICD — Statoil Autonomous ICD
5056.05	1.46	1552.83	ICD — Statoil Autonomous ICD
5057.51	1.83	1552.82	Packer
5059.34	32.71	1552.82	ICD — Statoil Autonomous ICD
5092.05	12.0	1552.75	ICD — Statoil Autonomous ICD
5104.05	12.0	1552.77	ICD — Statoil Autonomous ICD
5116.05	12.0	1552.83	ICD — Statoil Autonomous ICD
5128.05	12.0	1552.93	ICD — Statoil Autonomous ICD
5140.05	12.0	1553.08	ICD — Statoil Autonomous ICD
5152.05	12.0	1553.28	ICD — Statoil Autonomous ICD
5164.05	8.46	1553.55	ICD — Statoil Autonomous ICD
5172.51	2.21	1553.76	Packer
5174.72	30.79	1553.82	ICD — Statoil Autonomous ICD
5205.51	4.2	1554.69	Packer
5209.71	14.34	1554.82	ICD — Statoil Autonomous ICD
5224.05	12.0	1555.24	ICD — Statoil Autonomous ICD
5236.05	12.0	1555.55	ICD — Statoil Autonomous ICD
5248.05	12.0	1555.81	ICD — Statoil Autonomous ICD
5260.05	8.17	1555.99	ICD — Statoil Autonomous ICD
5268.22	15.83	1556.05	Packer
5284.05	12.0	1556.05	Blank pipe
5296.05	14.92	1555.99	Blank pipe
5310.97	9.08	1555.92	Blank pipe

5320.05	12.0	1555.88	Blank pipe
5332.05	12.0	1555.86	Blank pipe
5344.05	12.0	1555.87	Blank pipe
5356.05	12.0	1555.92	Blank pipe
5368.05	12.0	1556.02	Blank pipe

Appendix G: Horizontal Permeability BY1H NETool

Top MD [m]	Seg. length [m]	Top TVD [m]	κH [D]
2005.67	8.47	1553.01	-
2014.14	12.0	1554.08	1.01551
2026.14	12.0	1555.38	-
2038.14	12.0	1556.45	2.0951
2050.14	11.66	1557.27	-
2061.8	12.34	1557.87	4.84141
2074.14	12.0001	1558.1	4.47589
2086.14	12.0	1558.13	6.97598
2098.14	10.31	1558.14	5.19598
2108.45	10.15	1558.12	3.19359
2118.6	1.55	1558.09	-
2120.15	25.99	1558.09	3.48034
2146.14	12.0	1557.97	1.98453
2158.14	12.0	1557.89	4.72208
2170.14	8.27	1557.82	4.57321
2178.41	10.19	1557.79	4.0184
2188.6	1.42	1557.78	-
2190.02	28.12	1557.78	3.75194
2218.14	12.0	1557.76	4.5032
2230.14	12.0	1557.76	5.10993
2242.14	12.0	1557.76	6.51826
2254.14	12.0	1557.75	6.31486
2266.14	12.0	1557.74	6.26843
2278.14	12.0	1557.72	4.76998
2290.14	12.0	1557.7	2.85109
2302.14	12.0	1557.69	2.03178
2314.14	12.0	1557.68	3.27524
2326.14	12.0	1557.68	1.80046
2338.14	12.0	1557.68	0.531844
2350.14	12.0	1557.68	1.09488
2362.14	11.46	1557.69	5.79336
2373.6	3.82	1557.69	-
2377.42	20.72	1557.69	1.25706

2398.14	12.0	1557.7	0.314796
2410.14	13.88	1557.69	1.80666
2424.02	11.75	1557.65	2.00115
2435.77	2.83	1557.59	-
2438.6	8.86	1557.56	1.52955
2447.46	11.74	1557.48	5.84006
2459.2	11.59	1557.34	5.89224
2470.79	11.74	1557.15	7.62669
2482.53	11.7	1556.96	7.65615
2494.23	11.22	1556.81	9.07369
2505.45	11.68	1556.72	12.1766
2517.13	11.75	1556.66	9.44687
2528.88	11.69	1556.65	5.67087
2540.57	8.03	1556.68	5.67087
2548.6	3.71	1556.69	-
2552.31	37.83	1556.7	0.568343
2590.14	12.0	1556.99	0.0
2602.14	12.0	1557.16	9.95039
2614.14	12.0	1557.3	5.61074
2626.14	12.0	1557.41	8.27516
2638.14	6.97	1557.45	12.0301
2645.11	3.49	1557.45	12.0301
2648.6	2.11	1557.45	-
2650.71	29.34	1557.44	1.8573
2680.05	12.0	1557.39	0.494372
2692.05	12.0	1557.38	0.886714
2704.05	12.0	1557.4	0.472869
2716.05	15.52	1557.43	0.221267
2731.57	10.94	1557.51	0.518429
2742.51	0.75	1557.58	-
2743.26	20.79	1557.59	0.780416
2764.05	12.0	1557.7	1.61721
2776.05	12.0	1557.71	1.7041
2788.05	12.0	1557.63	4.91125
2800.05	12.0	1557.51	7.10793

2812.05	12.0	1557.38	3.4992
2824.05	12.58	1557.25	2.38641
2836.63	5.88	1557.15	3.06189
2842.51	5.81	1557.13	-
2848.32	23.73	1557.13	1.64861
2872.05	12.0	1557.18	1.96229
2884.05	12.0	1557.25	4.25888
2896.05	12.0	1557.39	3.91637
2908.05	12.0	1557.62	3.64131
2920.05	12.0	1557.85	6.00234
2932.05	8.14	1558.04	11.546
2940.19	11.32	1558.13	11.546
2951.51	1.0	1558.2	-
2952.51	22.9	1558.2	18.5508
2975.41	11.764	1558.05	23.9169
2987.17	11.4	1557.93	15.6833
2998.57	3.94	1557.83	15.6833
3002.51	7.84	1557.79	-
3010.35	29.7	1557.73	12.6881
3040.05	12.0	1557.67	13.7046
3052.05	12.0	1557.75	10.4543
3064.05	12.0	1557.88	9.76928
3076.05	12.0	1558.04	11.0186
3088.05	12.0	1558.2	12.76
3100.05	12.0	1558.32	5.26518
3112.05	12.0	1558.39	5.67258
3124.05	14.5	1558.43	7.90759
3138.55	3.96	1558.43	8.48615
3142.51	7.75	1558.43	-
3150.26	21.79	1558.43	9.007
3172.05	12.0	1558.49	7.34274
3184.05	12.0	1558.54	1.67531
3196.05	12.0	1558.62	5.82609
3208.05	12.0	1558.69	2.81383
3220.05	11.84	1558.74	4.34891

3231.89	10.62	1558.77	5.72652
3242.51	1.06	1558.78	-
3243.57	24.48	1558.78	4.16896
3268.05	12.0	1558.79	5.38003
3280.05	12.0	1558.79	3.6302
3292.05	12.0	1558.79	3.48989
3304.05	12.0	1558.79	8.29429
3316.05	12.0	1558.78	8.00047
3328.05	8.36	1558.78	2.26461
3336.41	6.1	1558.78	2.26461
3342.51	5.48	1558.78	-
3347.99	28.06	1558.78	2.4583
3376.05	12.0	1558.77	2.86321
3388.05	12.0	1558.76	5.213
3400.05	12.0	1558.74	3.45943
3412.05	12.0	1558.73	0.558806
3424.05	5.34	1558.72	1.13453
3429.39	10.12	1558.71	1.13453
3439.51	1.48	1558.7	1.13453
3440.99	31.06	1558.7	-
3472.05	12.0	1558.7	1.36535
3484.05	12.0	1558.66	2.85644
3496.05	12.0	1558.61	1.8808
3508.05	12.0	1558.52	2.10979
3520.05	13.88	1558.42	1.56209
3533.93	8.58	1558.28	2.46105
3542.51	3.03	1558.2	-
3545.54	22.51	1558.17	3.69842
3568.05	12.0	1557.97	2.74157
3580.05	12.0	1557.87	2.82409
3592.05	12.0	1557.77	2.85842
3604.05	12.0	1557.65	2.32246
3616.05	12.0	1557.55	2.3084
3628.05	10.65	1557.46	2.57977
3638.7	3.81	1557.39	2.27568

3642.51	7.79	1557.37	-
3650.3	25.75	1557.35	3.35393
3676.05	12.0	1557.26	3.69294
3688.05	12.0	1557.2	3.94036
3700.05	12.0	1557.11	4.70504
3712.05	12.0	1556.99	4.56807
3724.05	7.81	1556.86	4.03146
3731.86	10.65	1556.78	4.03146
3742.51	0.95	1556.68	-
3743.46	28.59	1556.67	4.72796
3772.05	12.0	1556.45	3.64004
3784.05	12.0	1556.39	3.98772
3796.05	12.0	1556.31	4.04176
3808.05	12.0	1556.22	4.17024
3820.05	16.75	1556.13	4.32054
3836.8	5.71	1555.99	4.42932
3842.51	5.89	1555.94	-
3848.4	19.65	1555.89	5.96915
3868.05	12.0	1555.71	6.23969
3880.05	12.0	1555.59	7.14085
3892.05	12.0	1555.48	8.75848
3904.05	12.0	1555.37	8.80278
3916.05	13.34	1555.28	8.52573
3929.39	10.12	1555.2	7.82654
3939.51	1.57	1555.16	-
3941.08	22.97	1555.15	6.71184
3964.05	12.0	1555.14	8.06536
3976.05	12.0	1555.18	8.44881
3988.05	12.0	1555.24	8.29549
4000.05	12.0	1555.33	8.76893
4012.05	12.0	1555.44	10.4616
4024.05	10.15	1555.51	11.0227
4034.2	8.31	1555.53	10.7798
4042.51	3.28	1555.53	-
4045.79	26.26	1555.52	13.2462

4072.05	12.0	1555.35	11.6005
4084.05	12.0	1555.23	8.59454
4096.05	12.0	1555.12	14.6084
4108.05	12.0	1555.02	9.81606
4120.05	12.0	1554.96	8.03249
4132.05	10.46	1554.93	8.05417
4142.51	8.3	1554.91	-
4150.81	17.24	1554.91	5.67967
4168.05	12.0	1554.92	5.93144
4180.05	12.0	1554.93	7.98957
4192.05	12.0	1554.92	8.98525
4204.05	12.0	1554.89	9.59807
4216.05	12.0	1554.85	10.1795
4228.05	12.0	1554.77	8.67087
4240.05	15.61	1554.68	10.0066
4255.66	10.85	1554.56	10.1603
4266.51	0.9	1554.51	-
4267.41	20.64	1554.5	5.85718
4288.05	12.0	1554.51	5.75046
4300.05	13.93	1554.58	4.42361
4313.98	8.53	1554.72	9.76877
4322.51	3.09	1554.81	-
4325.6	22.45	1554.84	12.9618
4348.05	12.0	1555.07	9.65786
4360.05	12.0	1555.13	6.31299
4372.05	12.0	1555.08	9.81497
4384.05	12.0	1554.93	11.3726
4396.05	12.0	1554.75	15.7918
4408.05	12.0	1554.56	9.07811
4420.05	12.0	1554.41	14.8638
4432.05	7.46	1554.34	13.7488
4439.51	1.93	1554.33	-
4441.44	26.61	1554.34	16.7363
4468.05	12.0	1554.42	11.8563
4480.05	12.0	1554.47	4.84085

4492.05	12.0	1554.52	17.4186
4504.05	12.0	1554.56	15.1012
4516.05	12.0	1554.59	5.89325
4528.05	14.46	1554.6	11.9031
4542.51	3.9	1554.6	-
4546.41	17.64	1554.59	12.7628
4564.05	12.0	1554.54	9.81412
4576.05	12.0	1554.47	8.00329
4588.05	12.0	1554.38	4.75369
4600.05	12.0	1554.29	2.14104
4612.05	12.0	1554.21	0.977806
4624.05	12.0	1554.14	2.9384
4636.05	12.0	1554.11	6.29026
4648.05	12.0	1554.08	0.537786
4660.05	12.0	1554.04	0.00960764
4672.05	12.0	1553.96	0.0134739
4684.05	12.0	1553.86	0.0357155
4696.05	19.46	1553.75	0.0876533
4715.51	5.08	1553.51	-
4720.59	11.46	1553.43	0.00494456
4732.05	12.0	1553.24	0.206129
4744.05	12.0	1553.05	0.0228094
4756.05	12.0	1552.88	0.00864293
4768.05	12.0	1552.76	0.125515
4780.05	12.0	1552.69	0.0134729
4792.05	12.0	1552.66	0.0131859
4804.05	12.0	1552.66	0.306422
4816.05	12.0	1552.64	1.16294
4828.05	12.0	1552.64	7.88066
4840.05	12.0	1552.65	3.19671
4852.05	12.0	1552.67	4.19963
4864.05	12.0	1552.7	2.64642
4876.05	12.0	1552.73	2.97299
4888.05	12.0	1552.77	0.784379
4900.05	15.46	1552.8	0.0441744

4915.51	4.14	1552.83	-
4919.65	16.4	1552.84	0.412436
4936.05	12.0	1552.87	0.0563139
4948.05	12.0	1552.88	0.0257665
4960.05	12.0	1552.91	0.281223
4972.05	12.0	1552.94	0.0212861
4984.05	5.46	1552.96	2.30426
4989.51	7.0	1552.96	2.30426
4996.51	4.69	1552.96	-
5001.2	30.85	1552.96	6.66067
5032.05	12.0	1552.9	1.20049
5044.05	12.0	1552.87	2.32841
5056.05	1.46	1552.83	2.32841
5057.51	1.83	1552.82	-
5059.34	32.71	1552.82	4.57779
5092.05	12.0	1552.75	2.16542
5104.05	12.0	1552.77	5.11972
5116.05	12.0	1552.83	6.26752
5128.05	12.0	1552.93	7.41971
5140.05	12.0	1553.08	6.62969
5152.05	12.0	1553.28	1.367
5164.05	8.46	1553.55	1.05489
5172.51	2.21	1553.76	-
5174.72	30.79	1553.82	8.11279
5205.51	4.2	1554.69	-
5209.71	14.34	1554.82	7.45904
5224.05	12.0	1555.24	0.68159
5236.05	12.0	1555.55	7.65074
5248.05	12.0	1555.81	7.36766
5260.05	8.17	1555.99	7.36766
5268.22	15.83	1556.05	-
5284.05	12.0	1556.05	4.29013
5296.05	14.92	1555.99	0.00141583
5310.97	9.08	1555.92	0.0
5320.05	12.0	1555.88	1.21067

5332.05	12.0	1555.86	1.21067
5344.05	12.0	1555.87	1.21067
5356.05	12.0	1555.92	1.21067
5368.05	12.0	1556.02	1.21067

Appendix H: Horizontal Permeability BY2H NETool

Top MD [m]	Seg. length [m]	Top TVD [m]	κH [D]
2005.67	8.47	1553.01	-
2014.14	12.0	1554.08	1.01551
2026.14	12.0	1555.38	-
2038.14	12.0	1556.45	2.0951
2050.14	11.66	1557.27	-
2061.8	12.34	1557.87	4.84141
2074.14	12.0001	1558.1	4.47589
2086.14	12.0	1558.13	6.97598
2098.14	10.31	1558.14	5.19598
2108.45	10.15	1558.12	3.19359
2118.6	1.55	1558.09	-
2120.15	25.99	1558.09	3.48034
2146.14	12.0	1557.97	1.98453
2158.14	12.0	1557.89	4.72208
2170.14	8.27	1557.82	4.57321
2178.41	10.19	1557.79	4.0184
2188.6	1.42	1557.78	-
2190.02	28.12	1557.78	3.75194
2218.14	12.0	1557.76	4.5032
2230.14	12.0	1557.76	5.10993
2242.14	12.0	1557.76	6.51826
2254.14	12.0	1557.75	6.31486
2266.14	12.0	1557.74	6.26843
2278.14	12.0	1557.72	4.76998
2290.14	12.0	1557.7	2.85109
2302.14	12.0	1557.69	2.03178
2314.14	12.0	1557.68	3.27524
2326.14	12.0	1557.68	1.80046
2338.14	12.0	1557.68	0.531844
2350.14	12.0	1557.68	1.09488
2362.14	11.46	1557.69	5.79336
2373.6	3.82	1557.69	-
2377.42	20.72	1557.69	1.25706

2398.14	12.0	1557.7	0.314796
2410.14	13.88	1557.69	1.80666
2424.02	11.75	1557.65	2.00115
2435.77	2.83	1557.59	-
2438.6	8.86	1557.56	1.52955
2447.46	11.74	1557.48	5.84006
2459.2	11.59	1557.34	5.89224
2470.79	11.74	1557.15	7.62669
2482.53	11.7	1556.96	7.65615
2494.23	11.22	1556.81	9.07369
2505.45	11.68	1556.72	12.1766
2517.13	11.75	1556.66	9.44687
2528.88	11.69	1556.65	5.67087
2540.57	8.03	1556.68	5.67087
2548.6	3.71	1556.69	-
2552.31	37.83	1556.7	0.568343
2590.14	12.0	1556.99	0.0
2602.14	12.0	1557.16	9.95039
2614.14	12.0	1557.3	5.61074
2626.14	12.0	1557.41	8.27516
2638.14	6.97	1557.45	12.0301
2645.11	3.49	1557.45	12.0301
2648.6	2.11	1557.45	-
2650.71	29.34	1557.44	1.8573
2680.05	12.0	1557.39	0.494372
2692.05	12.0	1557.38	0.886714
2704.05	12.0	1557.4	0.472869
2716.05	15.52	1557.43	0.221267
2731.57	10.94	1557.51	0.518429
2742.51	0.75	1557.58	-
2743.26	20.79	1557.59	0.780416
2764.05	12.0	1557.7	1.61721
2776.05	12.0	1557.71	1.7041
2788.05	12.0	1557.63	4.91125
2800.05	12.0	1557.51	7.10793

2812.05	12.0	1557.38	3.4992
2824.05	12.58	1557.25	2.38641
2836.63	5.88	1557.15	3.06189
2842.51	5.81	1557.13	-
2848.32	23.73	1557.13	1.64861
2872.05	12.0	1557.18	1.96229
2884.05	12.0	1557.25	4.25888
2896.05	12.0	1557.39	3.91637
2908.05	12.0	1557.62	3.64131
2920.05	12.0	1557.85	6.00234
2932.05	8.14	1558.04	11.546
2940.19	11.32	1558.13	11.546
2951.51	1.0	1558.2	-
2952.51	22.9	1558.2	18.5508
2975.41	11.764	1558.05	23.9169
2987.17	11.4	1557.93	15.6833
2998.57	3.94	1557.83	15.6833
3002.51	7.84	1557.79	-
3010.35	29.7	1557.73	12.6881
3040.05	12.0	1557.67	13.7046
3052.05	12.0	1557.75	10.4543
3064.05	12.0	1557.88	9.76928
3076.05	12.0	1558.04	11.0186
3088.05	12.0	1558.2	12.76
3100.05	12.0	1558.32	5.26518
3112.05	12.0	1558.39	5.67258
3124.05	14.5	1558.43	7.90759
3138.55	3.96	1558.43	8.48615
3142.51	7.75	1558.43	-
3150.26	21.79	1558.43	9.007
3172.05	12.0	1558.49	7.34274
3184.05	12.0	1558.54	1.67531
3196.05	12.0	1558.62	5.82609
3208.05	12.0	1558.69	2.81383
3220.05	11.84	1558.74	4.34891

3231.89	10.62	1558.77	5.72652
3242.51	1.06	1558.78	-
3243.57	24.48	1558.78	4.16896
3268.05	12.0	1558.79	5.38003
3280.05	12.0	1558.79	3.6302
3292.05	12.0	1558.79	3.48989
3304.05	12.0	1558.79	8.29429
3316.05	12.0	1558.78	8.00047
3328.05	8.36	1558.78	2.26461
3336.41	6.1	1558.78	2.26461
3342.51	5.48	1558.78	-
3347.99	28.06	1558.78	2.4583
3376.05	12.0	1558.77	2.86321
3388.05	12.0	1558.76	5.213
3400.05	12.0	1558.74	3.45943
3412.05	12.0	1558.73	0.558806
3424.05	5.34	1558.72	1.13453
3429.39	10.12	1558.71	1.13453
3439.51	1.48	1558.7	1.13453
3440.99	31.06	1558.7	-
3472.05	12.0	1558.7	1.36535
3484.05	12.0	1558.66	2.85644
3496.05	12.0	1558.61	1.8808
3508.05	12.0	1558.52	2.10979
3520.05	13.88	1558.42	1.56209
3533.93	8.58	1558.28	2.46105
3542.51	3.03	1558.2	-
3545.54	22.51	1558.17	3.69842
3568.05	12.0	1557.97	2.74157
3580.05	12.0	1557.87	2.82409
3592.05	12.0	1557.77	2.85842
3604.05	12.0	1557.65	2.32246
3616.05	12.0	1557.55	2.3084
3628.05	10.65	1557.46	2.57977
3638.7	3.81	1557.39	2.27568

3642.51	7.79	1557.37	-
3650.3	25.75	1557.35	3.35393
3676.05	12.0	1557.26	3.69294
3688.05	12.0	1557.2	3.94036
3700.05	12.0	1557.11	4.70504
3712.05	12.0	1556.99	4.56807
3724.05	7.81	1556.86	4.03146
3731.86	10.65	1556.78	4.03146
3742.51	0.95	1556.68	-
3743.46	28.59	1556.67	4.72796
3772.05	12.0	1556.45	3.64004
3784.05	12.0	1556.39	3.98772
3796.05	12.0	1556.31	4.04176
3808.05	12.0	1556.22	4.17024
3820.05	16.75	1556.13	4.32054
3836.8	5.71	1555.99	4.42932
3842.51	5.89	1555.94	-
3848.4	19.65	1555.89	5.96915
3868.05	12.0	1555.71	6.23969
3880.05	12.0	1555.59	7.14085
3892.05	12.0	1555.48	8.75848
3904.05	12.0	1555.37	8.80278
3916.05	13.34	1555.28	8.52573
3929.39	10.12	1555.2	7.82654
3939.51	1.57	1555.16	-
3941.08	22.97	1555.15	6.71184
3964.05	12.0	1555.14	8.06536
3976.05	12.0	1555.18	8.44881
3988.05	12.0	1555.24	8.29549
4000.05	12.0	1555.33	8.76893
4012.05	12.0	1555.44	10.4616
4024.05	10.15	1555.51	11.0227
4034.2	8.31	1555.53	10.7798
4042.51	3.28	1555.53	-
4045.79	26.26	1555.52	13.2462

4072.05	12.0	1555.35	11.6005
4084.05	12.0	1555.23	8.59454
4096.05	12.0	1555.12	14.6084
4108.05	12.0	1555.02	9.81606
4120.05	12.0	1554.96	8.03249
4132.05	10.46	1554.93	8.05417
4142.51	8.3	1554.91	-
4150.81	17.24	1554.91	5.67967
4168.05	12.0	1554.92	5.93144
4180.05	12.0	1554.93	7.98957
4192.05	12.0	1554.92	8.98525
4204.05	12.0	1554.89	9.59807
4216.05	12.0	1554.85	10.1795
4228.05	12.0	1554.77	8.67087
4240.05	15.61	1554.68	10.0066
4255.66	10.85	1554.56	10.1603
4266.51	0.9	1554.51	-
4267.41	20.64	1554.5	5.85718
4288.05	12.0	1554.51	5.75046
4300.05	13.93	1554.58	4.42361
4313.98	8.53	1554.72	9.76877
4322.51	3.09	1554.81	-
4325.6	22.45	1554.84	12.9618
4348.05	12.0	1555.07	9.65786
4360.05	12.0	1555.13	6.31299
4372.05	12.0	1555.08	9.81497
4384.05	12.0	1554.93	11.3726
4396.05	12.0	1554.75	15.7918
4408.05	12.0	1554.56	9.07811
4420.05	12.0	1554.41	14.8638
4432.05	7.46	1554.34	13.7488
4439.51	1.93	1554.33	-
4441.44	26.61	1554.34	16.7363
4468.05	12.0	1554.42	11.8563
4480.05	12.0	1554.47	4.84085

4492.05	12.0	1554.52	17.4186
4504.05	12.0	1554.56	15.1012
4516.05	12.0	1554.59	5.89325
4528.05	14.46	1554.6	11.9031
4542.51	3.9	1554.6	-
4546.41	17.64	1554.59	12.7628
4564.05	12.0	1554.54	9.81412
4576.05	12.0	1554.47	8.00329
4588.05	12.0	1554.38	4.75369
4600.05	12.0	1554.29	2.14104
4612.05	12.0	1554.21	0.977806
4624.05	12.0	1554.14	2.9384
4636.05	12.0	1554.11	6.29026
4648.05	12.0	1554.08	0.537786
4660.05	12.0	1554.04	0.00960764
4672.05	12.0	1553.96	0.0134739
4684.05	12.0	1553.86	0.0357155
4696.05	19.46	1553.75	0.0876533
4715.51	5.08	1553.51	-
4720.59	11.46	1553.43	0.00494456
4732.05	12.0	1553.24	0.206129
4744.05	12.0	1553.05	0.0228094
4756.05	12.0	1552.88	0.00864293
4768.05	12.0	1552.76	0.125515
4780.05	12.0	1552.69	0.0134729
4792.05	12.0	1552.66	0.0131859
4804.05	12.0	1552.66	0.306422
4816.05	12.0	1552.64	1.16294
4828.05	12.0	1552.64	7.88066
4840.05	12.0	1552.65	3.19671
4852.05	12.0	1552.67	4.19963
4864.05	12.0	1552.7	2.64642
4876.05	12.0	1552.73	2.97299
4888.05	12.0	1552.77	0.784379
4900.05	15.46	1552.8	0.0441744

4915.51	4.14	1552.83	-
4919.65	16.4	1552.84	0.412436
4936.05	12.0	1552.87	0.0563139
4948.05	12.0	1552.88	0.0257665
4960.05	12.0	1552.91	0.281223
4972.05	12.0	1552.94	0.0212861
4984.05	5.46	1552.96	2.30426
4989.51	7.0	1552.96	2.30426
4996.51	4.69	1552.96	-
5001.2	30.85	1552.96	6.66067
5032.05	12.0	1552.9	1.20049
5044.05	12.0	1552.87	2.32841
5056.05	1.46	1552.83	2.32841
5057.51	1.83	1552.82	-
5059.34	32.71	1552.82	4.57779
5092.05	12.0	1552.75	2.16542
5104.05	12.0	1552.77	5.11972
5116.05	12.0	1552.83	6.26752
5128.05	12.0	1552.93	7.41971
5140.05	12.0	1553.08	6.62969
5152.05	12.0	1553.28	1.367
5164.05	8.46	1553.55	1.05489
5172.51	2.21	1553.76	-
5174.72	30.79	1553.82	8.11279
5205.51	4.2	1554.69	-
5209.71	14.34	1554.82	7.45904
5224.05	12.0	1555.24	0.68159
5236.05	12.0	1555.55	7.65074
5248.05	12.0	1555.81	7.36766
5260.05	8.17	1555.99	7.36766
5268.22	15.83	1556.05	-
5284.05	12.0	1556.05	4.29013
5296.05	14.92	1555.99	0.00141583
5310.97	9.08	1555.92	0.0
5320.05	12.0	1555.88	1.21067

5332.05	12.0	1555.86	1.21067
5344.05	12.0	1555.87	1.21067
5356.05	12.0	1555.92	1.21067
5368.05	12.0	1556.02	1.21067

Appendix I: Water Saturation BY1H NETool

Top MD [m]	Seg. length [m]	Top TVD [m]	S_w
1978.05	11.97	1548.78	-
1990.02	12.0	1549.83	-
2002.02	3.6415	1552.21	-
2005.67	8.46	1553.01	-
2014.13	12.0	1554.07	0.234202
2026.13	12.0	1555.37	-
2038.13	17.84	1556.42	0.294247
2055.97	6.16	1557.58	0.440442
2062.13	12.0	1557.89	0.664937
2074.13	12.0001	1558.4	0.90769
2086.13	12.0	1558.76	0.909672
2098.13	12.0	1558.98	0.807162
2110.13	12.0	1559.08	0.659305
2122.13	12.0	1559.12	0.637588
2134.13	12.0	1559.12	0.668033
2146.13	12.0	1559.08	0.572044
2158.13	15.01	1559.0	0.79769
2173.14	8.99	1558.8	0.768379
2182.13	12.0	1558.63	0.821196
2194.13	2.52	1558.39	-
2196.65	21.48	1558.34	0.810817
2218.13	12.0	1557.95	0.460559
2230.13	12.0	1557.78	0.415009
2242.13	12.0	1557.64	0.479093
2254.13	12.0	1557.53	0.528574
2266.13	12.0	1557.44	0.384305
2278.13	12.0	1557.38	0.493334
2290.13	12.0	1557.36	0.619208
2302.13	12.0	1557.37	0.533734
2314.13	12.0	1557.36	0.530883
2326.13	12.0	1557.33	0.445837
2338.13	12.0	1557.28	0.453543

2350.13	10.35	1557.2	0.402384
2360.48	8.65	1557.13	0.402384
2369.13	2.98	1557.08	-
2372.11	26.02	1557.07	0.402384
2398.13	12.0	1556.99	0.427724
2410.13	12.0	1556.97	0.371775
2422.13	12.0	1556.98	0.327301
2434.13	7.59	1556.99	0.466716
2441.72	11.74	1557.01	0.862259
2453.46	9.67	1557.06	0.862259
2463.13	2.6	1557.14	-
2465.73	28.4	1557.16	0.862259
2494.13	12.0	1557.32	0.597668
2506.13	12.0	1557.28	0.514156
2518.13	12.0	1557.16	0.344743
2530.13	17.15	1556.98	0.356297
2547.28	9.64	1556.76	0.376752
2556.92	2.0	1556.68	-
2558.92	19.21	1556.67	0.612027
2578.13	12.0	1556.6	0.573199
2590.13	12.0	1556.58	0.361613
2602.13	12.0	1556.56	0.261149
2614.13	12.0	1556.51	0.267392
2626.13	12.0	1556.46	0.3149
2638.13	12.0	1556.44	0.376682
2650.13	14.16	1556.44	0.415247
2664.29	8.84	1556.47	0.267657
2673.13	2.85	1556.51	-
2675.98	22.15	1556.53	0.267657
2698.13	12.0	1556.67	0.360783
2710.13	12.0	1556.76	0.354822
2722.13	12.0	1556.83	0.281627
2734.13	12.0	1556.89	0.287326
2746.13	12.0	1556.94	0.368055
2758.13	12.0	1556.98	0.465164

2770.13	10.95	1557.02	0.597778
2781.08	9.05	1557.05	0.597778
2790.13	2.57	1557.07	0.597778
2792.7	25.43	1557.07	0.597778
2818.13	12.0	1557.12	0.307036
2830.13	12.0	1557.13	0.473818
2842.13	12.0	1557.12	0.494538
2854.13	8.77	1557.09	0.371969
2862.9	9.23	1557.07	0.371969
2872.13	2.37	1557.04	-
2874.5	27.63	1557.03	0.371969
2902.13	12.0	1556.97	0.356558
2914.13	12.0	1556.97	0.405396
2926.13	12.0	1556.97	0.324456
2938.13	12.0	1556.98	0.299405
2950.13	12.0	1557.0	0.289425
2962.13	12.0	1557.03	0.299014
2974.13	12.004	1557.06	0.326673
2986.13	16.93	1557.11	0.299882
3003.06	9.7	1557.18	0.270719
3012.76	2.49	1557.21	-
3015.25	19.51	1557.22	0.341328
3034.76	12.0	1557.27	0.490897
3046.76	12.0	1557.29	0.361385
3058.76	12.0	1557.32	0.469271
3070.76	12.0	1557.34	0.310996
3082.76	14.38	1557.36	0.292391
3097.14	9.62	1557.39	0.345384
3106.76	2.12	1557.42	-
3108.88	21.88	1557.43	0.433375
3130.76	13.24	1557.51	0.369522
3144.0	8.76	1557.56	0.828814
3152.76	2.87	1557.58	-
3155.63	23.13	1557.59	0.828814
3178.76	12.0	1557.57	0.518887

3190.76	12.0	1557.52	0.485503
3202.76	12.0	1557.45	0.433528
3214.76	11.14	1557.38	0.520003
3225.9	8.86	1557.33	0.487773
3234.76	2.62	1557.3	-
3237.38	25.38	1557.3	0.487773
3262.76	12.0	1557.31	0.419342
3274.76	12.0	1557.3	0.441537
3286.76	12.0	1557.27	0.315791
3298.76	12.0	1557.24	0.344313
3310.76	8.4	1557.2	0.341738
3319.16	8.6	1557.17	0.341738
3327.76	2.89	1557.13	-
3330.65	28.11	1557.12	0.341738
3358.76	12.0	1557.03	0.408032
3370.76	12.0	1556.99	0.429635
3382.76	12.0	1556.96	0.442128
3394.76	12.0	1556.92	0.407158
3406.76	12.0	1556.88	0.406862
3418.76	12.0	1556.85	0.38662
3430.76	5.0	1556.82	0.378816
3435.76	9.0	1556.79	0.378816
3444.76	2.7	1556.7	-
3447.46	31.3	1556.66	0.378816
3478.76	12.0	1556.15	0.353103
3490.76	12.0	1555.93	0.310397
3502.76	12.0	1555.75	0.272681
3514.76	12.0	1555.59	0.246667
3526.76	12.0	1555.46	0.300121
3538.76	12.0	1555.36	0.348447
3550.76	12.0	1555.28	0.328869
3562.76	12.0	1555.26	0.251346
3574.76	12.0	1555.26	0.267602
3586.76	12.0	1555.25	0.224784
3598.76	12.0	1555.23	0.22242

3610.76	12.0	1555.21	0.248177
3622.76	12.0	1555.18	0.240469
3634.76	10.56	1555.15	0.26216
3645.32	9.44	1555.15	0.26216
3654.76	2.23	1555.18	-
3656.99	25.77	1555.18	0.26216
3682.76	12.0	1555.34	0.275549
3694.76	12.0	1555.44	0.304958
3706.76	12.0	1555.53	0.317424
3718.76	12.0	1555.6	0.318945
3730.76	12.0	1555.66	0.340117
3742.76	12.0	1555.69	0.371602
3754.76	12.0	1555.69	0.423172
3766.76	12.0	1555.67	0.335457
3778.76	6.94	1555.62	0.291119
3785.7	9.06	1555.58	0.291119
3794.76	2.64	1555.52	-
3797.4	29.36	1555.51	0.291119
3826.76	12.0	1555.38	0.377434
3838.76	12.0	1555.37	0.49835
3850.76	12.0	1555.38	0.493673
3862.76	12.0	1555.4	0.591099
3874.76	12.0	1555.38	0.463687
3886.76	12.0	1555.32	0.322393
3898.76	12.0	1555.23	0.306752
3910.76	12.0	1555.15	0.34677
3922.76	14.74	1555.08	0.35844
3937.5	9.26	1555.04	0.438391
3946.76	2.49	1555.04	-
3949.25	21.51	1555.04	0.464355
3970.76	12.0	1554.98	0.587562
3982.76	12.0	1554.99	0.790155
3994.76	12.0	1555.13	0.805886
4006.76	12.0	1555.44	0.818061
4018.76	12.0	1555.91	0.770427

4030.76	12.0	1556.57	0.670452
4042.76	12.0	1557.22	0.60496
4054.76	12.0	1557.69	0.569937
4066.76	12.0	1558.0	0.577215
4078.76	12.0	1558.12	0.556922
4090.76	12.0	1558.05	0.547165
4102.76	12.0	1557.82	0.562077
4114.76	12.0	1557.43	0.691664
4126.76	9.69	1556.96	0.765277
4136.45	9.31	1556.53	0.765277
4145.76	2.43	1556.12	-
4148.19	26.57	1556.02	0.765277
4174.76	12.0	1555.18	0.485073
4186.76	12.0	1554.98	0.36123
4198.76	12.0	1554.85	0.322517
4210.76	12.0	1554.77	0.352342
4222.76	12.0	1554.72	0.34377
4234.76	12.0	1554.7	0.341713
4246.76	12.0	1554.72	0.387367
4258.76	12.0	1554.81	0.474635
4270.76	17.79	1554.93	0.452566
4288.55	9.21	1555.06	0.419337
4297.76	2.47	1555.1	-
4300.23	18.53	1555.11	0.475277
4318.76	12.0	1555.05	0.476142
4330.76	12.0	1554.95	0.484297
4342.76	12.0	1554.83	0.393031
4354.76	12.0	1554.69	0.321561
4366.76	12.0	1554.56	0.316499
4378.76	12.0	1554.44	0.342194
4390.76	12.0	1554.35	0.34749
4402.76	12.0	1554.29	0.301871
4414.76	12.0	1554.27	0.334301
4426.76	13.21	1554.27	0.27727
4439.97	8.79	1554.28	0.263003

4448.76	2.59	1554.3	-
4451.35	23.41	1554.3	0.263003
4474.76	12.0	1554.37	0.371432
4486.76	12.0	1554.42	0.212182
4498.76	12.0	1554.48	0.276879
4510.76	12.0	1554.53	0.275953
4522.76	12.0	1554.55	0.379205
4534.76	12.0	1554.56	0.406163
4546.76	12.0	1554.57	0.501338
4558.76	12.0	1554.56	0.104064
4570.76	12.0	1554.5	0.100594
4582.76	12.0	1554.41	0.100594
4594.76	7.82	1554.3	0.581962
4602.58	9.18	1554.22	0.581962
4611.76	2.44	1554.13	-
4614.2	28.56	1554.11	0.581962
4642.76	12.0	1553.9	0.187035
4654.76	12.0	1553.83	0.362711
4666.76	12.0	1553.75	0.340762
4678.76	12.0	1553.69	0.354898
4690.76	12.0	1553.66	0.496136
4702.76	16.8	1553.65	0.538768
4719.56	9.2	1553.61	0.490603
4728.76	2.54	1553.58	0.620071
4731.3	19.46	1553.57	0.620071
4750.76	12.0	1553.44	0.67869
4762.76	12.0	1553.32	0.620892
4774.76	12.0	1553.18	0.399079
4786.76	12.0	1553.01	0.694076
4798.76	12.0	1552.81	0.684311
4810.76	12.0	1552.58	0.699583
4822.76	12.0	1552.32	0.491853
4834.76	12.0	1552.03	0.351858
4846.76	12.0	1551.76	0.29185
4858.76	12.0	1551.54	0.286984

4870.76	12.0	1551.41	0.321164
4882.76	12.0	1551.33	0.414955
4894.76	12.0	1551.32	0.492392
4906.76	12.0	1551.33	0.47829
4918.76	12.0	1551.33	0.498856
4930.76	12.0	1551.31	0.476365
4942.76	12.0	1551.33	0.474772
4954.76	12.0	1551.41	0.519869
4966.76	12.0	1551.53	0.542832
4978.76	12.0	1551.7	0.542788
4990.76	12.0	1551.9	0.515082
5002.76	12.0	1552.07	0.50353
5014.76	12.0	1552.18	0.48061
5026.76	12.0	1552.25	0.477726
5038.76	12.0	1552.28	0.506303
5050.76	8.32	1552.27	0.471269
5059.08	9.68	1552.24	0.154502
5068.76	2.08	1552.15	-
5070.84	11.73	1552.13	0.154502
5082.57	11.75	1551.98	0.154502
5094.32	28.44	1551.78	0.154502
5122.76	6.66	1551.4	0.229216
5129.42	9.34	1551.4	0.351067
5138.76	2.3	1551.45	-
5141.06	23.49	1551.47	0.450582
5164.55	9.21	1551.9	0.5
5173.76	2.52	1552.09	-
5176.28	23.35	1552.14	0.156976
5199.63	11.62	1552.42	-
5211.25	19.51	1552.45	0.156976
5230.76	12.0	1552.44	0.400415
5242.76	12.0	1552.47	0.5
5254.76	12.0	1552.57	0.5
5266.76	12.0	1552.77	0.5
5278.76	7.02	1553.08	0.5

Appendix J: Water Saturation BY2H NETool

Top MD [m]	Seg. length [m]	Top TVD [m]	Sw
2005.67	8.47	1553.01	-
2014.14	12.0	1554.08	0.443662
2026.14	12.0	1555.38	-
2038.14	12.0	1556.45	0.906735
2050.14	11.66	1557.27	-
2061.8	12.34	1557.87	0.843981
2074.14	12.0001	1558.1	0.600475
2086.14	12.0	1558.13	0.638302
2098.14	10.31	1558.14	0.638302
2108.45	10.15	1558.12	0.57154
2118.6	1.55	1558.09	-
2120.15	25.99	1558.09	0.779253
2146.14	12.0	1557.97	0.778798
2158.14	12.0	1557.89	0.813811
2170.14	8.27	1557.82	0.813811
2178.41	10.19	1557.79	0.460538
2188.6	1.42	1557.78	-
2190.02	28.12	1557.78	0.416506
2218.14	12.0	1557.76	0.478327
2230.14	12.0	1557.76	0.52698
2242.14	12.0	1557.76	0.384753
2254.14	12.0	1557.75	0.492082
2266.14	12.0	1557.74	0.616545
2278.14	12.0	1557.72	0.534217
2290.14	12.0	1557.7	0.532272
2302.14	12.0	1557.69	0.447189
2314.14	12.0	1557.68	0.454449
2326.14	12.0	1557.68	0.434799
2338.14	12.0	1557.68	0.4
2350.14	12.0	1557.68	0.408485
2362.14	11.46	1557.69	0.408485
2373.6	3.82	1557.69	-

2377.42	20.72	1557.69	0.364913
2398.14	12.0	1557.7	0.330525
2410.14	13.88	1557.69	0.375487
2424.02	11.75	1557.65	0.399923
2435.77	2.83	1557.59	-
2438.6	8.86	1557.56	0.823777
2447.46	11.74	1557.48	0.531896
2459.2	11.59	1557.34	0.346076
2470.79	11.74	1557.15	0.358487
2482.53	11.7	1556.96	0.356704
2494.23	11.22	1556.81	0.56574
2505.45	11.68	1556.72	0.56574
2517.13	11.75	1556.66	0.56574
2528.88	11.69	1556.65	0.361261
2540.57	8.03	1556.68	0.361261
2548.6	3.71	1556.69	-
2552.31	37.83	1556.7	0.260831
2590.14	12.0	1556.99	0.267383
2602.14	12.0	1557.16	0.31431
2614.14	12.0	1557.3	0.4
2626.14	12.0	1557.41	0.334795
2638.14	6.97	1557.45	0.245348
2645.11	3.49	1557.45	0.245348
2648.6	2.11	1557.45	-
2650.71	29.34	1557.44	0.36126
2680.05	12.0	1557.39	0.354684
2692.05	12.0	1557.38	0.276814
2704.05	12.0	1557.4	0.299251
2716.05	15.52	1557.43	0.436183
2731.57	10.94	1557.51	0.355007
2742.51	0.75	1557.58	-
2743.26	20.79	1557.59	0.397774
2764.05	12.0	1557.7	0.531276
2776.05	12.0	1557.71	0.682569
2788.05	12.0	1557.63	0.307633

2800.05	12.0	1557.51	0.477782
2812.05	12.0	1557.38	0.4
2824.05	12.58	1557.25	0.390302
2836.63	5.88	1557.15	0.352664
2842.51	5.81	1557.13	-
2848.32	23.73	1557.13	0.404454
2872.05	12.0	1557.18	0.356789
2884.05	12.0	1557.25	0.405446
2896.05	12.0	1557.39	0.325011
2908.05	12.0	1557.62	0.294296
2920.05	12.0	1557.85	0.30274
2932.05	8.14	1558.04	0.264101
2940.19	11.32	1558.13	0.264101
2951.51	1.0	1558.2	-
2952.51	22.9	1558.2	0.406627
2975.41	11.764	1558.05	0.406627
2987.17	11.4	1557.93	0.361459
2998.57	3.94	1557.83	0.361459
3002.51	7.84	1557.79	-
3010.35	29.7	1557.73	0.469226
3040.05	12.0	1557.67	0.310476
3052.05	12.0	1557.75	0.289447
3064.05	12.0	1557.88	0.338134
3076.05	12.0	1558.04	0.429128
3088.05	12.0	1558.2	0.429692
3100.05	12.0	1558.32	0.379263
3112.05	12.0	1558.39	0.4
3124.05	14.5	1558.43	0.832779
3138.55	3.96	1558.43	0.518474
3142.51	7.75	1558.43	-
3150.26	21.79	1558.43	0.485388
3172.05	12.0	1558.49	0.433294
3184.05	12.0	1558.54	0.533623
3196.05	12.0	1558.62	0.519912
3208.05	12.0	1558.69	0.4

3220.05	11.84	1558.74	0.442646
3231.89	10.62	1558.77	0.440827
3242.51	1.06	1558.78	-
3243.57	24.48	1558.78	0.31586
3268.05	12.0	1558.79	0.344356
3280.05	12.0	1558.79	0.33072
3292.05	12.0	1558.79	0.309633
3304.05	12.0	1558.79	0.336677
3316.05	12.0	1558.78	0.413841
3328.05	8.36	1558.78	0.442041
3336.41	6.1	1558.78	0.442041
3342.51	5.48	1558.78	-
3347.99	28.06	1558.78	0.407082
3376.05	12.0	1558.77	0.406798
3388.05	12.0	1558.76	0.386698
3400.05	12.0	1558.74	0.359663
3412.05	12.0	1558.73	0.4
3424.05	5.34	1558.72	0.35304
3429.39	10.12	1558.71	0.35304
3439.51	1.48	1558.7	0.35304
3440.99	31.06	1558.7	-
3472.05	12.0	1558.7	0.272493
3484.05	12.0	1558.66	0.24678
3496.05	12.0	1558.61	0.30549
3508.05	12.0	1558.52	0.4
3520.05	13.88	1558.42	0.286661
3533.93	8.58	1558.28	0.268273
3542.51	3.03	1558.2	-
3545.54	22.51	1558.17	0.224261
3568.05	12.0	1557.97	0.222723
3580.05	12.0	1557.87	0.248198
3592.05	12.0	1557.77	0.240401
3604.05	12.0	1557.65	0.216178
3616.05	12.0	1557.55	0.262199
3628.05	10.65	1557.46	0.262199

3638.7	3.81	1557.39	0.275677
3642.51	7.79	1557.37	-
3650.3	25.75	1557.35	0.304978
3676.05	12.0	1557.26	0.317426
3688.05	12.0	1557.2	0.319027
3700.05	12.0	1557.11	0.356157
3712.05	12.0	1556.99	0.381737
3724.05	7.81	1556.86	0.307806
3731.86	10.65	1556.78	0.307806
3742.51	0.95	1556.68	-
3743.46	28.59	1556.67	0.265374
3772.05	12.0	1556.45	0.284032
3784.05	12.0	1556.39	0.315592
3796.05	12.0	1556.31	0.400539
3808.05	12.0	1556.22	0.4
3820.05	16.75	1556.13	0.54961
3836.8	5.71	1555.99	0.46311
3842.51	5.89	1555.94	-
3848.4	19.65	1555.89	0.32228
3868.05	12.0	1555.71	0.306689
3880.05	12.0	1555.59	0.346939
3892.05	12.0	1555.48	0.352425
3904.05	12.0	1555.37	0.4
3916.05	13.34	1555.28	0.459382
3929.39	10.12	1555.2	0.588066
3939.51	1.57	1555.16	-
3941.08	22.97	1555.15	0.790473
3964.05	12.0	1555.14	0.805817
3976.05	12.0	1555.18	0.818061
3988.05	12.0	1555.24	0.770177
4000.05	12.0	1555.33	0.626395
4012.05	12.0	1555.44	0.572618
4024.05	10.15	1555.51	0.572618
4034.2	8.31	1555.53	0.556967
4042.51	3.28	1555.53	-

4045.79	26.26	1555.52	0.547202
4072.05	12.0	1555.35	0.562079
4084.05	12.0	1555.23	0.692261
4096.05	12.0	1555.12	0.786044
4108.05	12.0	1555.02	0.4
4120.05	12.0	1554.96	0.743115
4132.05	10.46	1554.93	0.484168
4142.51	8.3	1554.91	-
4150.81	17.24	1554.91	0.361113
4168.05	12.0	1554.92	0.322387
4180.05	12.0	1554.93	0.352506
4192.05	12.0	1554.92	0.34366
4204.05	12.0	1554.89	0.341796
4216.05	12.0	1554.85	0.408264
4228.05	12.0	1554.77	0.472287
4240.05	15.61	1554.68	0.438844
4255.66	10.85	1554.56	0.449461
4266.51	0.9	1554.51	-
4267.41	20.64	1554.5	0.487396
4288.05	12.0	1554.51	0.4
4300.05	13.93	1554.58	0.43412
4313.98	8.53	1554.72	0.321486
4322.51	3.09	1554.81	-
4325.6	22.45	1554.84	0.316582
4348.05	12.0	1555.07	0.34234
4360.05	12.0	1555.13	0.347239
4372.05	12.0	1555.08	0.301964
4384.05	12.0	1554.93	0.334238
4396.05	12.0	1554.75	0.277828
4408.05	12.0	1554.56	0.262084
4420.05	12.0	1554.41	0.262084
4432.05	7.46	1554.34	0.371622
4439.51	1.93	1554.33	-
4441.44	26.61	1554.34	0.211786
4468.05	12.0	1554.42	0.277083

4480.05	12.0	1554.47	0.276037
4492.05	12.0	1554.52	0.379655
4504.05	12.0	1554.56	0.430206
4516.05	12.0	1554.59	0.199375
4528.05	14.46	1554.6	0.100594
4542.51	3.9	1554.6	-
4546.41	17.64	1554.59	0.100599
4564.05	12.0	1554.54	0.388958
4576.05	12.0	1554.47	0.642084
4588.05	12.0	1554.38	0.63619
4600.05	12.0	1554.29	0.479
4612.05	12.0	1554.21	0.187405
4624.05	12.0	1554.14	0.362728
4636.05	12.0	1554.11	0.340677
4648.05	12.0	1554.08	0.355043
4660.05	12.0	1554.04	0.496718
4672.05	12.0	1553.96	0.534611
4684.05	12.0	1553.86	0.4
4696.05	19.46	1553.75	0.540771
4715.51	5.08	1553.51	-
4720.59	11.46	1553.43	0.678784
4732.05	12.0	1553.24	0.620152
4744.05	12.0	1553.05	0.399651
4756.05	12.0	1552.88	0.694331
4768.05	12.0	1552.76	0.684312
4780.05	12.0	1552.69	0.699193
4792.05	12.0	1552.66	0.491255
4804.05	12.0	1552.66	0.351521
4816.05	12.0	1552.64	0.5
4828.05	12.0	1552.64	0.5
4840.05	12.0	1552.65	0.5
4852.05	12.0	1552.67	0.5
4864.05	12.0	1552.7	0.5
4876.05	12.0	1552.73	0.5
4888.05	12.0	1552.77	0.5

4900.05	15.46	1552.8	0.5
4915.51	4.14	1552.83	-
4919.65	16.4	1552.84	0.5
4936.05	12.0	1552.87	0.5
4948.05	12.0	1552.88	0.5
4960.05	12.0	1552.91	0.5
4972.05	12.0	1552.94	0.5
4984.05	5.46	1552.96	0.5
4989.51	7.0	1552.96	0.5
4996.51	4.69	1552.96	-
5001.2	30.85	1552.96	0.5
5032.05	12.0	1552.9	0.5
5044.05	12.0	1552.87	0.5
5056.05	1.46	1552.83	0.5
5057.51	1.83	1552.82	-
5059.34	32.71	1552.82	0.5
5092.05	12.0	1552.75	0.5
5104.05	12.0	1552.77	0.5
5116.05	12.0	1552.83	0.5
5128.05	12.0	1552.93	0.5
5140.05	12.0	1553.08	0.5
5152.05	12.0	1553.28	0.5
5164.05	8.46	1553.55	0.5
5172.51	2.21	1553.76	-
5174.72	30.79	1553.82	0.5
5205.51	4.2	1554.69	-
5209.71	14.34	1554.82	0.5
5224.05	12.0	1555.24	0.5
5236.05	12.0	1555.55	0.5
5248.05	12.0	1555.81	0.5
5260.05	8.17	1555.99	0.5
5268.22	15.83	1556.05	-
5284.05	12.0	1556.05	0.5
5296.05	14.92	1555.99	0.5
5310.97	9.08	1555.92	0.4

5320.05	12.0	1555.88	0.4
5332.05	12.0	1555.86	0.4
5344.05	12.0	1555.87	0.4
5356.05	12.0	1555.92	0.4
5368.05	12.0	1556.02	0.4